



January 2013

A Mass Spectrometry-Based Method For Quantification Of Human Metallothionein Isoforms And Usefulness In Biomarker Detection Of Cancers And Metal Toxicity

Aaron Andrew Mehus

Follow this and additional works at: <https://commons.und.edu/theses>

Recommended Citation

Mehus, Aaron Andrew, "A Mass Spectrometry-Based Method For Quantification Of Human Metallothionein Isoforms And Usefulness In Biomarker Detection Of Cancers And Metal Toxicity" (2013). *Theses and Dissertations*. 1454.
<https://commons.und.edu/theses/1454>

This Dissertation is brought to you for free and open access by the Theses, Dissertations, and Senior Projects at UND Scholarly Commons. It has been accepted for inclusion in Theses and Dissertations by an authorized administrator of UND Scholarly Commons. For more information, please contact zeinebyousif@library.und.edu.

A MASS SPECTROMETRY-BASED METHOD FOR QUANTIFICATION OF HUMAN
METALLOTHIONEIN ISOFORMS AND USEFULNESS IN BIOMARKER DETECTION OF
CANCERS AND METAL TOXICITY

by

Aaron Andrew Mehus
Bachelor of Science, Mayville State University, 2007
Masters of Science, University of North Dakota, 2009

A Dissertation

Submitted to the Graduate Faculty

of the

University of North Dakota

in partial fulfillment of the requirements

for the degree of

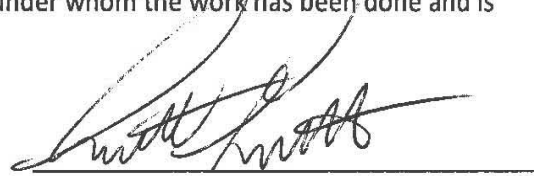
Doctor of Philosophy

Grand Forks, ND

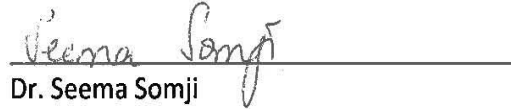
May

2013

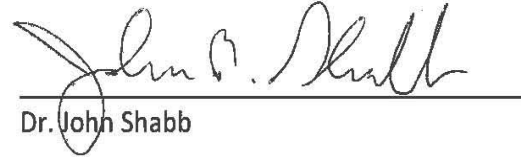
This dissertation, submitted by Aaron A. Mehus in partial fulfillment of the requirements for the Degree of Doctor of Philosophy from the University of North Dakota, has been read by the Faculty Advisory Committee under whom the work has been done and is hereby approved.



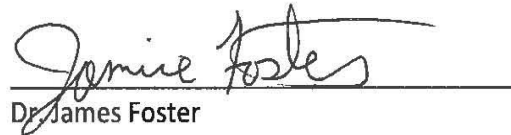
Dr. Scott Garrett,
Chairperson



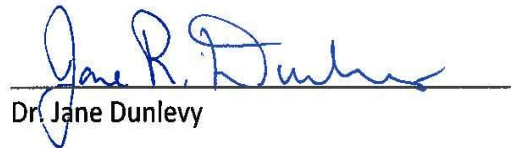
Dr. Seema Somji



Dr. John Shabb



Dr. James Foster



Dr. Jane Dunlevy

This dissertation is being submitted by the appointed advisory committee as having met all of the requirements of the Graduate School at the University of North Dakota and is hereby approved.



Dr. Wayne Swisher,
Dean of the Graduate School

April 23, 2013
Date

PERMISSION

Title A Mass Spectrometry-Based Method for Quantification of Human Metallothionein Isoforms and Usefulness in Biomarker Detection of Cancers and Metal Toxicity

Department Biochemistry and Molecular Biology

Degree Doctor of Philosophy

In presenting this dissertation in partial fulfillment of the requirements for a graduate degree from the University of North Dakota, I agree that the library of this University shall make it freely available for inspection. I further agree that permission for extensive copying for scholarly purposes may be granted by the professor who supervised my dissertation work or, in their absence, by the chairperson of the department or the dean of the Graduate School. It is understood that any copying or publication or other use of this dissertation or part thereof for financial gain shall not be allowed without my written permission. It is also understood that due recognition shall be given to me and to the University of North Dakota in any scholarly use which may be made of any material in my dissertation.

Name: Aaron A. Mehus

Date: 4-19-13

TABLE OF CONTENTS

LIST OF FIGURES.....	vii
LIST OF TABLES.....	ix
ACKNOWLEDGEMENTS.....	x
ABSTRACT.....	xii
CHAPTER	
I. INTRODUCTION	1
Background of metallothioneins.....	1
The MT gene cluster	2
MTs in cancer	3
MT isoforms: potential biomarkers of cancers.....	4
Diagnostics and MT protein isoforms.....	5
MT proteomics.....	6
STATEMENT OF PURPOSE	11
II. METHODS	12
Materials and reagents	12
Cell culture	12
Cytosol preparation	13
Human kidney and brain tissue	14
Reconstituted human urine	14

Formalin-fixed paraffin-embedded uterine specimens.....	15
Reduction and alkylation of cytosolic, urine, and fixed-tissue protein	17
Preparation of ¹⁵ N-labeled peptide standards	17
Trypsin digestion.....	18
Chromatography	19
Mass spectrometry	20
Relative and absolute quantitation	20
Real-time analysis of MT isoform mRNA expression.....	21
III. RESULTS	23
Initial method development and detection of MTs in prostate cells.....	23
N-terminal modifications of endogenous MTs.....	36
Identification of endogenous N-terminal MT peptides in HK-2 MT-3 cells...	37
Validation of ¹⁴ N and ¹⁵ N iodoacetamide for quantitation of N-terminal MT peptides	39
Cd-induction of MT isoforms in HK-2 MT-3 cells: relative quantitation...	48
Synthetic N-terminal acetylated MT peptides for absolute MT quantitation	48
MT Isoform expression in HK-2 MT-3 Cells: absolute protein quantitation..	55
MT mRNA transcript levels in the HK-2 MT-3 cells.....	55
Absolute protein quantitation of MT isoforms in human tissue	60
Extraction of pure intact MT-3 from human urine for proteomic analysis	64

Proteomic analysis of formalin-fixed paraffin-embedded uterine specimens	66
MT isoform expression in malignant and non-malignant human breast cells with different estrogen receptor (ER) status: absolute protein quantitation	68
MT mRNA transcript levels in the human breast cells	70
IV. DISCUSSION	72
V. APPENDICES	82
Appendix A- abbreviations used in text.....	83
Appendix B- MSMS spectra of endogenous and synthetic MT peptides .	86
BIBLIOGRAPHY	104

LIST OF FIGURES

Figure	Page
1. Initial work flow for identifications of human MTs from complex cell lysates	26
2. Liquid chromatography of control RWPE-1 cell tryptic peptides	27
3. Liquid chromatography of Zn-induced RWPE-1 cell tryptic peptides.....	28
4. 1D LC-MS heat map of control RWPE-1 tryptic peptides	30
5. 1D LC-MS heat map of Zn-induced RWPE-1 tryptic peptides.....	31
6. Enlarged view of “MT zone” in Zn-induced RWPE-1 1D LC-MS heat map	32
7. 1D LC-MS heat map of “MT zone” after optimization of sample preparation.	35
8. 1D LC-MS heat map of “MT zone” in control HK-2 MT-3	40
9. Strong cation exchange chromatography profile	41
10. 2D LC-MS heat map of “MT zone” in control HK-2 MT-3 cells	42
11. MS spectra of ¹⁴ N and ¹⁵ N labeled N-term acetylated MT-2 peptide in HK-2 MT-3 cytosol	44
12. Retention time vs. monoisotopic peak intensity of N-term acetylated MT-2 peptide in HK-2 MT-3 cytosol	45
13. 3D nano-rpHPLC-MS heat map of the MT zone showing the 1:1 (¹⁴ N: ¹⁵ N) labeling MT peptides in HK-2 MT-3 cytosol.....	46
14. Sensitivity and dynamic range of MT-2 relative quantitation	47

15. 3D nano-rpHPLC-MS heat map of MT zone in control (¹⁴ N) vs. Cd-induced (¹⁵ N) HK-2 MT-3 cytosol	49
16. Relative quantitation of MTs in HK-2 MT-3 cells exposed to 9 μM Cd for 3 days	50
17. Ratios (heavy/light) vs. monoisotopic peak intensities for MTs in control and Cd-induced HK-2 MT-3 cells.....	51
18. Work flow for absolute quantitation	56
19. Absolute protein levels of the MT isoforms in HK-2 MT-3 cells	57
20. Fold induction comparison of MT isoform protein and mRNA	58
21. Absolute mRNA transcript levels of the MT isoforms in HK-2 MT-3 cells	59
22. Absolute protein levels of the MT isoforms in human cortex kidney tissue ..	62
23. Absolute protein levels of the MT isoforms in human cerebrum brain tissue....	63
24. Absolute protein levels of the MT isoforms in human breast cells	69
25. Absolute mRNA transcript levels of the MT isoforms in human breast cells	71

LIST OF TABLES

Table	Page
1. Amino acid sequence alignment of human MT isoforms	7
2. Tryptic MT peptides identified in RWPE-1 cells.....	33
3. Unique N-terminal acetylated tryptic MT peptides detected in HK-2 MT-3 cells	38
4. All endogenous and synthetic human N-terminal tryptic MT peptides	52
5. Initial purity and total ionizations synthetic MT peptides.....	54
6. Absolute quantitation values of MT proteins in HK-2 MT-3 cells.....	57
7. Fold induction values for MT protein and mRNA	58
8. Absolute quantitation values of MT mRNA transcripts in HK-2 MT-3 cells.....	59
9. Absolute quantitation values of MT proteins in human cortex kidney tissue.	62
10. Absolute quantitation values of MT proteins in human cerebrum brain tissues	63
11. Absolute quantitation values of MT proteins in human breast cells	69
12. Absolute quantitation values of MT mRNA transcripts in human breast cells	71

ACKNOWLEDGEMENTS

I would like to take this opportunity to express my sincere gratitude to my lab advisor Dr. Scott Garrett. Dr. Garrett was very helpful with giving me guidance on where to start my research and gave continued support throughout the entire project. I am also very grateful for his knowledge of the metallothionein family which was a big help throughout the project. Additionally, I need to thank my committee member/proteomics core director, Dr. John Shabb. Dr. Shabb was a great help from the start of this project until the end. When I first began this project I knew very little in the field of proteomics but he was able to give me guidance with everything from mass spec-based sample preparation to data analysis. I owe much of what I know about the field of proteomics to him. I also need to thank my committee member, Dr. Seema Somji who was part of our lab group. She taught me everything I know about cell culture and was also very helpful in many technical aspects of experiments. I would also like to thank all the members of our lab for their support, especially the senior students who went the extra mile to give advice and training. I need to thank Wallace Muhonen who is a research assistant in the proteomics lab. I owe him for training me on the machines in the lab. He is full of ideas and was always there for technical support or trouble shooting. I also need to thank my fourth committee member, Dr. Jane Dunlevy, she has collaborated with our lab on many different projects including my Masters project where she was a big help. She was always there for help if needed.

I would especially like to thank Dr. Kathy Sukalski, the interim chair of our department. She truly helped in scheduling courses and making sure my graduate experience went smoothly. She was always there for advice, personally and academically, and truly cared about my well being, making me feel welcome.

I also need to express my gratitude to the faculty, staff, and students of the biochemistry department. The faculty truly contributed to my graduate education. The graduate students were all very helpful, supportive, and great to talk with. I also need to thank Marlys Kennedy, Mary Bohlman, Kim Hansen, Cathy Perry, and Jennifer Hershey for their clerical help and making sure all my paper-work was in order throughout the years. They are always a pleasure to talk to.

I need to give a special thanks to Dr. Don Sens. My project would not exist without him letting me work under his grant. I had many meetings with him throughout my project and considered it an honor for him to take time and listen to my results and give positive support of the work I was doing.

Last but not least, I would like to thank my family. My parents, Jeroy and Debbie, gave constant support of what I was doing and also showed interest in my project even though I'm not sure they truly understood it! I would also like to recognize my three older brothers and two sisters for their support, it was greatly appreciated.

ABSTRACT

Current methods for detecting metallothionein (MT) protein expression lack the specificity to distinguish between all twelve human isoforms. Each, however, can be distinguished by the masses of their acetylated, cysteine-rich, hydrophilic N-terminal tryptic peptides. These properties were exploited to develop a mass spectrometry-based method for their simultaneous quantification.

Human kidney HK-2 epithelial cells expressing recombinant MT-3 were grown in the presence or absence of cadmium. Cytosolic proteins were alkylated with ^{14}N - or ^{15}N -iodoacetamide and digested with trypsin. The N-terminal MT peptides were enriched by two-dimensional liquid chromatography and analyzed by MALDI-TOF/TOF mass spectrometry. Relative expression was measured by combining ^{14}N -labeled control and ^{15}N -labeled cadmium-treated cytosols before trypsin digestion and determining monoisotopic peak ratios of the targeted peptides. Absolute quantification was accomplished with ^{15}N -labeled synthetic peptides.

Seven isoforms (MT-1E, MT-1F, MT-1G2, MT-1M, MT-1X, MT-2, and MT-3) were detected and quantified. The dynamic range was sufficient to detect 67-fold differences in abundance and 12-fold induction for some isoforms. Combined, MTs represented 0.3% to 1.5% of total cytosolic protein. The mRNA isoform expression levels differed in both the rank order and fold induction.

The assay was also applied to four malignant (MCF-7, Hs578T, T-47D, and MDA-MB-231) and one non-malignant (MCF-10A) human breast cell lines. The malignant cell lines were either estrogen receptor positive (ER⁺) or estrogen receptor negative (ER⁻). Three MT isoforms (MT-2, MT-1E, and MT-1X) were quantified in the breast cells. In regards to the ER status of the cells, the ER⁺ malignant cells had low MT protein levels while the ER⁻ malignant cells had a significant overexpression of MTs compared to the control. When comparing the ER⁺ to ER⁻ cells, there was between a 5.5 – 14.5 fold increase in protein expression of the individual MT isoforms or a 38-fold difference in abundance between all MT isoforms. This method expands the usefulness of human MT isoforms as potential biomarkers for specific diseases or environmental exposures to heavy metals.

CHAPTER I

INTRODUCTION

Background of Metallothioneins

Metallothioneins (MTs) were first identified in equine kidney by Margoshes and Vallee in 1957¹ and are a family of small, highly conserved proteins with the specific capacity to bind metal ions²⁻⁴. The mammalian MTs are typically 61- to 68-amino acid proteins possessing a large number of highly catalytic cysteine residues. These cysteine residues are strictly conserved among species with arrangement in motifs that form two distinct metal-binding domains linked by a short peptide. There are several biological roles that the MTs are proposed to have in cellular homeostasis. The first is derived from their exceptional metal binding capacity and as such they contribute to the homeostasis of metal ions within the cell. Due to the fact that high concentrations of both essential and non-essential metal ions, like zinc, cadmium, mercury and lead can be toxic, the MTs are also involved in protection of the cell from acute heavy metal toxicity²⁻⁴. The MTs also can function in zinc metabolism by regulating the activity of fast-exchanging metalloproteins, such as the zinc finger-containing protein Sp1 and the tumor suppressor gene, p53⁵⁻⁸. The MTs are also looked upon as stress proteins participating in a variety of protective functions since they are also induced by many stimuli other than metals, such as hormones and cytokines. Because the MTs are capable of scavenging free radicals they can play a role in the protection of cells and

tissues against oxidative injury associated with such insults as radiation, lipid peroxidation, and inflammation.

The MT Gene Cluster

The study of the role that alterations in metallothionein expression may have in human disease is complicated by differences in the gene organization between humans and rodent animal models². A gene duplication event occurred in the metallothionein gene family between rodents and primates. Rodents express four MT isoforms, MT1, MT2, MT3 and MT4 while all primates to date possess multiple copies of the MT1 isoform². In contrast to the 4 rodent MT isoforms, 18 human MT isoforms and 4 human MT-like genes have been identified, most of which contain only small differences in specific amino acids. The duplication event was at the level of DNA since all active genes contain an intact promoter. Currently, there are at least 11 active human MT genes; MT4, MT3, MT2A, MT1A, MT1B, MT1E, MT1F, MT1G, MT1H, MT1M and MT1X. Seven of the MT isoforms are classified as non-processed pseudogenes (MT1IP, MT1P2, MT1JP, MT1L, MT1CP, MT1DP, and MT2P1); although it is not clear if some of the proposed pseudogenes are functional². The MT1JP and MT1DP genes contain a promoter and are transcribed, but they also encode a premature stop codon. Seventeen of the 18 isoforms are clustered together on chromosome 16q13 and chromosome 16 is known to be enriched for intrachromosomal duplications². The various MT isoforms do differ in their patterns of expression. In general, the MT3 and MT4 are constitutively expressed in a narrow range of cell types; whereas, the MT1 and MT2 isoforms are highly inducible and constitutively expressed upon stimulation. The

human MT1 isoforms show less divergence from human MT2 than from mouse MT1 based on the coding sequences of the genes, suggesting that the MT1 and MT2 isoforms arose after the emergence of primates⁹. In contrast, phylogenetic analysis of the mouse and human MT3 and MT4 isoforms proteins suggest that these isoforms diverged prior to the primate/rodent divergence². Both the human and mouse MT1 and MT2 isoforms are clearly distinct from the MT3 and MT4 clusters, in line with the unique tissue distributions and inducibility of the two sets of isoforms.

MT gene expression is known to be induced by oxidative stress and metal ions which suggests that MTs are an important component in the cells protection against and recovery from environmental insult, specifically those associated with heavy metals¹⁰⁻¹⁴. MT isoforms are ubiquitous and basally expressed at low levels but are also inducible by cytokines, xenobiotics and hormones¹⁵⁻¹⁷. MT expression has also been implicated to play a role in many types of diseases including cancers, Alzheimers disease (AD), amyotrophic lateral sclerosis (ALS), autism, Parkinsons disease (PD), and even prion disease¹⁸⁻²³.

MTs in Cancer

Although MTs have shown to be associated with various diseases, their association with cancers is predominantly reported. MTs have been shown to have either increased or decreased expression in a tissue-dependent manner in carcinogenesis with no general consensus of expression levels seen for all cancer types. The mRNA and/or protein for MTs has been shown to be overexpressed in cancers of the human kidney, urinary bladder, breast, ovary, pancreas, testes, lung, nasopharynx,

leukemia, and non-Hodgkin's lymphoma (NHL)²⁴. On the other hand, a decreased expression of MT mRNA and/or protein has been shown in cancers of the human colon, liver, thyroid, central nervous system (CNS), and prostate²⁴. The level of increased or decreased expression of MT isoforms in these tumors has been suggested to have a relationship with tumor growth, prognosis, and/or patient resistance/response to cancer treatments²⁴.

MT Isoforms: Potential Biomarkers of Cancers

On an MT isoform-specific basis, human MT-3 was first considered to be brain-specific in expression but was shown to be expressed (mRNA and protein) in normal and malignant kidney and bladder, and quantifying levels of this MT isoform and/or other isoforms in the urine or tissue may be of potential use as a prognostic marker of tumor progression¹⁹⁻²². Clinically, breast tumors are routinely immunohistochemically stained and classified as ER⁺ or ER⁻ depending on the presence (ER⁺) or absence (ER⁻) of the estrogen receptor, and patients with ER⁻ tumors tending to have worse patient prognosis due to tamoxifen resistance. The ER status of the tumor is a good prognostic biomarker of breast cancers but ~25% of tumors will not stain exclusively ER⁺ or ER⁻ and the pathologist will classify the tumor as “unknown ER status”. In these patients, the chemotherapeutic regimen is not entirely clear and some individuals may get treated with drugs that will not aid in treating the disease but actually make them sicker. In these cases it would be beneficial to have an alternative biomarker for use as a prognostic marker or help guide the therapeutic decisions and the MT status could potentially be this type of marker. MT-1E mRNA has been shown to be highly

expressed in ER⁻ human breast cells and invasive ductal breast cancer tissue compared to absent or low expression of MT-1E mRNA in ER⁺ cells and tissue^{29,30}, suggesting a relationship between this gene and the estrogen receptor status of the tumor cells. In a larger study that suggests MT-2As association with cell proliferation in breast cancer, MT-2A transcript was the highest among all other MT isoforms detected in seventy-nine cases of human invasive ductal breast carcinoma and the total MT protein was significantly higher in histological grade 3 compared to grade 1 and 2 tumors³¹. These are a small sub-set of examples but specific MT isoforms have been hypothesized to play roles or be potential biomarkers in many cancers. Taken together, the MT isoforms are an attractive biomarker in the clinical and toxicological community.

Diagnostics and MT Protein Isoforms

A major factor compromising the study of the role of the individual MT isoforms in human disease is the lack of isoform-specific antibodies to the individual MT family proteins. Due to similarities in amino acid sequence, the only isoform-specific antibody that can be produced is against the MT-3 isoform³². However, there is an antibody (Dako, clone E-9) that recognizes all the MT1, MT2 and MT4 protein isoforms that has been widely used for the histochemical determination of the expression of this family of proteins in cells and tissues³³. In fact, it is research using the E-9 antibody that has identified the need to develop methodology to quantify the individual MT isoform specific proteins. The E-9 antibody against the human MT1, 2 and 4 family members has been widely used to demonstrate the immunohistochemical overexpression of MT in a wide variety of human cancers and has been the subject of several excellent reviews³³⁻

³⁵. In general, the overexpression of MT in various cancers, as determined using the E-9 antibody, has been associated with resistance to anticancer therapies and linked to a poor prognosis. While there is methodology to determine the expression of mRNA from the individual MT isoform genes^{36, 37}, there are no available methods to determine the individual expression of the isoform-specific proteins in cells and tissues. This prevents studies to determine if the expression of individual MT proteins may have diagnostic and prognostic significance beyond that found for the family members as determined as an undefined group of proteins or through their mRNA expression patterns. The goal of the present study was to develop a proteomic method to identify and quantify the individual proteins that comprise the human metallothionein gene family.

MT Proteomics

The N-terminal tryptic peptide of each human MT isoform has a unique sequence that may be used for their identification and quantification in complex biological samples from human cells and tissues³⁸ (Table 1). Any attempt at quantification of this family of small, highly conserved, cysteine rich proteins therefore requires reproducible detection of these signature peptides. A number of studies have shed light on the nature of the N termini of MT isoforms which help inform the design of their mass spectrometry-based quantitation. In the 1970's and 1980's, Edman sequencing of several mammalian MTs demonstrated that its N-terminal methionine was acetylated³⁹⁻⁴³. This conclusion is consistent with more recent general studies of N-termini which show that proteins beginning with Met-Asp, such as human MTs, are almost completely acetylated⁴⁴⁻⁴⁶. Other studies utilizing capillary electrophoresis

and mass spectrometry detected trace amounts of unacetylated MTs⁴⁷⁻⁵⁰. The fraction of unacetylated MT2 reached 20% in livers of zinc-treated rats⁴⁸. Though a minor form, unacetylated MT may have physiological relevance since its metal-binding properties are distinct from the acetylated form⁴⁹. Taken together, MTs are likely stoichiometrically N-acetylated except possibly under metal-stressed conditions when a minor degree of under-acetylation may be observed.

Structural studies based on Edman sequencing or amino acid analysis do not address whether the N-terminal methionine might be oxidized. This is likely because of reversion of methionine sulfoxide to methionine under the acidic conditions of these procedures^{51, 52} or because cyanogen bromide may not have cleaved the N-terminal methionine sulfoxide⁵³ preventing Met-oxidized MTs from being sequenced.

In more recent years a few mass spectrometry-based studies have succeeded in identifying the complement of MT isoforms in human cells^{38, 54}. Though top-down approaches hold promise for quantitation of MTs based on the unique masses of intact isoforms^{38, 55}, this has yet to be exploited. Bottom-up quantitative approaches specifically targeting MTs have not yet been reported.

Detection of MT peptides, especially the critical N-terminal peptides, appears to be sporadic in global proteomic profiling studies. A survey of the Human 2012-10-11 build of the PeptideAtlas database^{56, 57} reveals that N-terminal MT peptides are identified in only ten of 467 samples in the repository. Seven of the data sets have been published⁵⁸⁻⁶². Combined, these studies identified three MT N-terminal peptides (MT-2, MT-1E, MT-1X). Only one study detected the acetylated forms of MT-1X and MT-1E⁵⁹.

The rest detected only unacetylated forms because N-terminal protein acetylation was not selected as a variable modification as a parameter for database searches.

Even when N-terminal acetylated proteins are specifically targeted for profiling, detection of MT peptides is still limited to MT-2 and MT-1X⁴⁶. The COFRADIC (combined fractional diagonal chromatography) approach that has been successfully applied to the mass spectrometric characterization of many blocked N-termini^{63, 45} unfortunately excludes acetylated N-terminal MT peptides because the method requires cleavage at arginine residues which are absent from all human MTs except MT-4.

Since human MT isoforms are distinguished by only one to three tryptic peptides (Table 1), the label-free methods utilized by the two PeptideAtlas-referenced studies that reported MT abundance^{58, 59} are not sufficiently robust for their accurate quantitation even if N-terminal acetylated peptides are measured. Accurate quantitation is further compromised in global studies that do not incorporate N-terminal acetylation into their search parameters. One can conclude from this survey that most global proteomic profiling strategies are not optimized for MT quantification and may even yield misleading results. In order to develop a robust peptide-based quantitative profiling strategy, existing LC-MS approaches needed to be optimized for this family of proteins.

Given the high cysteine content of the N-terminal MT peptides, the use of isotopically labeled alkylating agents as a means of introducing mass tags for quantitative profiling was chosen. The demonstration that deuterated acrylamide could be used as a cysteine-directed mass tag for proteomics⁶⁴ and the development of the

commonly used iodoacetamide-based “isotopic-coded affinity tags” (ICAT) method of quantitative analysis⁶⁵ spurred the development of numerous variants of isotopically-labeled alkylating agents⁶⁶⁻⁷¹, all potentially applicable to quantitative proteomics of MTs. Some of these agents, particularly the deuterated compounds have the disadvantage of isotope effects that may cause differences in chromatography^{72, 73}, making them less desirable for LC-MS/MS-based quantitative profiling. Others are not commercially available. All of these alkylating agents give mass shifts of from 3 to 7 Da, which is reasonable for singly or doubly modified peptides. Mass shifts for N-terminal MT peptides would be five times as great, and any isotope effects would be magnified accordingly.

STATEMENT OF PURPOSE

The first goal of this study was to develop a mass spectrometry-based method of identifying metallothionein isoforms in complex cell or tissue lysates. The second goal of this study was to develop a means to quantify (relative and absolute) MT isoforms in complex cell or tissue lysate using mass spectrometry. Furthermore, I wanted to apply this assay to quantify inductions of MTs from metal treatment. I also wanted to develop a method for extracting MTs from urine then quantifying levels which has biomarker potential of renal or bladder cancer. Lastly, I wanted to apply this assay in malignant and non-malignant breast cells with differing estrogen receptor status. Since MTs have been widely used diagnostically, they may be a good place to look for prognostic/diagnostic biomarkers for cancers or heavy metal exposure.

CHAPTER II

Methods

Materials and Reagents - ^{15}N -iodoacetamide, ^{14}N -iodoacetamide, absolute ethanol, EDTA, urea, sodium chloride, Tris, dimethyl sulfide, xylene, tris(2-carboxyethyl)phosphine and dithiothreitol was from Sigma-Aldrich (St. Louis, MO). SDS was from Bio-Rad (Hercules, CA). RapiGest SF was from Waters Corporation (Milford, MA). Human urine (freeze-dried)- KOVA-Trol III was from HYCOR Biomedical (Garden Grove, CA). Microcon Centrifugal Filter Devices were from Millipore Corporation (Bedford, MA). Formic acid was from Thermo Scientific (Waltham, MA). MS-grade water, acetonitrile, and methanol were from Fisher Scientific (Pittsburgh, PA). Pure intact MT-3 was from Bastenbalt (Tallinn, Estonia). Isoform-specific N-terminal acetylated MT peptides were synthesized by Elim Biopharmaceuticals (Hayward, CA).

Cell Culture-

Human Prostate Cells- The RWPE-1 cells were obtained from the American Type Culture Collection (ATCC, Manassas, VA). The RWPE-1 cells were grown in keratinocyte serum-free medium (K-SFM) containing 50 $\mu\text{g}/\text{ml}$ bovine pituitary extract and 5 ng/ml epidermal growth factor. Cultures were incubated at 37 °C in a humidified atmosphere containing 5% CO_2 . The cells were fed fresh growth medium every 3 days and at

confluence the cells were subcultured at a 1:4 ratio using trypsin-EDTA (0.05%, 0.02%). For use in experimental protocols, cells were subcultured at a 1:4 ratio in T-75 flasks, allowed to reach confluence, and then exposed to 75 μ M zinc sulfate for 4 days. The cells were fed fresh medium containing zinc on day 3 and harvested for total protein or RNA on day 4.

Human Kidney Cells- Epithelial HK-2 cells containing the stably transfected human MT-3 were grown as described previously^{74, 75}. The cells were allowed to reach confluency with doming. After cells domed they were maintained for three days in the presence or absence of 9 μ M CdCl₂ to induce the expression of metallothioneins.

Human Breast Cells- Five breast cell lines (MCF-10A, MCF-7, T-47D, Hs578T, MDA-MB-231) were obtained from the American Type Culture Collection. The MCF-10A cells were grown in a 1:1 mixture of Ham's F-12 medium and DMEM supplemented with 5% (v/v) fetal calf serum, 10 μ g/ml insulin, 0.5 μ g/ml hydrocortisone, 20 ng/ml epidermal growth factor, and 0.1 μ g/ml cholera toxin. The MCF-7, T-47D, Hs578T, and MDA-MB-231 cells were grown in DMEM supplemented with 5% (v/v) fetal calf serum. The cells were fed fresh growth medium every 3 days, and at confluence (normally 6-12 days post subculture), the cells were subcultured at a 1:4 ratio using trypsin-EDTA (0.25%, 1 mM).

Cytosol Preparation - All data from cells listed above represent biological replicates done in triplicates. Cell monolayers from two T-75 flasks were washed twice with phosphate-buffered saline (PBS), detached by scraping, and pelleted by centrifugation

at 197 x g for 5 min at 4°C. Cell pellets were either stored at -80°C or used immediately. Cells were resuspended in 0.5 mL of hypotonic buffer (10mM Tris pH 8.0, 1.5 mM MgCl₂, 10 mM KCl, 1 mM DTT, and 0.5 μL protease inhibitor cocktail (Sigma-Aldrich)). The cells were then passed through a 25-gauge, 5/8 inch needle three times to disrupt membranes. The nuclei were pelleted by centrifugation (800 x g for 10 min at 4°C) and the supernatant was further clarified by centrifugation at 100,000 x g, 30 min at 4°C. Total protein was determined by the Bio-Rad Protein Assay (Bio-Rad, Hercules, CA). Typical yields of 0.5 mL cytosol per two T-75 flasks containing 3.0-3.5 mg/ml protein were obtained. Cytosols were stored at -80 °C.

Human Kidney and Brain Tissue- Data from these tissues represent three technical replicates of one biological replicate. Frozen cortical kidney tissue and cerebrum brain tissue was also used in these studies. The frozen kidney tissue came from an elderly renal cancer patient's kidney that was removed due to cancer. The kidney tissue came from healthy cortex of the diseased organ. No data was available for the human brain tissue. Tissues did not have patient identifiers. A small piece of these tissues was manually homogenized and processed in hypotonic lysis buffer as listed above to extract cytosolic protein.

Reconstituted Human Urine- Methods for total protein extraction from urine were analyzed to discover the most efficient way to extract MTs from this biological fluid and look for potential modifications of the MT proteins or peptides. Freeze dried human urine (KOVA-Trol III-HYCOR Biomedical (Garden Grove, CA)) was purchased and

reconstituted in H₂O for use in development of MT protein extractions. Methanol precipitation showed highest recovery of protein. Briefly, 5 µg of intact pure unacetylated MT-3 was spiked into 1 ml of urine or MS-grade H₂O for a control. The samples were then incubated for 5 hours at 37 °C in a water bath to mimic conditions in human bladder. Samples were centrifuged immediately at 10,000 X g at 4 °C to remove particulate matter and cell debris. Pelleted material was discarded and supernatant was transferred to a fresh tube. 100% stock solution of methanol was added to urine at a ratio of 9:1. 3.5 mM EDTA was added to chelate any metals bound to MTs and to aid in their precipitation. The samples were then incubated overnight (12-16 hr.) at -20 °C then centrifuged at 14,000 X g for 30 mins. at 4 °C. Methanolic supernatant was decanted off and protein pellet was resuspended in MS-grade H₂O and transferred to fresh eppendorf tube. Ultrafiltration (3000 Da MWCO membrane) was also used as an extraction method for MTs in the urine according to the manufacturer's instructions. After extraction of total urine protein, the concentration of the protein was estimated by area under curve analysis by 214 nm absorbance. The protein was then either analyzed immediately as described below or stored at -80 °C.

Formalin-Fixed Paraffin-embedded Uterine Specimens- Slices of tissue (2 X 10 µM) were minced and placed in clean 1.5 ml Eppendorf tubes. Paraffin was removed with three washes in 1 ml of pure (99.0+%) xylene, and rehydration was achieved with three washes each in 1 ml of 100, 90, and 70% absolute ethanol. Uterine tissues were resuspended in 100 µl of 0.2% (w/v) RapiGest in 50 mM ammonium bicarbonate with 5 mM DTT or 100 µL of Qproteome Extraction Buffer (Qiagen, Germantown, MD). For

RapiGest protein extraction, the samples were vortexed aggressively then incubated on ice for 5 min. and then mixed again by vortexing. The samples were then incubated at 100 °C for 30 min. then cooled on ice for 5 min. followed by vortexing vigorously. The samples were heated at 80 °C for 2 hr. with agitation at 750 rpm followed by 5 min. incubation on ice. Samples were then centrifuged for 15 min. at 14,000 X g at 4 °C. The supernatant containing the extracted proteins was transferred to a new microcentrifuge tube. A 10 µl aliquot was removed from samples to estimate protein concentration using a BCA assay. The proteins were reduced, alkylated, and digested as described below. After digestion the RapiGest surfactant was precipitated from samples with 0.5% formic acid before LC-MS described below. Extraction of proteins using the Qproteome kit was achieved by using the manufacturer's standard protocol. Filter-Aided Separation of Proteins (FASP) was required to remove detergent from the extracted proteins from the Qproteome kit before digestion and LC-MS. Briefly, 50 µL of lysate was mixed with 200 µL 8M urea in 0.1M Tris pH 8.0 in the filter unit (YM-3) and was centrifuged at 14,000 X g for 30 min. Then 200 µL of urea solution was added to the filter unit followed by centrifugation at 14,000 X g for 20 min. The flow-through was discarded from collection tube and the recovered samples were reduced and alkylated as described below in the filter unit followed by centrifugation at 14,000 X g for 10 min. 100 µL of the urea solution was added to the filter units followed by centrifugation at 14,000 X g for 15 min., and then this step was repeated twice. 100 µL ammonium bicarbonate (ABC) was added to filter units, they were then centrifuged at 14,000 X g for 10 min. This step was repeated twice. 40 µL ABC with 2% trypsin was added to filter

units and incubated at 37 °C overnight. The filter units were then transferred to new collection tubes and centrifuged at 14,000 X g for 10 min. 50 µL of ABC was added to filter units followed by centrifugation at 14,000 X g for 10 min. The resulting peptides were used in LC-MS experiments as described below.

Reduction and Alkylation of Cytosolic, Urine, and Fixed-tissue Protein – 300 µg of protein (~100 µl) was incubated with 3.5 mM EDTA. Samples were then denatured with 8 M urea, then reduced with 5 mM dithiothreitol (DTT) or tris(2-carboxyethyl) phosphine (TCEP) in 100 mM Tris pH 8.0 for 1 hour at room temperature in a final volume of ~190 µl. Proteins were then alkylated at room temperature in the dark for 1 hour by the addition of ~27 µl of 200 mM ¹⁴N- or ¹⁵N-iodoacetamide to a final concentration of 28 mM. Urea and excess alkylating agent were removed from the samples by passing them through ~1 ml of Bio Gel P-6 in micro Bio-Spin chromatography columns (Bio-Rad Laboratories, Hercules, CA) equilibrated with 100 mM Tris pH 8.0.

Preparation of ¹⁵N-labeled Peptide Standards -The purity of the seven metallothionein peptides as received from the manufacturer ranged from 11 to 90% even though >95% purity was requested. This was primarily because of the difficulty of synthesis related to the high cysteine content and peptide-specific sequences. Thirty µg of each peptide was reduced with 5 mM DTT or 5 mM TCEP in 100 mM Tris pH 8.0 for 1 hour at room temperature in a final volume of 31.5 µL. The reduced peptides were then alkylated with 28 mM ¹⁵N-iodoacetamide for 1 hour in the dark at room temperature. The ¹⁵N-labeled peptides were then purified by reversed-phase chromatography using a narrow-

bore 2.1 x 150 mm Zorbax 300SB-C18, 5- μ m bead-size column (Agilent Technologies, Santa Clara, CA) on a Shimadzu 10-AVP HPLC (Shimadzu, Kyoto, Japan). Peptides were separated with a linear 35 min gradient using 97% Buffer A (0.1% formic acid, 2% acetonitrile) to 38% Buffer B (0.1% formic acid, 98% acetonitrile) at 0.3 ml/min. Peptides were detected by absorbance at 214 nm. The peak corresponding to the peptide with the correct mass as determined by mass spectrometry was collected, dried and reconstituted in MS grade H₂O. All ¹⁵N-labeled peptides were at least 95 % pure as assessed by rpHPLC. Peptide concentration was determined using area under the curve analysis at 214 nm based on the absorbance of a known amount of MT peptide for which the peptide concentration using elemental analysis was provided by the manufacturer represented a product of >95% purity. Aliquots of the purified ¹⁵N absolute MT standard peptides were stored at -80°C. A reference mixture containing 145 pmol/ μ L of each of the seven ¹⁵N-labeled peptides (MT-2, MT-3, MT-1E, MT-1G2, MT-1X, MT-1M, MT-1F) served as the internal standard for absolute quantitation experiments in the HK-2 MT-3 cells. For the breast cells, a reference mixture containing 100 pmol/ μ L of each of the three ¹⁵N-labeled peptides (MT-2, MT-1E, MT-1X) was used as the internal standard for absolute quantitation.

Trypsin Digestion - For relative quantification, 300 μ g each of ¹⁴N-labeled control cytosol and ¹⁵N-labeled Cd-treated cytosol were combined. For absolute quantification, 1 μ l of ¹⁵N-labeled MT peptide reference mix was added to 300 μ g of ¹⁴N-labeled sample. Samples were incubated with modified trypsin, 2% w/w (Trypsin Gold, Promega, Madison, WI) overnight at 37°C. The reaction was stopped by the addition of

formic acid to 0.1% final concentration. Peptides were desalted online via HPLC through a self-packed Magic C18AQ column (200A pore size, 5 micron diameter particles, MICHROM Bioresources, Auburn, CA) using 0.15 ml/min Buffer A (0.1% formic acid) for ~20 minutes. The peptides were then eluted onto a strong cation exchange (SCX) column using a 500 μ l injection of 75% acetonitrile and 0.1% formic.

Chromatography - Peptides were then fractionated on a 2.1 mm x 25 cm poly LC polysulfoethyl A self-packed SCX analytical column with a 60 min linear gradient using Buffer A (0.1 % formic acid) and from 0-25% Buffer B (0.1% formic acid; 1 M NaCl; 10% acetonitrile) at 0.15 ml/min. Fractions were collected every seven minutes and screened by mass spectrometry to locate the MT peptides. The MT peptide-containing fraction was evaporated to dryness, and reconstituted in 24 μ l 8 M HCl containing 0.5 M dimethyl sulfide. The reaction was incubated 30 minutes at room temperature to reduce methionine sulfoxides⁷⁶. The reaction was then quenched by the addition of 12 μ l 5 M NaOH. Precipitated salt was pelleted by centrifugation at 14,000 x g for 2 minutes at room temperature and the supernatant was collected. The sample was immediately injected into a self-packed 100 μ m x 10 cm Magic C18AQ column (200A pore size, 5 micron diameter particles, MICHROM Bioresources, Auburn, CA) using a Tempo LC-MALDI (ABI SCIEX, Framingham, MA) integrated nano-HPLC/spotter. The column was equilibrated with 97% Buffer A (0.1% formic acid, 2% acetonitrile) and 3% Buffer B (0.1% formic acid, 98% acetonitrile) at a flow rate of 0.8 μ l/min and peptides were fractionated with a 70 min linear gradient of 3% Buffer B/97% Buffer A to 20% Buffer B/80% Buffer A. Fractions were spotted every 0.18 seconds onto a MALDI target plate

with post-column mixing of an equal volume of 10 mg/mL α -cyano-4-hydroxycinnamic acid (CHCA) in 75% acetonitrile, 0.1% formic acid. The column was recycled with 70% Buffer B/30% Buffer A for 5 minutes and then re-equilibrated with 3% pump B for 10 minutes.

Mass Spectrometry - The samples were analyzed by MS and MS/MS using an ABI 4800 MALDI-TOF/TOF mass spectrometer. For MS, laser intensity was 3200 to 3500 and 900 spectra were accumulated over 30 subspectra at 30 shots per subspectrum. The precursor ion mass range was limited to m/z 1800-3000. Resolution was typically 15000. Metallothionein peptide identities were confirmed by MSMS. Laser intensity was 4000. Spectra were accumulated over 30 subspectra at 30 shots per subspectrum.

Unprocessed .t2d files were centroided and converted to .mgf files using the Peaks to Mascot tool on the AB Sciex 4000 Explorer software (version 3.5.28193). MT peptides were identified using Mascot version 2.3.02 (Matrix Science Inc., Boston, MA). Spectra were searched against the human proteome in the UniProt protein database (version 15.15). Search parameters were set at precursor peptide mass tolerance of 1.2 Da; fragment ion tolerance of 0.6 Da; enzyme – trypsin; fixed modification - cysteine ^{15}N -carbamidomethylation; variable modifications - acetylation (protein N-term), methionine oxidation, cysteine ^{14}N -carbamidomethylation; missed cleavages - up to two. Peptide mass errors were typically less than 100 ppm. Mascot ion scores were routinely 60-150.

Relative and absolute quantification - The mean monoisotopic peak intensity was determined for each MT ^{14}N and ^{15}N precursor ion across three to five spots spanning

the precursor ion peak. The minimum signal to noise ratio accepted for a given peak was 20. The mass difference between pairs of ^{14}N - and ^{15}N -labeled MT precursor ion pairs was 5 Da. Intensities of the ^{15}N -labeled monoisotopic peaks were corrected for the contribution of the overlapping ^{14}N peptide n+6 isotopic peak using the equation $H_{corr} = H - (L * C) - (H - L * C)(P * P')$ where H and L are the intensities of the monoisotopic peak of the heavy- and light- labeled precursor ions respectively, C is the percent contribution of the n+6 isotopic peak of the light precursor ion, P is the atom percent ^{14}N contamination in ^{15}N iodoacetamide, P' is the atom percent purity of ^{15}N iodoacetamide. The ^{14}N contamination was based on 99 atom percent according to the manufacturer.

Real Time Analysis of MT Isoform mRNA Expression - Total RNA was purified from RWPE-1, HK-2 MT-3, MCF-10A, Hs578T, MDA-MB-231, MCF-7, and T-47D cell pellets (biological replicates done in triplicates) using the manufacturer's standard TRI REAGENT (Molecular Research Center, Cincinnati, OH) protocol. The measurement of MT isoform mRNA expression was assessed with real time RT-PCR utilizing previously described MT isoform-specific primers³⁶. The primers sequences used for MT-1M consisted of: Up- GGGCCTAGCAGTCG, Low- TGGCTCAGTATCGTATTG. The primer sequences used for 18S mRNA expression were: Up- CGCCGCTAGAGGTGAAATTC, Low- TTGGCAAATGCTTTCGCTC. Forty nanograms of total RNA was subjected to RT-PCR amplification using the iScript One-Step RT-PCR kit (Bio-Rad Laboratories, Hercules CA) with SYBR Green using 0.2 μM of primers in a total reaction volume of 20 μL in an iCycler iQ real-time detection system (Bio-Rad Laboratories). Amplification was

monitored by SYBR Green fluorescence and compared with that of a standard curve of each MT isoform gene cloned into pcDNA3.1/hygro (+) and linearized with *Fsp* I. Cycling parameters consisted of a reverse transcription step at 50 °C for 10 minutes, denaturation at 95 °C for 15 seconds, annealing at 65 °C for 40 seconds, and extension at 72 °C for 40 seconds which gave the optimal amplification efficiency of each standard. For MT-1M, 62 °C was used for the annealing temperature while the other cycling parameters listed above remained the same. The level of MT isoform expression was normalized to that of 18S assessed by the same assay.

CHAPTER III

Results

Initial method development and detection of MTs in prostate cells

The RWPE-1 cell line was used for the development of the method used to identify MTs in a complex lysate. These cells were used based on prior experiments from our laboratory that demonstrated there is a large induction of MTs when these cells are treated with 75 μ M zinc sulfate for four days. The high levels of MTs in these cells would increase the likelihood of detecting MTs with MS.

A major limitation to overcome in targeted MS experiments with complex lysates is ion suppression. Ion suppression is defined as the simultaneous presence of more than one component in the ion source which can result in competition in the ionization process and lead to a subsequent reduction in MS signals. Ion suppressors can be ionic species (electrolytes and salts), highly polar compounds (phenols or pigments), or various organic molecules (carbs, lipids, urea, metabolites, and peptides). For proteomic studies, various top-down and/or bottom-up separation/enrichment techniques to overcome suppression can be employed to identify the proteins or peptides of interest. Size exclusion chromatography (SEC), ion exchange (IEX), isoelectric focusing, and reverse-phase liquid chromatography (RPLC) are just a handful of examples employed to reduce sample complexity.

The very first technique used in this study to reduce sample complexity to enrich for and identify MTs was OFFGEL electrophoresis coupled with nano-rpHPLC (data not shown). OFFGEL focuses proteins or peptides in solution according to their isoelectric points (PI). Unfortunately, this technique was unsuccessful for a number of reasons. The chemical properties of the MT proteins or peptides inhibit the successful use of this technique. Studying the sequences of the MT family of proteins revealed that the very first N-terminal tryptic peptide (T1) is required to distinguish all of the MT isoforms so isolating this peptide is imperative for successful identification of the MT isoforms (Table 1). The main limitation with OFFGEL is the pH strips used to focus the proteins or peptides. The strips have a limited pH range of 3-10 but in actuality the pH range focused is much narrower, such as 4-7. This is a problem when it comes to using OFFGEL to focus MT peptides or proteins because the T1 peptide PI is very acidic (below the low pH range of OFFGEL) and the intact protein PI is basic (above the high pH range of OFFGEL). So, the extreme pH range of the MT T1 or the intact protein isoforms prevent the successful use of OFFGEL as a first dimension separation technique. Ampholytes used in the OFFGEL experiments are another problem for LC-MS experiments. Ampholytes are molecules that carry both acidic and basic groups and are used to help focus the peptides or proteins in OFFGEL experiments. The problem is that they mimic peptides as well and are suppressive in LC-MS requiring special measures to remove them from samples.

After OFFGEL was deemed unsuccessful, it was necessary to develop an alternative enrichment strategy to detect the MT isoforms in cells or tissue. Heat depletion of intact proteins was then used to enrich for MTs. The physical properties of the MT proteins add attractiveness to this method. MTs are very small and have been known to stay in solution when the sample is heated to 95-100 °C and this method has been used for years to isolate MTs. If the MTs are bound to metals they are even more stable and resist precipitation. Figure 1 displays the initial work flow used for detection of MTs in the RWPE-1 cells. Early experiments with this technique involved preparing a cytosolic lysate in hypotonic lysis buffer (methods) then heating the sample to 95 °C for five minutes which precipitates the majority of intact proteins in the lysate. Precipitates were spun out and proteins remaining in solution were treated with EDTA followed by reduction, alkylation, and tryptic digestion. The resulting peptides were then separated based on their hydrophobicity using nano-rpHPLC and then analyzed by MS. Figures 2 and 3, respectively, show the reversed-phase chromatography of the peptide peaks based on 214 nm absorbance of the heat depleted control and Zn-induced cytosolic lysates. There are clear differences in the chromatographic profiles of peptides of the control and Zn-induced samples. The Zn-induced chromatograph displays multiple peaks early in the acetonitrile gradient that are absent in the control sample. After the samples had been separated by nano-rpHPLC and spotted onto a MALDI target plate, the samples were analyzed by MS and MSMS.

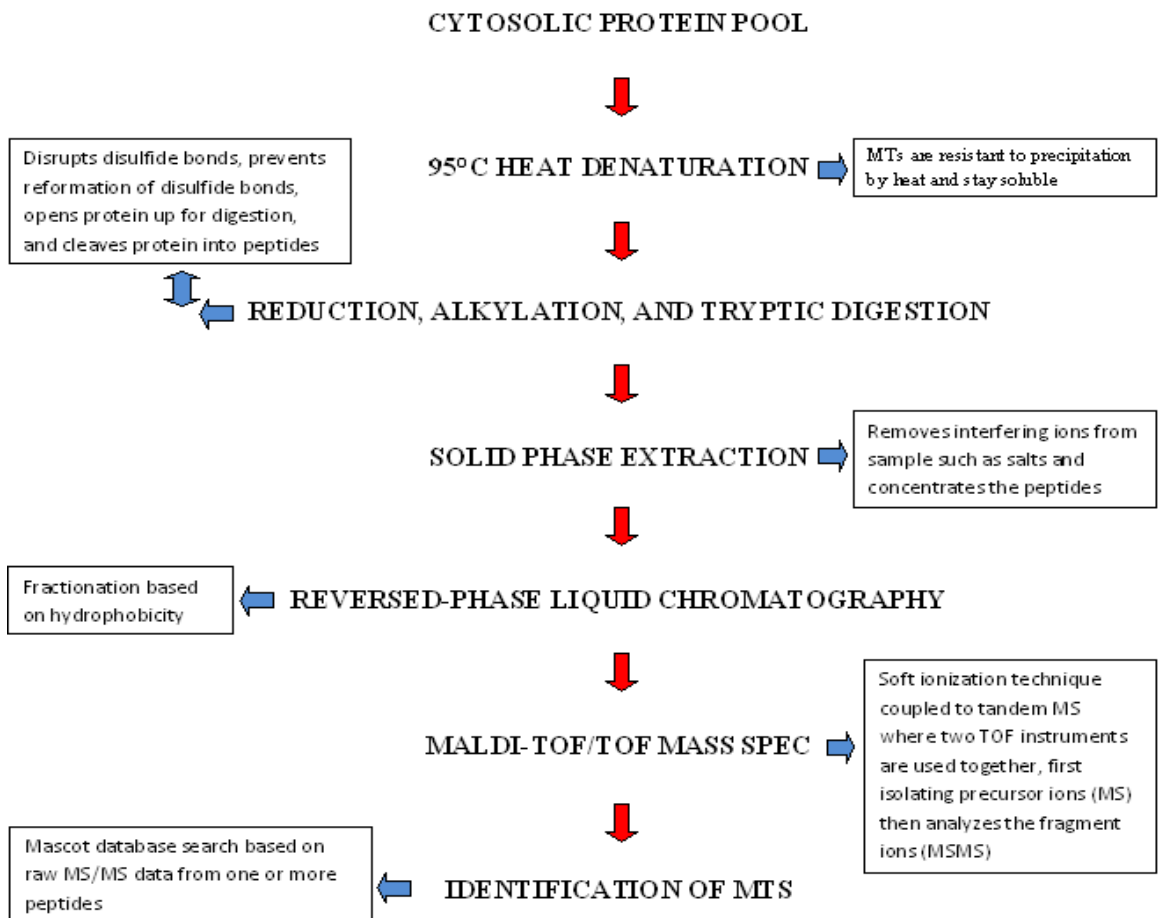


Figure 1. Initial work flow for identifications of human MTs from complex cell lysates.

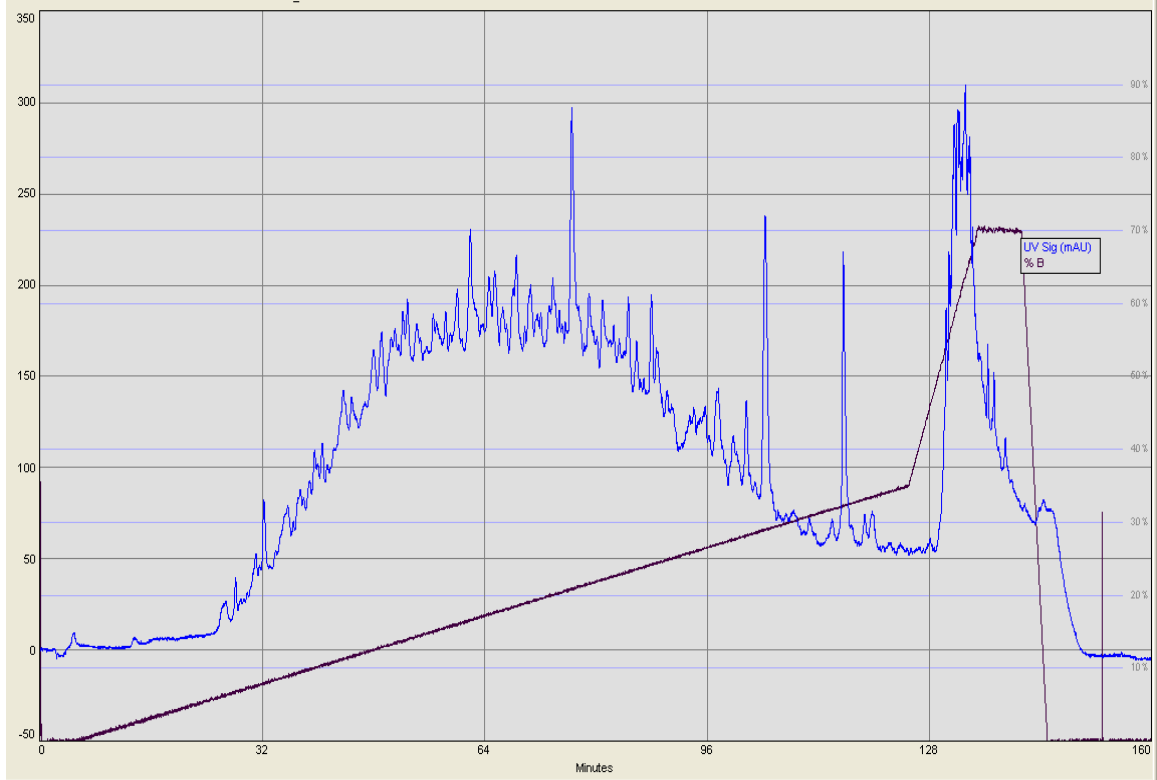


Figure 2. Liquid chromatography of control RWPE-1 cell tryptic peptides.



Figure 3. Liquid chromatography of Zn-induced RWPE-1 cell tryptic peptides.

Figures 4 and 5, respectively show the LC-MS heat maps of the sequenceable peptides within the control and Zn-induced lysates. Again, there is a distinct difference when comparing the two heat maps. The Zn-induced sample (Figure 5) has a high abundance of early eluting peptides that were identified using MSMS as being various MT peptides from multiple isoforms and also modified MT peptides (Figure 5, MT-zone). A remarkable feature of the heat maps was that the MT peptides were segregated almost completely from the typical smaller early-eluting and larger more hydrophobic peptides (Figure 5). Appendix B contains MSMS spectra and fragmentation tables for all MTs identified and studied in this project. The only identifiable MT in the control sample (Figure 4) in these initial experiments was the higher abundant MT-2 isoform. Figure 6 displays an enlarged view of the MT zone of the LC-MS heat map from the Zn-induced sample. Seven MT isoforms were identified in these Zn-induced heat depleted samples (MT-1E, 1F, 1G1, 1G2, 1X, 1M, 2) but there were also multiple modifications on these peptides (Table 2). Some of the peptide modifications were endogenous (acetylated N-term, +42 Da) but most were exogenous sample preparation artifacts such as ammonia-loss of N-term cysteines (-17 Da), dethiomethylation (-48 Da) of methionine, truncations of 1 or 2 residues on N- and C-term (Δ M, Δ MD, Δ CA), and oxidation of methionine (+16 Da). The presence of these exogenous modifications needed to be resolved since quantitation was an eventual goal of this project. Not only does having multiple species (modifications) of the same peptide affect reproducibility and accuracy of quantitation, it also limits the sensitivity of the assay.

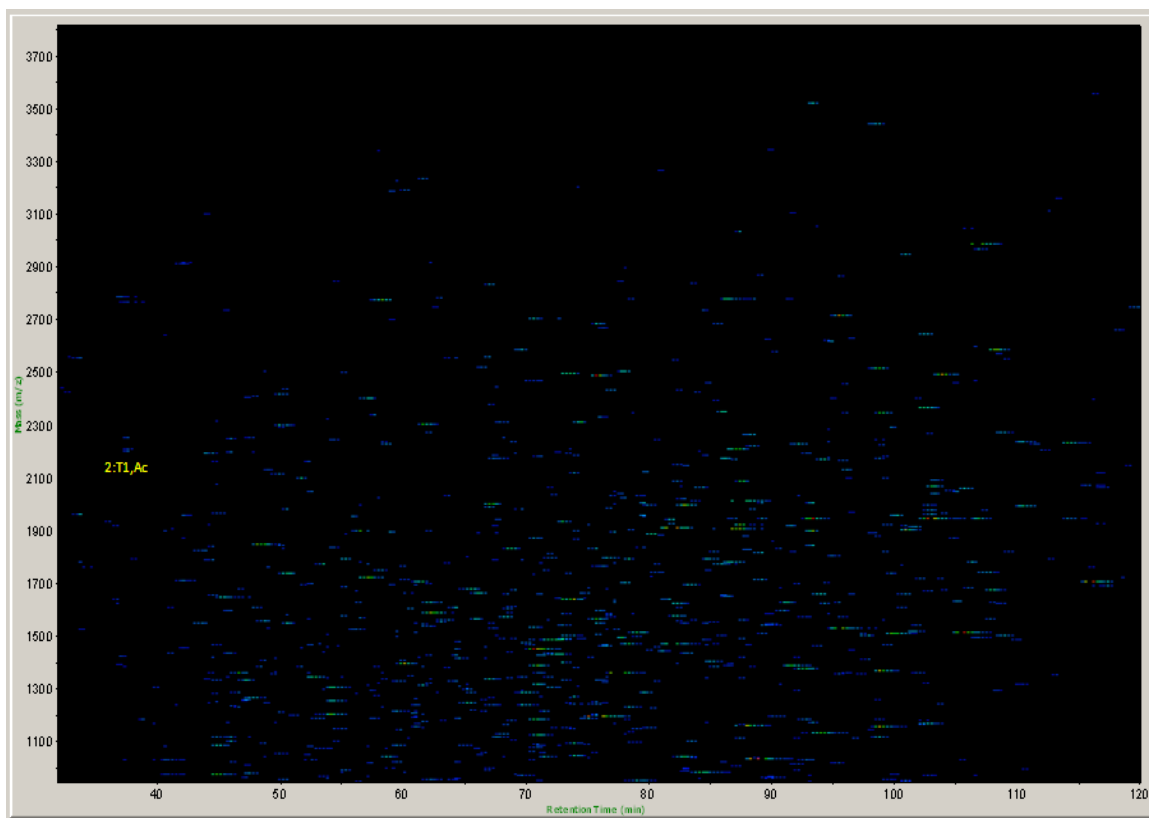


Figure 4. 1D LC-MS heat map of control RWPE-1 tryptic peptides.

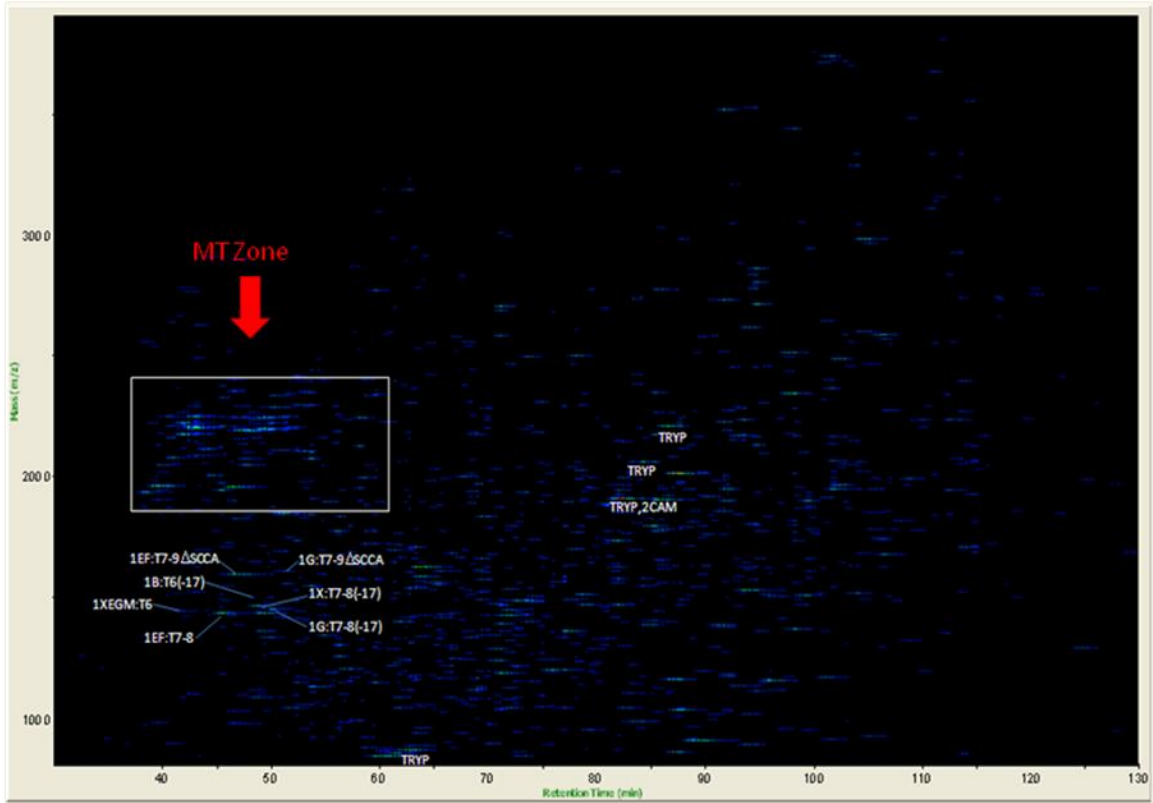


Figure 5. 1D LC-MS heat map of Zn-induced RWPE-1 tryptic peptides.

Table 2. Tryptic peptides identified for each MT isoform.

Tryptic Peptides Identified for Each MT Isoform

MT-1X				
Observed Mass	Miss Cleavages	Peptide	Modifications	Heat Map Name
1445.5	0	(K) SCCSCCPVGCAR(C)	0	1XEGM: T6
1467.6	1	(K) CAQGCICKGTSDK(C)	Ammonia Loss(N-term C)	1X: T7-8(-17)
1874.7	2	(K) CAQGCICKGTSDKGTSDKSC(C)	Ammonia Loss(N-term C)	1X: T7-9, ΔCA(-17)
1958.7	0	(D) PNCSCSPVGSACAGSCK(C)	0	1X: T1, ΔMD
2105.7	2	(K) CAQGCICKGTSDKGTSDKSCCA	Ammonia Loss(N-term C)	1X: T7-9(-17)
2156.8	0	(-) MDPNCSCSPVGSACAGSCK(C)	Dethiomethyl(M)	1X: T1(-48)
2192.8	2	(K) CTSCRK KSCCS CCPVGCAR(C)	Ammonia Loss(N-term C)	1XEGM: 2: T4-6(-17)
2198.8	0	(-) MDPNCSCSPVGSACAGSCK(C)	Acetyl(Protein N-term); Dethiomethyl(M)	1X: T1, Ac(-48)
2204.8	0	(-) MDPNCSCSPVGSACAGSCK(C)	0	1X: T1
2209.8	2	(K) CTSCRK KSCCS CCPVGCAR(C)	0	1XEGM: 2: T4-6
2246.8	0	(-) MDPNCSCSPVGSACAGSCK(C)	Acetyl(Protein N-term)	1X: T1, Ac
MT-2A				
1962.7	0	(D) PNCSCAAGDSCTCAGSCK(C)	0	2: T1, ΔMD
2075.7	2	(K) CAQGCICKGASDK GASDKSCCA	Ammonia Loss(N-term C)	2: T7-9(-17)
2077.7	0	(M) DPNCSCAAGDSCTCAGSCK(C)	0	2: T1, ΔM
2160.7	0	(-) MDPNCSCAAGDSCTCAGSCK(C)	Dethiomethyl(M)	2T1(-48)
2192.8	2	(K) CTSCRK KSCCS CCPVGCAR(C)	Ammonia Loss(N-term C)	1XEGM: 2: T4-6(-17)
2202.8	0	(-) MDPNCSCAAGDSCTCAGSCK(C)	Acetyl(Protein N-term); Dethiomethyl(M)	2: T1, Ac(-48)
2209.8	2	(K) CTSCRK KSCCS CCPVGCAR(C)	0	1XEGM: 2: T4-6
2250.7	0	(-) MDPNCSCAAGDSCTCAGSCK(C)	Acetyl(Protein N-term)	2: T1, Ac
MT-1E				
1437.6	1	(K) CAQGCVCKGASEK(C)	Ammonia Loss(N-term C)	1EF: T7-8
1445.5	0	(K) SCCSCCPVGCAR(C)	0	1XEGM: T6
1597.6	2	(K) CAQGCVCKGASEK(S)	Ammonia Loss(N-term C)	1EF: T7-9ΔSCCA
1934.7	0	(D) PNCSCATGGSCCTCAGSCK(C)	0	1E: T1, ΔMD
2049.7	0	(M) DPNCSCATGGSCCTCAGSCK(C)	0	1E: T1, ΔM
2174.8	0	(-) MDPNCSCATGGSCCTCAGSCK(C)	Acetyl(Protein N-term); Dethiomethyl(M)	1E: T1, Ac(-48)
2180.7	0	(-) MDPNCSCATGGSCCTCAGSCK(C)	0	1E: T1
2192.8	2	(K) CTSCRK KSCCS CCPVGCAR(C)	Ammonia Loss(N-term C)	1XEGM: 2: T4-6(-17)
2209.8	2	(K) CTSCRK KSCCS CCPVGCAR(C)	0	1XEGM: 2: T4-6
2222.8	0	(-) MDPNCSCATGGSCCTCAGSCK(C)	Acetyl(Protein N-term)	1E: T1, AC

Table 2 Cont.

MT-1G1				
1445.5	0	(K) SCCSCCPVGCAK (C)	0	1XEGM: T6
1451.6	1	(K) CAQGCIKGA SEK (C)	Ammonia Loss (N-term C)	1G: T7-8 (-17)
1611.6	2	(K) CAQGCIKGA SEK (S)	Ammonia Loss (N-term C)	1G: T7-9ASCCA
2047.7	0	(D) PNCSCAAGV SCTCASSCK (C)	0	1G1: T1, AMD
2162.8	0	(M) DPNCSCAAGV SCTCASSCK (C)	0	1G1: T1, AM
2192.8	2	(K) CTSCRK KSCCS CCPVGCAK (C)	Ammonia Loss (N-term C)	1XEGM: 2: T4-6 (-17)
2209.8	2	(K) CTSCRK KSCCS CCPVGCAK (C)	0	1XEGM: 2: T4-6
2287.8	0	(-) MDPNCSCAAGV SCTCASSCK (C)	Acetyl (Protein N-term); Dethiomethyl (M)	1G1: T1, Ac (-48)
		(-) MDPNCSCAAGV SCTCASSCK (C)	Acetyl (Protein N-term)	1G1: T1, Ac
MT-1F				
1437.6	1	(K) CAQGCVC KGA SEK (C)	Ammonia Loss (N-term C)	1EF: T7-8
1597.6	2	(K) CAQGCVC KGA SEK (S)	Ammonia Loss (N-term C)	1EF: T7-9ASCCA
1946.7	0	(D) PNCSCAAGV SCTCAGSCK (C)	0	1F: T1, AMD
2234.8	0	(-) MDPNCSCAAGV SCTCAGSCK (C)	Acetyl (Protein N-term)	1F: T1, Ac
MT-1M				
1445.5	0	(K) SCCSCCPVGCAK (C)	0	1XEGM: T6
1895.7	1	(K) CAHGCVC KGTLENCSC (C)	Ammonia Loss (N-term C)	1M: T7-8, ΔCA (-17)
2006.7	0	(D) PNCSCCTGV SCACTG SCK (C)	0	1M: T1, AMD
2126.8	1	(K) CAHGCVC KGTLENCSC (-)	Ammonia Loss (N-term C)	1M: T7-8 (-17)
2192.8	2	(K) CTSCRK KSCCS CCPVGCAK (C)	Ammonia Loss (N-term C)	1XEGM: 2: T4-6 (-17)
2209.8	2	(K) CTSCRK KSCCS CCPVGCAK (C)	0	1XEGM: 2: T4-6
2246.0	0	(M) DPNCSCCTGV SCACTG SCK (C)	Acetyl (Protein N-term); Dethiomethyl (M)	1M: T1, Ac (-48)
2294.8	0	(M) DPNCSCCTGV SCACTG SCK (C)	Acetyl (Protein N-term)	1M: T1, AC
MT-1G2				
1445.5	0	(K) SCCSCCPVGCAK (C)	0	1XEGM: T6
1451.6	1	(K) CAQGCIKGA SEK (C)	Ammonia Loss (N-term C)	1G: T7-8 (-17)
1611.6	2	(K) CAQGCIKGA SEK (S)	Ammonia Loss (N-term C)	1G: T7-9ASCCA
1976.7	0	(D) PNCSCAAGV SCTCASSCK (C)	0	1G2: T1, AMD
2192.8	2	(K) CTSCRK KSCCS CCPVGCAK (C)	Ammonia Loss (N-term C)	1XEGM: 2: T4-6 (-17)
2209.8	2	(K) CTSCRK KSCCS CCPVGCAK (C)	0	1XEGM: 2: T4-6
2264.8	0	(M) DPNCSCAAGV SCTCASSCK (C)	Acetyl (Protein N-term)	1G2: T1, AC

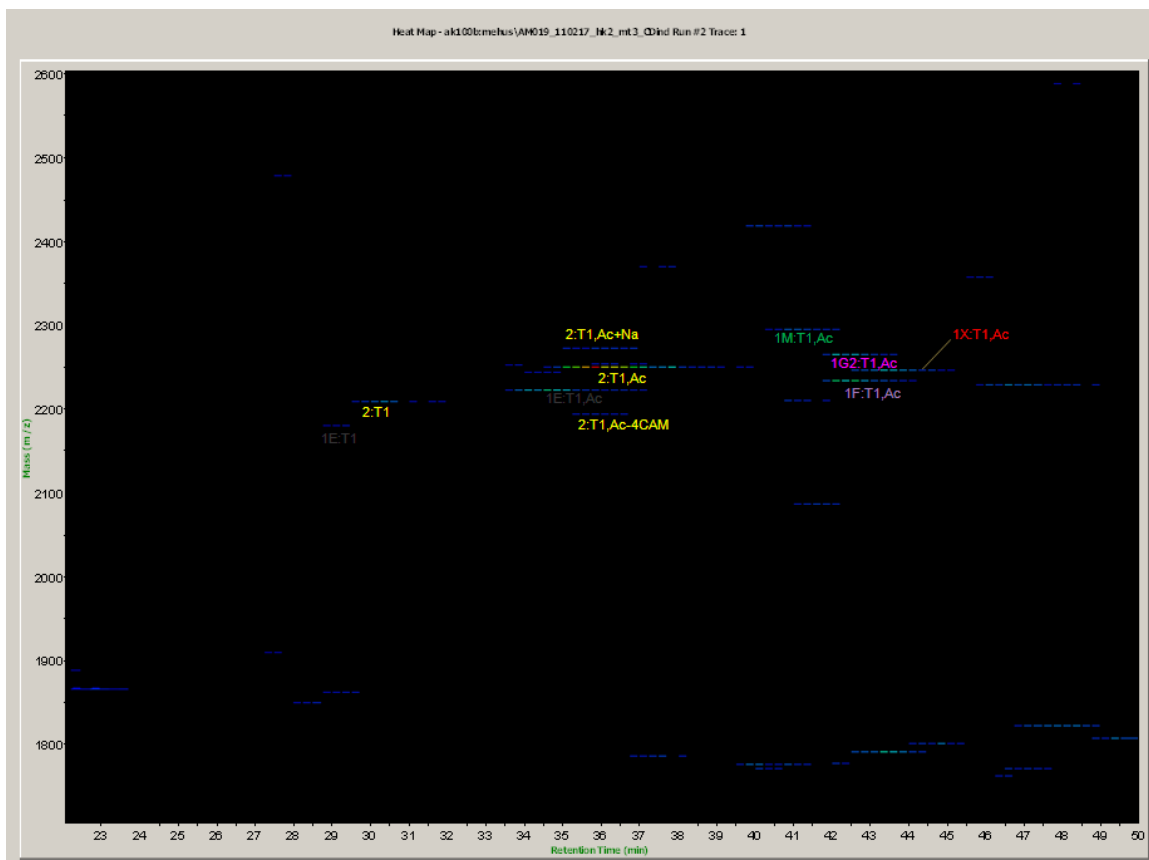


Figure 7. 1D LC-MS heat map of “MT zone” after optimization of sample preparation.

To resolve the unwanted modifications the entire sample preparation procedure had to be revised and optimized. This required many experiments to optimize every step which required changes in pH, reagents, concentrations, temperatures, and incubation times. The 95 °C heat depletion step was a very efficient way to enrich the MT peptides but it was probably the biggest catalyst of the unwanted modifications. After removing this step from the preparations, most of the unwanted modifications disappeared. The optimized MT sample preparation and gradient conditions used for the remainder of this project is listed in the methods section. Figure 7 displays a LC-MS heat map from a Zn-induced sample after optimization showing the MTs in mostly one form without the additional modifications. After optimization, only three MT isoforms in the control cells could be identified, MT-2, 1E, and 1X (data not shown).

N-terminal modifications of endogenous MTs

Almost all N-terminal peptides from endogenous MTs were N-acetylated. A small amount of unacetylated MT2 (10% or less of total MT2 signal; not shown) was routinely detected in Cd-induced HK-2 cytosol. A trace amount of unacetylated MT1E was observed once, but not for any of the other MTs. In addition to acetylation, early experiments showed some truncations of the N-termini – most notably the loss of the acetyl-Met-Asp dipeptide (Table 2). Refinement of the isolation and enrichment strategy greatly reduced the relative intensities of these truncated precursors, suggesting that they may have been artifacts of sample preparation. The acetyl-Met-Asp dipeptide of mammalian MTs precedes a proline residue. The Asp-Pro bond in general⁷⁸ and that of mammalian MTs in particular^{42, 41} are acid labile. This

susceptibility to cleavage may explain in part why multiple N-terminal MT truncations are observed in the PeptideAtlas database^{56, 57}. As much as 40% of the total ion signal for a given N-terminal MT peptide was in the Methionine sulfoxide form. This is considered a high degree of oxidation based on a recent quantitative proteomic study of intracellular methionine oxidation in human Jurkat cells⁷⁹. As described earlier, the COFRADIC approach does not capture N-terminal MT peptides. Even so, the acetyl-Met-Asp-Pro sequence of MT N-termini would classify it as highly susceptible to oxidation based on sequence preferences revealed by this study. The susceptibility of these peptides to oxidation was reinforced by the observation that addition of synthetic MT peptides to cytosol caused them to achieve a similar degree of oxidation as the cognate peptides from endogenous MTs. This oxidation appeared to occur before the chromatography steps. Further experiments are needed to determine if methionine oxidation of MTs occurs intracellularly or if it is a sample handling artifact. For purposes of quantitation, it was important to control for the potential variability of methionine oxidation in MTs. Reduction with dimethyl sulfide^{80, 76} quantitatively reverted methionine sulfoxides to methionine, collapsing the MT zone into single dominant precursors for each isoform.

Identification of endogenous N-terminal MT peptides in HK-2 MT-3 cells

The next step of this project was to characterize a cell line (HK-2 MT-3) that was expressing the MT-3 isoform. Optimized one-dimensional reversed-phase chromatography followed by mass spectrometry was sufficient to identify seven MT isoforms in Cd-induced HK-2 human kidney epithelial cell cytosol (Table 3) and

Table 3. Unique N-terminal Acetylated Tryptic MT Peptides Detected in HK-2 MT-3 Cells.

Isoform	Sequence	Modifications Identified by Mascot	<i>m/z</i> +1H (¹⁴N-C) (¹⁵N-C)	Ret. (min.)
MT-1E	MDPNCSCATGGSC TCAGSCK	Acetylation (protein N-term), 5 Carbamidomethylations (¹⁴ N- or ¹⁵ N-C)	2222.8 2227.8	36.9
MT-1F	MDPNCSCAAGV SCTCAGSCK	Acetylation (protein N-term), 5 Carbamidomethylations (¹⁴ N- or ¹⁵ N-C)	2234.8 2239.8	46.9
MT-1G2	MDPNCSCAAGV SCTCASSCK	Acetylation (protein N-term), 5 Carbamidomethylations (¹⁴ N- or ¹⁵ N-C)	2264.8 2269.8	47.2
MT-1M	MDPNC SCTTGVSCACTGSCK	Acetylation (protein N-term), 5 Carbamidomethylations (¹⁴ N- or ¹⁵ N-C)	2294.8 2299.8	45.6
MT-1X	MDPNC SCSPVGSCACAGSCK	Acetylation (protein N-term), 5 Carbamidomethylations (¹⁴ N- or ¹⁵ N-C)	2246.8 2251.8	48.4
MT-2	MDPNC SCAAGDSCTCAGSCK	Acetylation (protein N-term), 5 Carbamidomethylations (¹⁴ N- or ¹⁵ N-C)	2250.7 2255.8	38.5
MT-3	MDPET CPPSGGSCTCADSCK	Acetylation (protein N-term), 5 Carbamidomethylations (¹⁴ N- or ¹⁵ N-C)	2418.8 2423.8	45.1

The five conserved cysteine residues are highlighted in red and the N-terminal methionine (acetylated) residues are highlighted in blue. The masses are listed for the fully alkylated ¹⁴N and ¹⁵N peptides along with elution times.

(Appendix B). Only three isoforms could be detected in cytosol from uninduced cells and their signals were very weak (Figure 8). A second chromatography step was needed to reduce sample complexity and get better sampling depth. Strong cation exchange (SCX) chromatography effectively separated the MT peptides, which eluted early in the gradient away from the bulk of tryptic peptides (Figure 9). This result was consistent with the general SCX fractionation pattern of N-terminally acetylated peptides⁷⁷. The two-dimensional separation of uninduced HK-2 samples increased the sensitivity sufficiently to detect all of the MTs found in the Cd-induced sample except MT-1M (Figure 10). Increasing the starting amount of cytosol from 300 ug to 800 ug did not produce additional detections of N-terminal MT peptides (data not shown).

Validation of ¹⁴N and ¹⁵N iodoacetamide for quantitation of N-terminal MT peptides

The enhanced sensitivity gained with two-dimensional LC and the simplification of precursor ion complexity with dimethyl sulfide treatment set the stage for quantitative profiling of MT isoforms. We selected ¹⁵N-iodoacetamide as a stable isotope labeled compound because it is commercially available, gives a cumulative mass shift of 5 Da for N-terminal MT peptides, and is well-characterized for its cysteine-specific reactivity in peptides. To our knowledge this reagent has not been used in typical stable isotope labeling experiments probably because a single Dalton mass shift would complicate quantitation due to the high degree of isotopic envelope overlap.

The commercially available ¹³C₂-iodoacetic acid was also tested. This compound gave a cumulative mass shift and no isotope effects were observed (not shown). The increased hydrophilicity introduced by the carboxylates weakened their retention

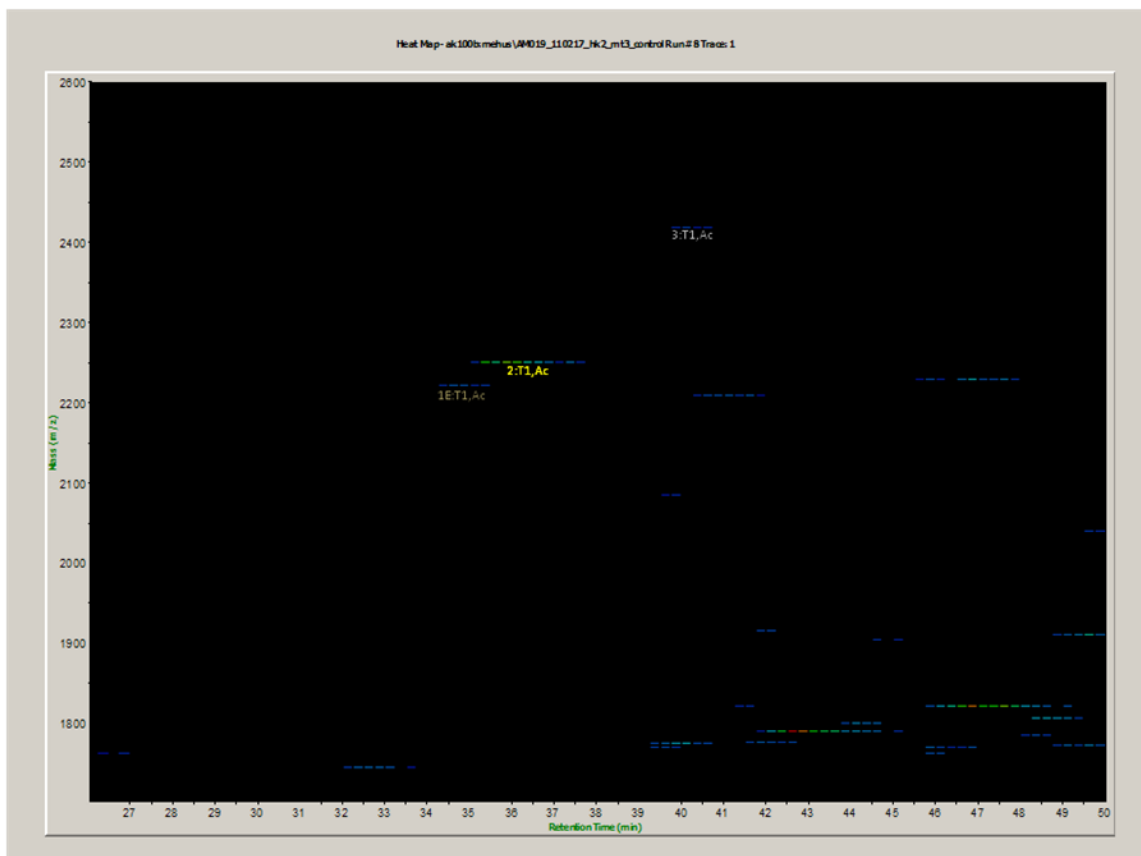


Figure 8. 1D LC-MS heat map of “MT zone” in control HK-2 MT-3 cells.

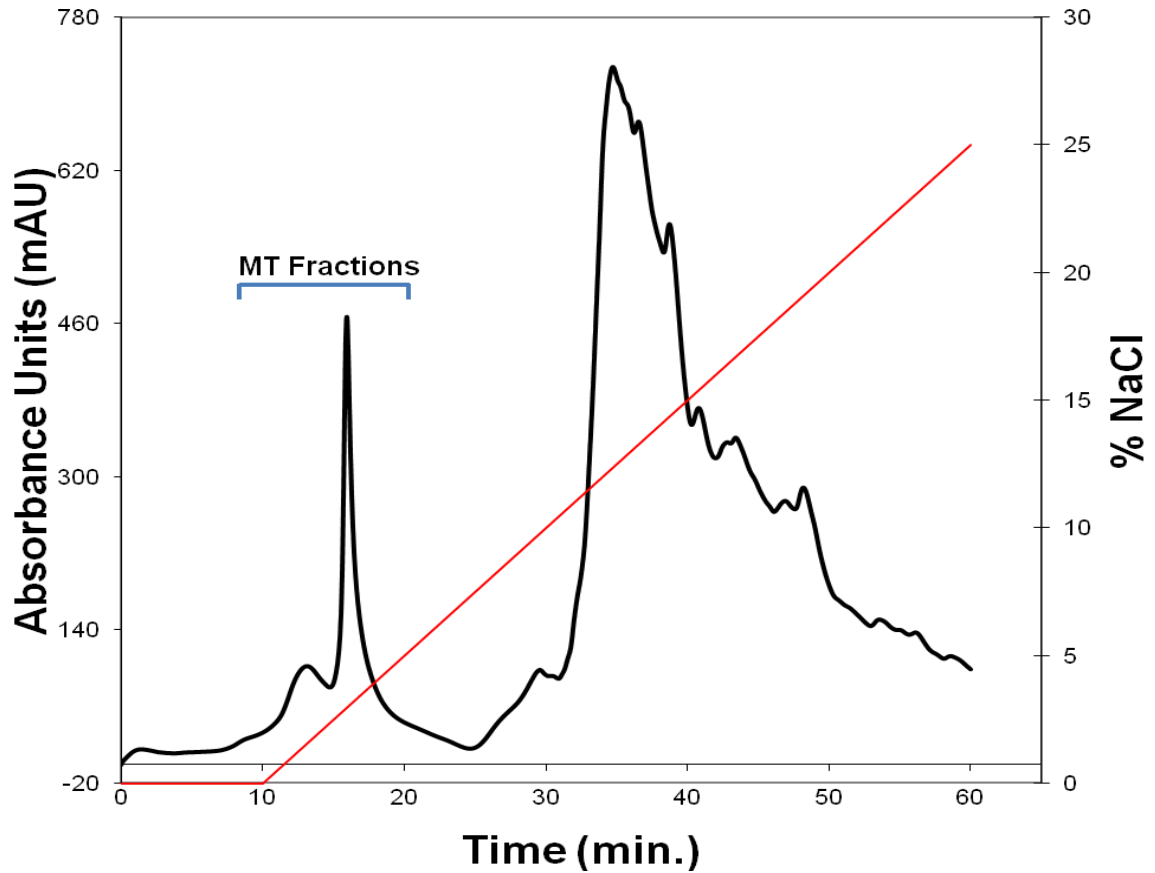


Figure 9. Strong cation exchange chromatography profile. Optimized strong cation exchange (SCX) chromatography of tryptic digested cytosolic lysate with ~100 pmol/isoform pure acetylated N-term MT peptide standards added. Fractions two and three (7-21 mins.) contain the acetylated N-term tryptic MT peptides along with other non-MT 0 and +1 charged peptides. The red line indicates NaCl gradient. The black line indicates 214 nm absorbance of the tryptic peptides. The acetylated N-term MT peptides elute with ~20-25 mM NaCl.

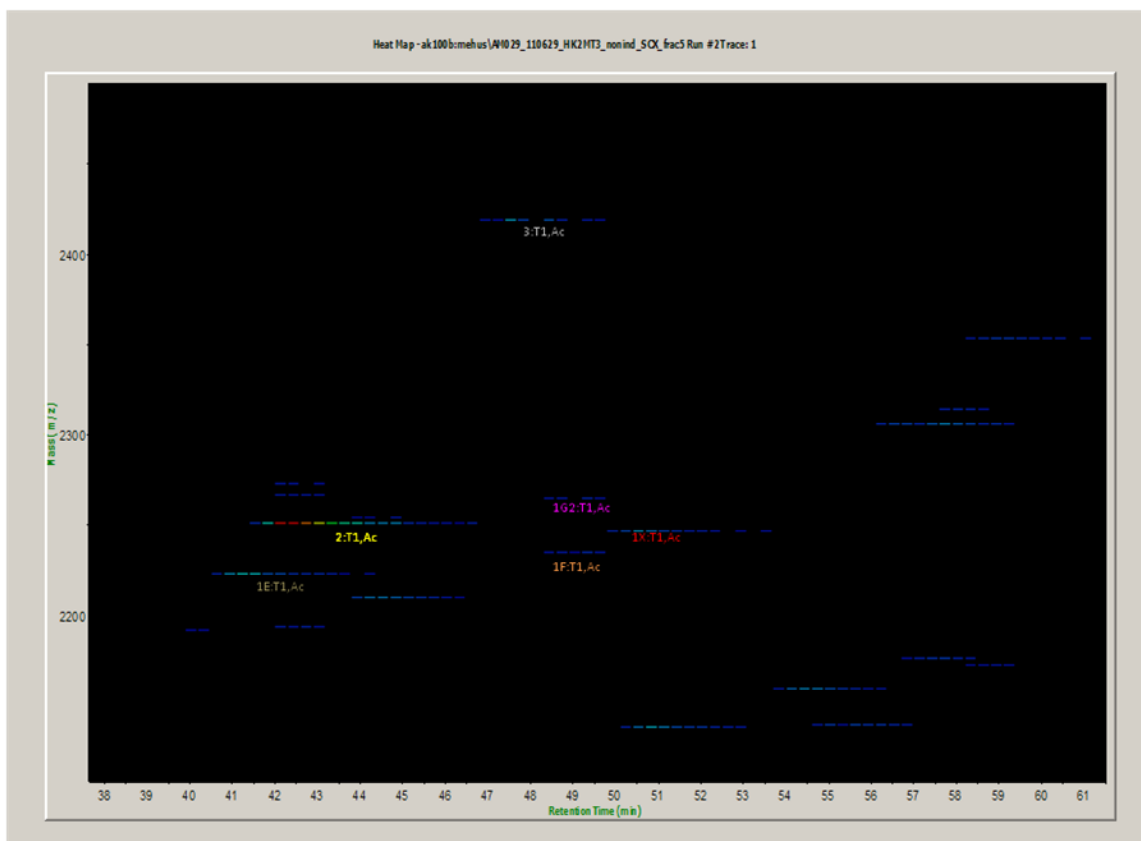


Figure 10. 2D LC-MS heat map of “MT zone” in control HK-2 MT-3 cells.

during reversed phase chromatography sufficiently to compromise reproducible quantitation. 300 µgs of cytosol from the Cd-induced HK-2 cells were alkylated with ¹⁴N-iodoacetamide (light) and 300 µgs of the same cytosol was alkylated with ¹⁵N-iodoacetamide (heavy), respectively. Equal amounts of alkylated samples were mixed and proteins were digested with trypsin. The N-terminal MT peptides were enriched as described in Methods and analyzed by MALDI-TOF/TOF MS. Figure 11 illustrates the isotopic envelopes for the light and heavy labeled N-terminal acetylated tryptic peptides of MT-2 precursor ions. As expected, a 5 Da shift between the light (*m/z* 2250.7) and heavy (*m/z* 2255.7) monoisotopic peaks was observed. The monoisotopic peak intensities for the light and heavy precursors were plotted after correcting for isotopic overlap and purity of the ¹⁵N label (Figure 12). The 1:1 ratio of light to heavy monoisotopic peak intensities across the entire MT-2 peak indicates that there is no isotope effect on the chromatographic behavior of the light and heavy-labeled MT peptides. This reproducibility was maintained for all observed N-terminal MT peptides (Figure 13). The sensitivity and dynamic range of the relative quantitation assay was determined next. A serial dilution of light cytosol was mixed with a constant amount of heavy cytosol and the samples were digested, fractionated and analyzed as before. A 1:1 correlation was observed for experimental vs. theoretical light/heavy MT2 ratio over two orders of magnitude (Figure 14). The signal to noise ratio for these samples ranged from 3.24 to 109.33. The signal-to-noise ratio of the weakest observed endogenous N-terminal MT peptide was 3.24 for MT-1G2.

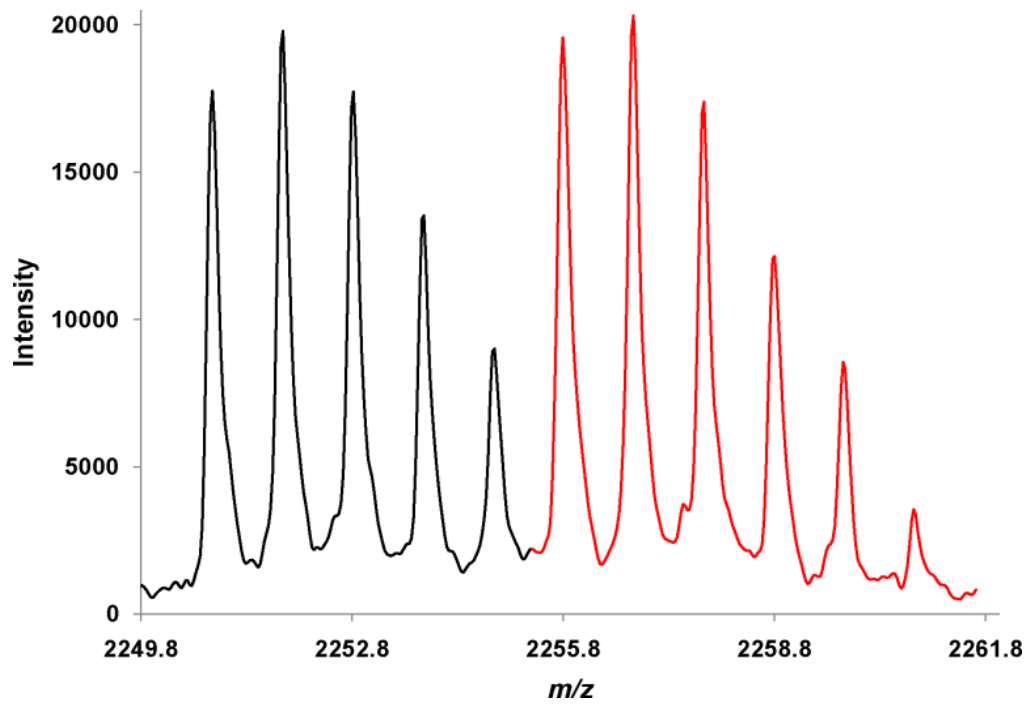


Figure 11. MS spectra of ¹⁴N and ¹⁵N labeled N-term acetylated MT-2 peptide in HK-2 MT-3 cytosol. The isotopic envelop of the light-labeled peptide is outlined in black while the isotopic envelop of the heavy-labeled peptide is outlined in red.

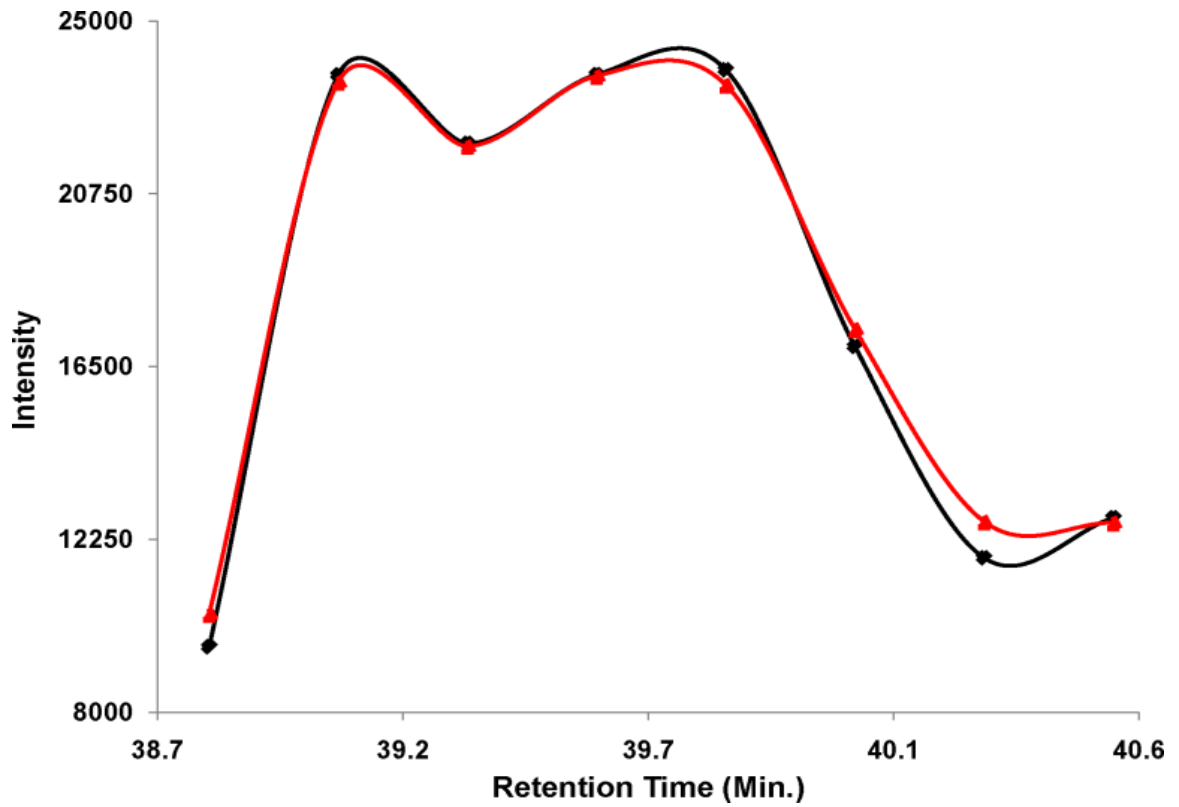


Figure 12. Retention time vs. monoisotopic peak intensity of N-term acetylated MT-2 peptide in HK-2 MT-3 cytosol. The black points represent data from the light-labeled peptide while the red points represent data from the heavy-labeled peptide after de-isotoping spectra.

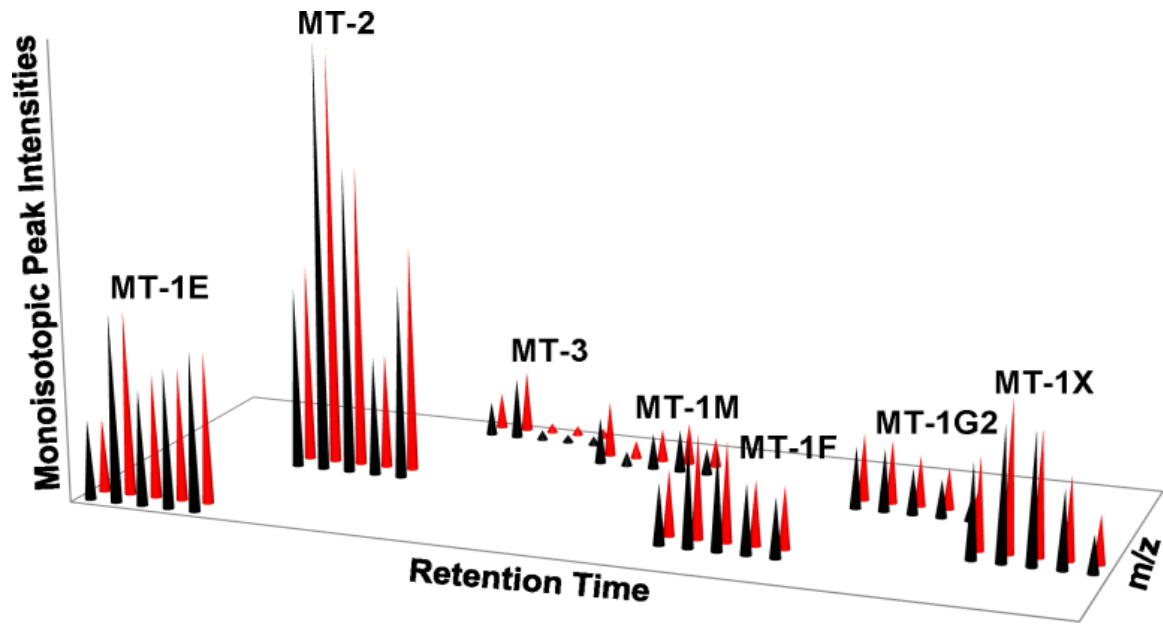


Figure 13. 3D nano-rpHPLC-MS heat map of the MT zone showing the 1:1 ($^{14}\text{N}:$ ^{15}N) labeling MT peptides in HK-2 MT-3 cytosol. The black cones represent data from the light-labeled peptide while the red cones represent data from the heavy-labeled peptide.

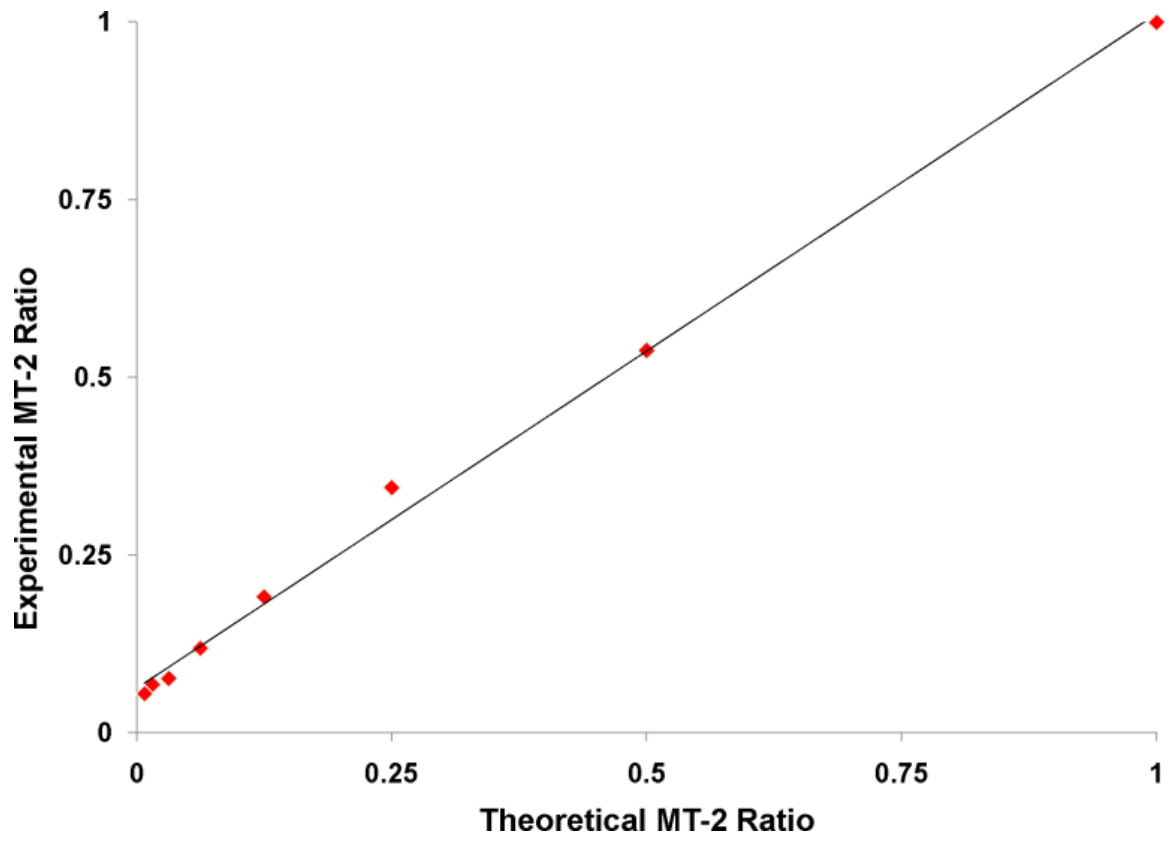


Figure 14. Sensitivity and dynamic range of MT-2 relative quantitation.

Cd-induction of MT isoforms in HK-2 MT-3 cells: Relative quantitation

In order to determine the fold induction of individual MT isoforms in response to Cd treatment, equal volumes of HK-2 cytosol from control (light) and Cd-induced (heavy) cells were mixed, trypsin-digested, fractionated and analyzed as above. Figure 15 is a representative three-dimensional LC-MS heat map of the MT zone. The fold induction were calculated for six MT isoforms (Figure 16). A value could not be calculated for MT-1M since it was not detected in control cells. The range of inductions for MT1/2 isoforms was 1.7 to 12-fold with MT-1F showing the highest induction. The MT-3 isoform, under the control of the non-metal-responsive CMV promoter, was induced 1.70-fold. Figure 17 displays the fold inductions (ratio of heavy/light) compared to the average monoisotopic peak intensities of the six MT isoforms measured by the relative assay. In proteomics, relative abundance of proteins or peptides is commonly estimated (sometimes inaccurately) by the relative peak intensities (assuming equal ionization of each MT peptide). Assuming that all the diagnostic N-term acetylated MT peptides ionize similarly, Figure 17 demonstrates that MT-2 was the most abundant peptide in both the control and Cd-induced cells and that MT-1G2 was the least abundant in both these cells. According to peak intensities, MT-1F showed equal abundance to MT-1G2 in the control cells but was the 4th most abundant peptide in the Cd-induced cells, which accounted for the 12-fold induction of this isoform.

Synthetic N-terminal acetylated MT peptides for absolute MT quantitation

Table 4 (Appendix C) displays all the acetylated N-terminal tryptic peptides for human MT isoforms that were commercially synthesized, ¹⁵N-labeled, and purified

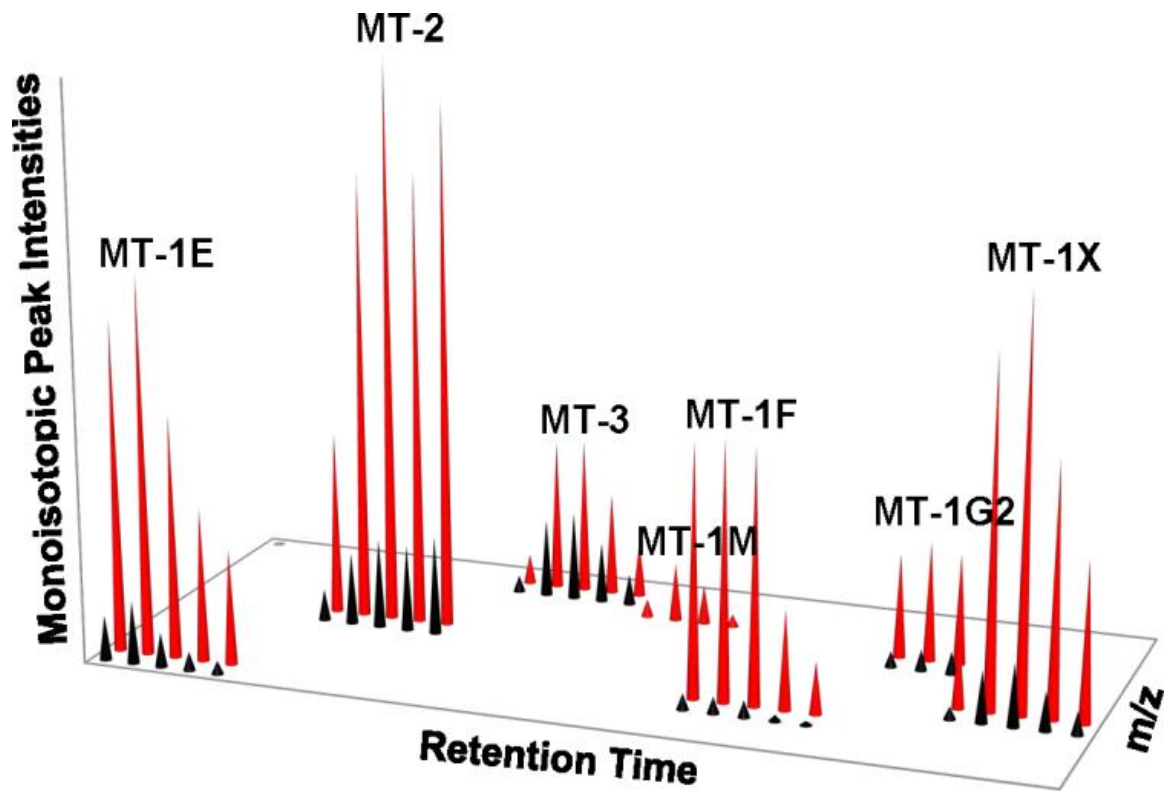


Figure 15. 3D nano-rpHPLC-MS heat map of MT zone in control (¹⁴N) vs. Cd-induced (¹⁵N) HK-2 MT-3 cytosol. The black cones represent data from the control and the red cones represent data from the Cd-induced acetylated N-terminal tryptic peptides in HK-2 MT-3 cells.

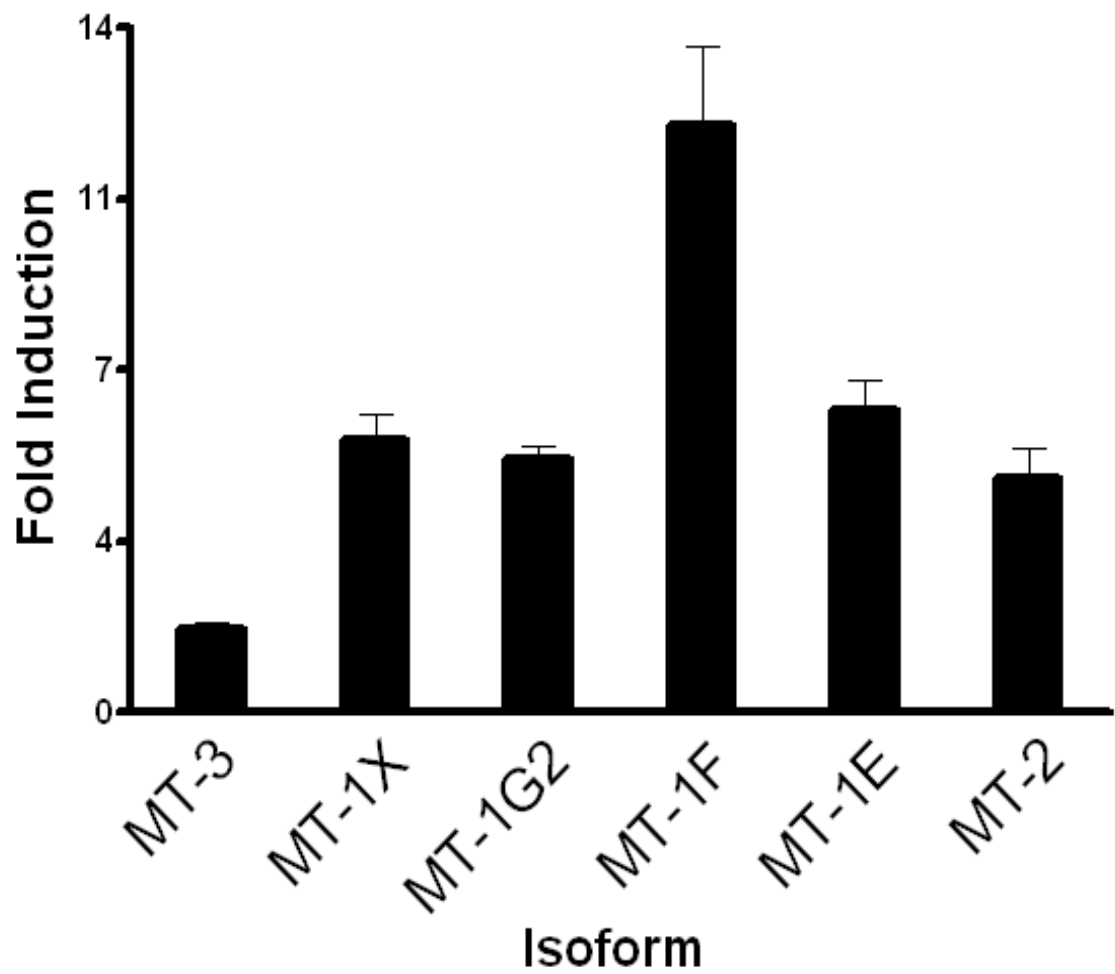


Figure 16. Relative quantitation of MTs in HK-2 MT-3 cells exposed to 9 μ M Cd for 3 days. Errors bars represent mean \pm S.D. where n=3.

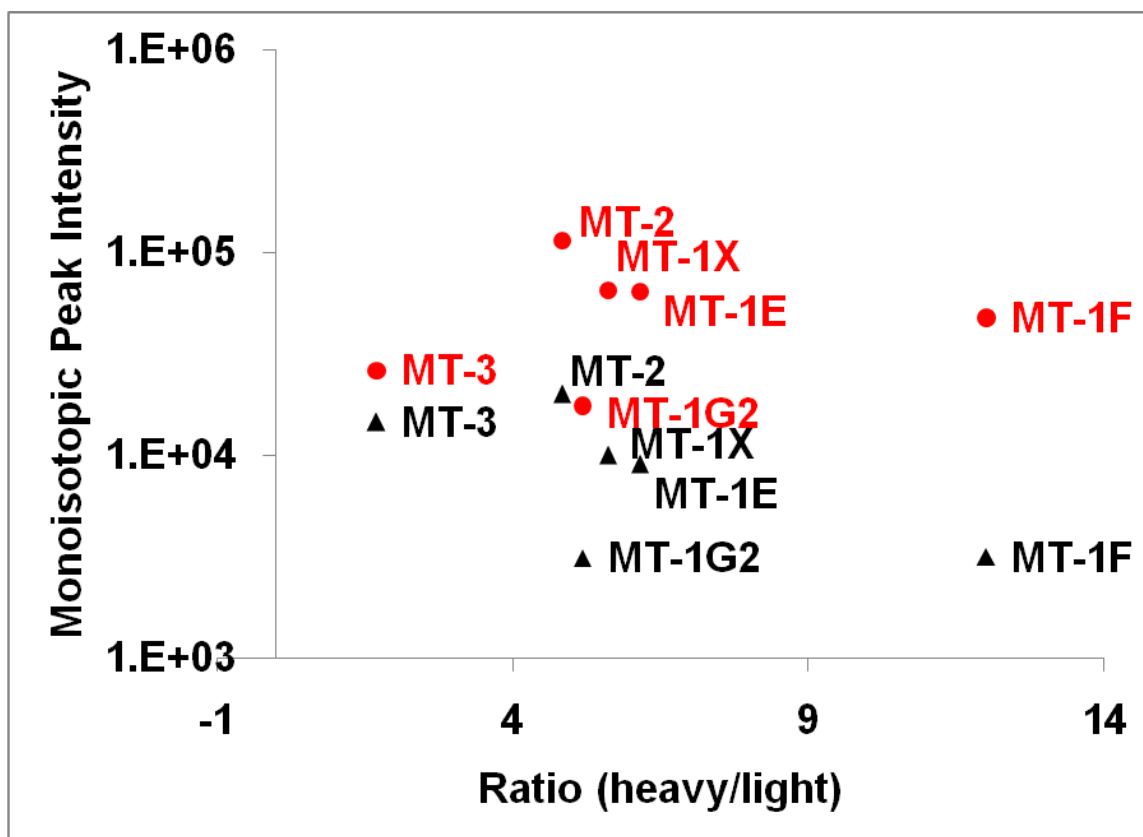


Figure 17. Ratios (heavy/light) vs. monoisotopic peak intensities for MTs in control (black) and Cd-induced (red) HK-2 MT-3 cells.

Table 4. All endogenous and synthetic human N-terminal tryptic MT peptides. **m/z* includes N-terminal acetylation and five ¹⁴N carbamidomethyl modifications of the Cys residues. The ¹⁵N carbamidomethylated peptides have a *m/z* 5 Da greater than the *m/z* shown. *ppm errors were consistently less than 50 for all MT isoforms in experimental runs. N-terminal tryptic MT peptides account for 30-36% sequence coverage across all isoforms. `MT-1G1 was not successfully synthesized but was endogenously detected in alternative cells and tissues.

Acc. #	MT Isoform	Sequence	Expected <i>m/z</i> *	Retention Time (min.)
P04731	MT-1A	MDPNCSCATGGCTCTGSCK	2252.8	36.5
P07438	MT-1B	MDPNCSCCTGGSCACAGSCK	2222.8	36.5
P04732	MT-1E	MDPNCSCATGGCTCAGSCK	2222.8	37.0
P04733	MT-1F	MDPNCSCAAGVSCTCAGSCK	2234.8	46.9
P13640	`MT-1G1	MDPNCSCAAAGVSCTCASSCK	2335.9	48.2
P13640-2	MT-1G2	MDPNCSCAAGVSCTCASSCK	2264.8	47.2
P80294	MT-1H	MDPNCSCAAGVSCTCAGSCK	2220.8	38.3
Q93083	MT-1L	MDPNCSCATGGSCSCASSCK	2238.8	35.8
Q8N339	MT-1M	MDPNCSCCTGGVSCACTGSCK	2294.8	45.8
P80297	MT-1X	MDPNCSCSPVGSACAGSCK	2246.8	48.4
P02795	MT-2	MDPNCSCAAGDSCTCAGSCK	2250.8	38.5
P25713	MT-3	MDPETCPCPSGGCTCADSCK	2418.8	45.1

for this study. Initially, the synthetic peptides were found to be of lower purity levels than what was requested (>95% purity) because the high cysteine level of these peptides made them very reactive. The company synthesized the peptides and ran elemental analysis of the peptides to determine the absolute amount of the peptides before shipping them. Table 5 lists the initial purity levels of the peptides that were ordered. After alkylating (¹⁵N-labeling) these peptides, the peptides of interest were able to be purified-out from the contaminating synthesis products. The identities of each ¹⁵N peptide were confirmed by MSMS (Appendix B) after re-purification. During the purification process the total abundance of the pure peptides recovered was estimated by area under the curve analysis (AUC) using 214 nm absorbance. After purification of all peptides, equal amounts of each isoform were mixed together then total MS ionizations were calculated for each (Table 5). The ionization intensities of these peptides were comparable when analyzed in this experiment but there was still a 2-3 fold difference for some of the peptides. So, equal amounts of the purified peptides were re-run on the same nano-rpHPLC gradient and AUC analysis was re-calculated once more. The re-calculated AUCs displayed similar 2-3 fold differences for the same isoforms that were seen in the total MS ionization experiment so a correction factor was calculated. The correction factor was the normalization of the individual MTs AUCs to that of MT-1X because this isoform had the greatest initial purity (90%) and likely represents the absolute concentration most closely. These ¹⁵N-labeled peptides would serve as absolute standards to quantify endogenous levels of the various MTs isoforms in cells and tissues.

Table 5. Initial purities and total ionizations of synthetic peptides.

<u>Isoform</u>	<u>Initial Purity (%)</u>	<u>Total Ionization</u>	<u>Normalized Ionization</u>
MT-3	73.32	265429.84	0.81
MT-1L	34.52	294155.78	0.90
MT-1X	90.28	325968.10	1.00
MT-1H	17.65	234696.60	0.72
MT-1E	44.86	273031.63	0.84
MT-1B	34.65	273031.63	0.84
MT-2	73.27	154424.32	0.47
MT-1M	25.69	126377.40	0.39
MT-1G2	10.15	138968.18	0.43
MT-1F	12.84	163048.02	0.50
MT-1A	11.01	110516.85	0.34

MT Isoform expression in HK-2 MT-3 Cells: Absolute protein quantitation

The ¹⁵N-labeled synthetic MT peptides described earlier were used as internal standards to determine the absolute amount of human MT isoforms in HK-2 MT-3 cells. A cocktail containing seven N-terminal MT peptides observed in HK-2 MT-3 cells was added to cytosols that had been alkylated with ¹⁴N-iodoacetamide. Figure 18 outlines the work flow for absolute quantitation. The spiked cytosols were then trypsin-digested and the N-terminal MT peptides were enriched and analyzed as above. Metallothionein isoforms were quantified for both control and Cd-induced cells (Figure 19, Table 6). Absolute abundance was expressed as ng intact MT isoform per µg of total protein. 300 µg total cytosolic protein was used for each experiment. This is equivalent to the cytosolic protein content of ~3.7 X 10⁶ cells. The protein expression for the seven detected MT isoforms ranged from 0.11 to 7.28 ng per µg total protein for MT-1F in the control and MT-2 in the Cd-induced cells respectively. The six MTs detected in the uninduced cells accounted for 0.33% of total protein whereas the seven MTs detected in Cd-induced cells accounted for 1.46% of the total cytosolic protein. The fold inductions of individual MT isoforms determined by the absolute method were comparable to those measured by the relative method (Figure 20, Table 7).

MT mRNA transcript levels in the HK-2 MT-3 Cells

The mRNA expression of human MT isoforms in HK-2 MT-3 cells was determined by a quantitative polymerase chain reaction assay (Figure 21, Table 8). The same MT isoforms were detected at the protein and mRNA levels with one exception. A low level of MT-1M mRNA, not seen at the protein level, was detected in uninduced cells. This

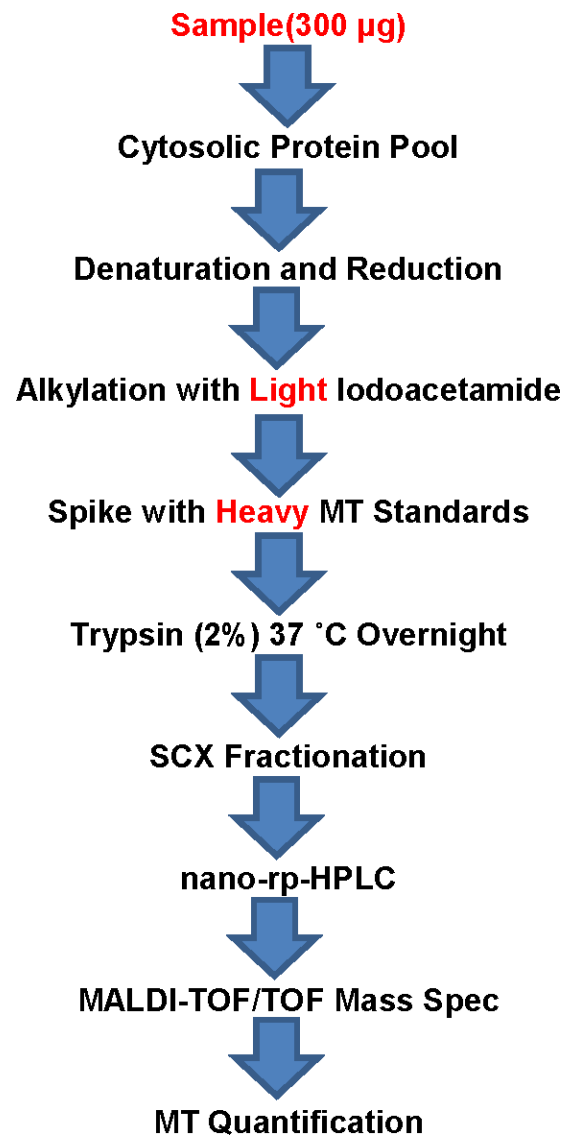


Figure 18. Work flow for absolute quantitation.

Table 6. Absolute quantitation values of MT proteins in HK-2 MT-3 cells. Δ (no detection). Values are average ng/ μ g \pm S.D. and represent three biological replicates. Fold inductions were calculated by comparing levels of each MT isoform from Cd-treated cells to that of the MT levels found in the control.

	Control	Cd-treated	Fold Induction
MT-1M	Δ	0.3757 \pm .1257	--
MT-3	0.6013 \pm .0431	1.0544 \pm .1550	1.8
MT-1X	0.3486 \pm .0639	1.6396 \pm .2841	4.7
MT-1G2	0.1513 \pm .0212	0.8253 \pm .1717	5.5
MT-1F	0.1083 \pm .0030	1.0742 \pm .1912	9.9
MT-1E	0.4150 \pm .0181	2.4364 \pm .1187	5.9
MT-2	1.6955 \pm .2169	7.2757 \pm .5457	4.3

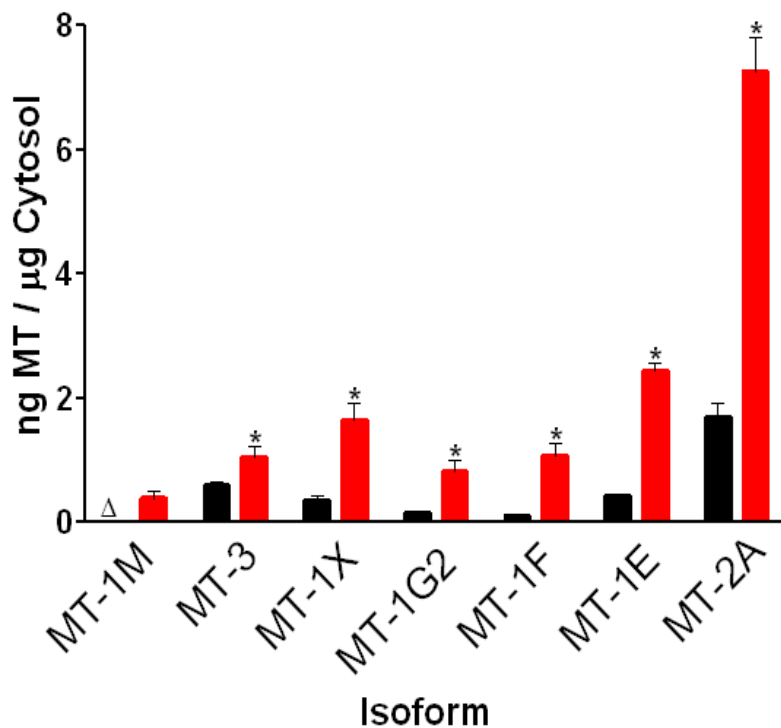


Figure 19. Absolute protein levels of the MT isoforms in HK-2 MT-3 cells. Protein data represents biological replicates where n=3. Error bars indicate the standard deviation around the mean. A two-way ANOVA followed with a Bonferroni posttest was run on all data sets. Significance was based on variation between control (black) and Cd-induced (red) levels for each isoform. * P < 0.01. Δ (no detection).

Table 7. Fold induction values for MT protein and mRNA. Fold inductions (protein and mRNA) from control to Cd-Induced HK-2 MT-3 cells were measured by relative and absolute methods. Values are average fold inductions \pm S.D. and represent three biological replicates.

Isoform	Protein		mRNA
	Absolute Fold Induction	Relative Fold Induction	Transcripts Fold Induction
MT-3	1.7 \pm 0.1	1.8 \pm 0.2	1.7 \pm 0.1
MT-1X	5.6 \pm 0.9	4.7 \pm 1.8	5.1 \pm 0.4
MT-1G2	5.2 \pm 0.5	5.4 \pm 1.3	4.9 \pm 0.6
MT-1F	12.0 \pm 2.8	9.9 \pm 1.9	3.1 \pm 0.3
MT-1E	6.2 \pm 1.1	5.9 \pm 0.5	3.0 \pm 0.4
MT-2	4.8 \pm 1.1	4.3 \pm 0.9	3.1 \pm 0.9

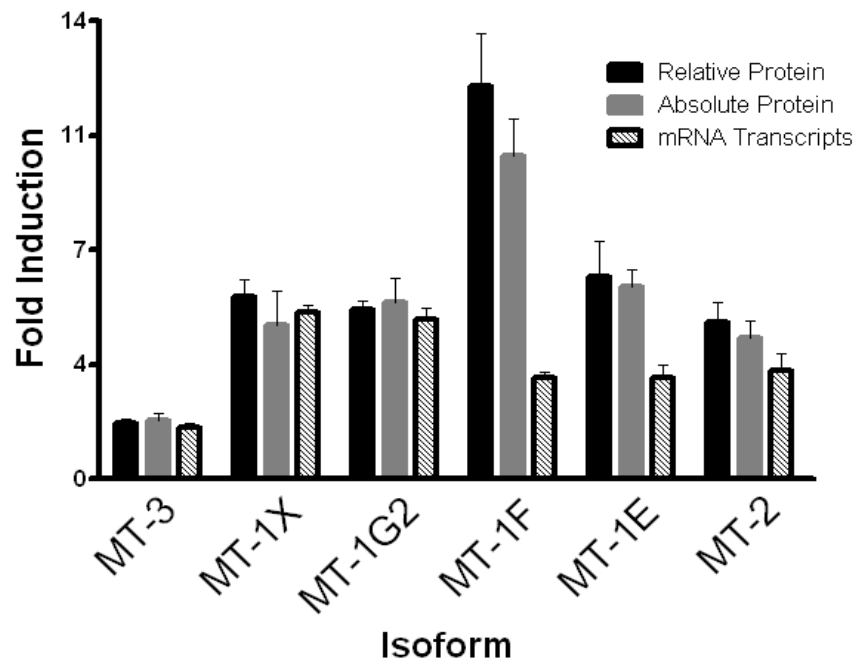


Figure 20. Fold induction comparison of MT isoform protein and mRNA.

Table 8. Absolute quantitation values of MT mRNA transcripts in HK-2 MT-3 cells. Values are average MT transcripts/1000 18S \pm S.D. and represent three biological replicates. Fold inductions were calculated by comparing levels of each MT isoform from Cd-treated cells to that of the MT levels found in the control.

	Control	Cd-treated	Fold Induction
MT-1M	0.0021 \pm .0006	0.0031 \pm .0001	1.5
MT-3	0.0013 \pm .0002	0.0022 \pm .0002	1.7
MT-1X	0.0069 \pm .0023	0.0351 \pm .0084	5.1
MT-1G2	0.0027 \pm .0003	0.0135 \pm .0008	4.9
MT-1F	0.0027 \pm .0004	0.0085 \pm .0021	3.1
MT-1E	0.1078 \pm .0259	0.3265 \pm .0572	3.0
MT-2	0.0352 \pm .0091	0.1090 \pm .0265	3.1

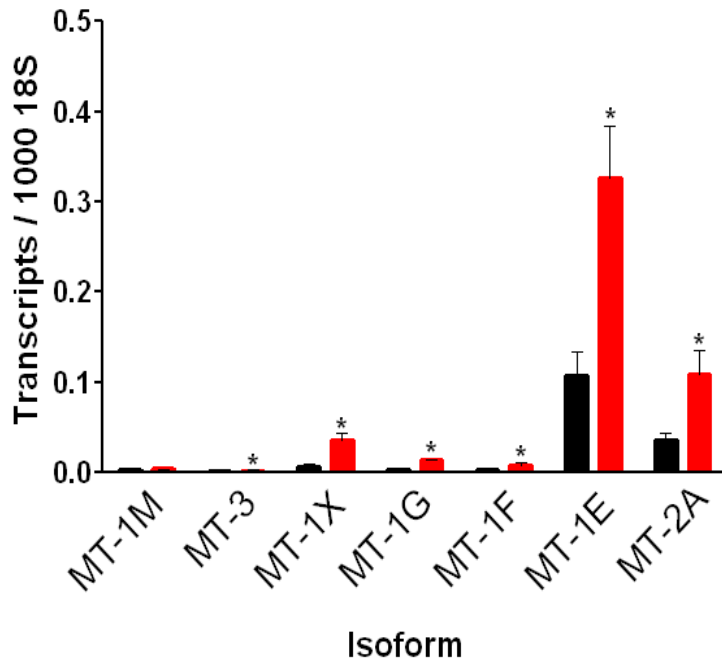


Figure 21. Absolute mRNA transcript levels of the MT isoforms in HK-2 MT-3 cells. Absolute mRNA transcripts were normalized to 18S. mRNA data represents biological replicates where n=3. Error bars indicate the standard deviation around the mean. A two-way ANOVA followed with a Bonferroni posttest was run on all data sets. Significance was based on variation between control (black) and Cd-induced (red) levels for each isoform. * P < 0.01. Δ (no detection).

level of concordance suggests that the mass spectrometry-based method has adequate sampling depth. The relative order of MT isoform abundance differs somewhat between mRNA and protein expression. For example, MT-1E mRNA is the most abundant whereas MT-2 protein levels are greatest. Technical limitations associated with quantification of peptide standards may be partly responsible for this difference, but other factors such as isoform-dependent differences in protein stability may also be in play. Cadmium-induced mRNA induction was comparable to that of protein for MT-1G2, MT-1X, MT-2 and MT-3, but induction of protein expression was greater than that of mRNA for MT-1E, and MT-1F (Figure 20, Table 7).

This suggests that MT isoforms may display differential post-translational stabilization upon metal induction. The influence of metal binding on MT stabilization and proteolytic susceptibility must be considered since it has been shown that MTs bound to Cd are significantly more protected from degradation and proteolytic cleavage⁸¹⁻⁸⁵. Half-life measurements of MT isoform mRNAs and proteins are needed to address this possibility. Lastly, the translational efficiencies of the individual MT isoforms are also something that needs consideration when comparing mRNA transcripts to protein levels.

Absolute protein quantitation of MT isoforms in human tissue

The next step of this study was to characterize MT levels in human tissue. Two different types of human tissue were used to achieve this: normal kidney cortex and normal brain cerebrum. The kidney tissue came from an elderly (~75 years old) patient's kidney that had been removed due to cancer. The actual tissue that was used in this study was

from a healthy part of the cortex of that kidney. It is known that cadmium ingested through diet accumulates in the kidney and keeps accumulating over the life-time of an individual. In a sense, it can be thought that this tissue represents what is happening in a low-level chronic exposure (decades) to cadmium compared to the HK-2 MT-3 cells exposed to a high-level acute exposure (3 days) which was previously explained.

Seven MT isoforms were detected in this tissue. Figure 22 and Table 9 display the absolute protein levels of MT isoforms in human kidney tissue. Interestingly, MT-1G1 was the most abundant isoform present in this tissue (1.6 ng/ μ g) while this isoform was completely absent in the HK-2 MT-3 cells but its sub-isoform, MT-1G2, which only differs from MT-1G1 by a deletion of one alanine, was present at low levels in the Cd-induced HK-2 MT-3 cells (0.8 ng/ μ g). MT-1F was the least abundant MT isoform in the kidney tissue (0.2 ng/ μ g). There is likely going to be some biological variation in the expression of MT isoforms from individual to individual and this data is only representative of one tissue but perhaps there is a potential role of the individual isoforms or sub-isoforms in relation to acute, chronic, high-dose, or low-dose exposures to cadmium. More tissue needs to be analyzed to confirm or reject this. The MT levels in normal human brain cerebrum were then analyzed. It is well published that MT-3 is highly expressed in human brain so this tissue was characterized as a positive control tissue for the MT-3 isoform (Figure 23 and Table 10). Six different MT isoforms were detected in this tissue. MT-3 displayed this highest level of protein (4.1 ng/ μ g) being 4-fold more abundant than the next highest abundant isoform, MT-2 (1.1 ng/ μ g). Again, MT-1F was the lowest abundant (0.1 ng/ μ g) followed by MT-1G1 (0.2 ng/ μ g). This

Table 9. Absolute quantitation values of MT proteins in human cortex kidney tissue. Values are average ng/ μ g \pm S.D. and represent three technical replicates.

MT-1F	0.1620 \pm 0.0099
MT-1H	0.3982 \pm 0.0835
MT-1E	0.3413 \pm 0.0140
MT-1X	0.5571 \pm 0.0152
MT-1G2	0.3709 \pm 0.0363
MT-2	0.4382 \pm 0.0195
MT-1G1	1.5888 \pm 0.1720

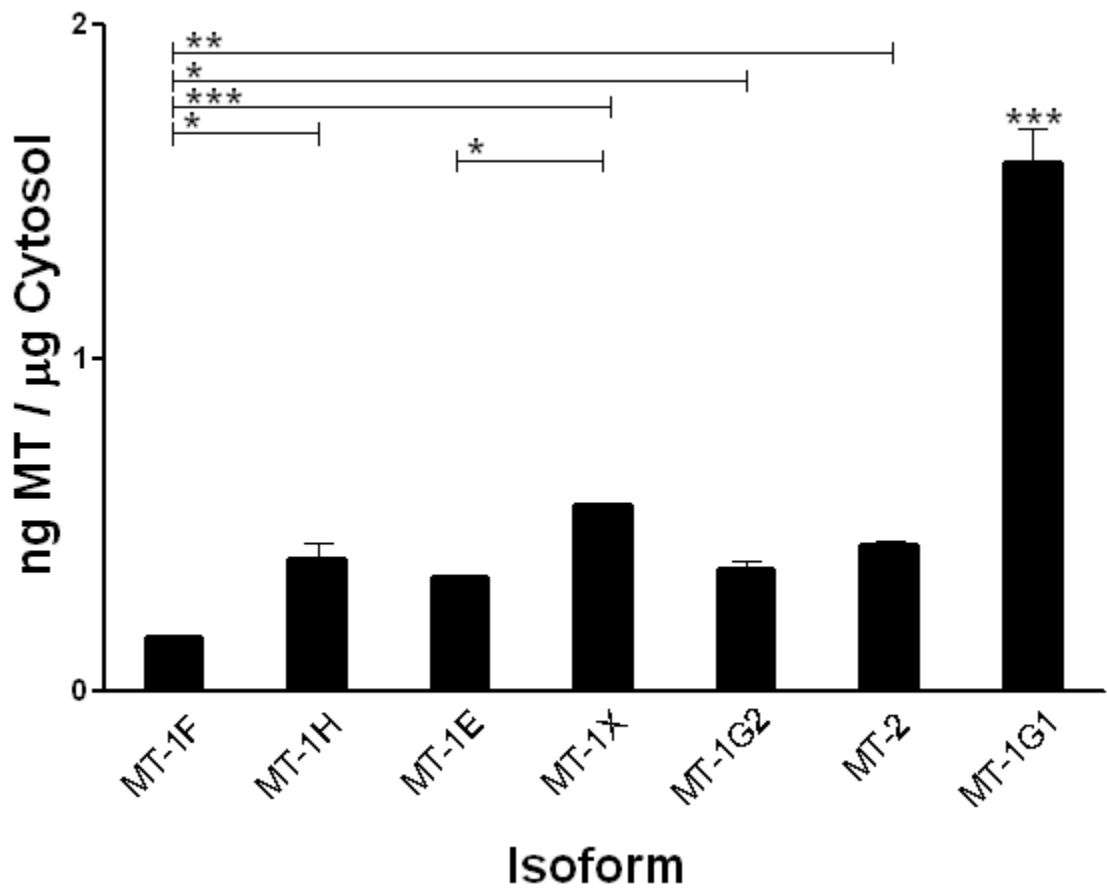


Figure 22. Absolute protein levels of the MT isoforms in human cortex kidney tissue. Protein data represents biological replicates where n=1. Error bars indicate the standard deviation around the mean from 3 independent technical replicates of 1 biological replicate. A One-way analysis of variation was run on all data sets. * P < 0.05, ** P < 0.01, and *** P < 0.001.

Table 10. Absolute quantitation values of MT proteins in human cerebrum brain tissues. Values are average ng/ μ g \pm S.D. and represent three technical replicates.

MT-3	4.1242 \pm 0.1065
MT-2	1.0820 \pm 0.0715
MT-1E	0.8083 \pm 0.0281
MT-1G1	0.2381 \pm 0.0056
MT-1X	0.6257 \pm 0.0141
MT-1F	0.1084 \pm 0.0003

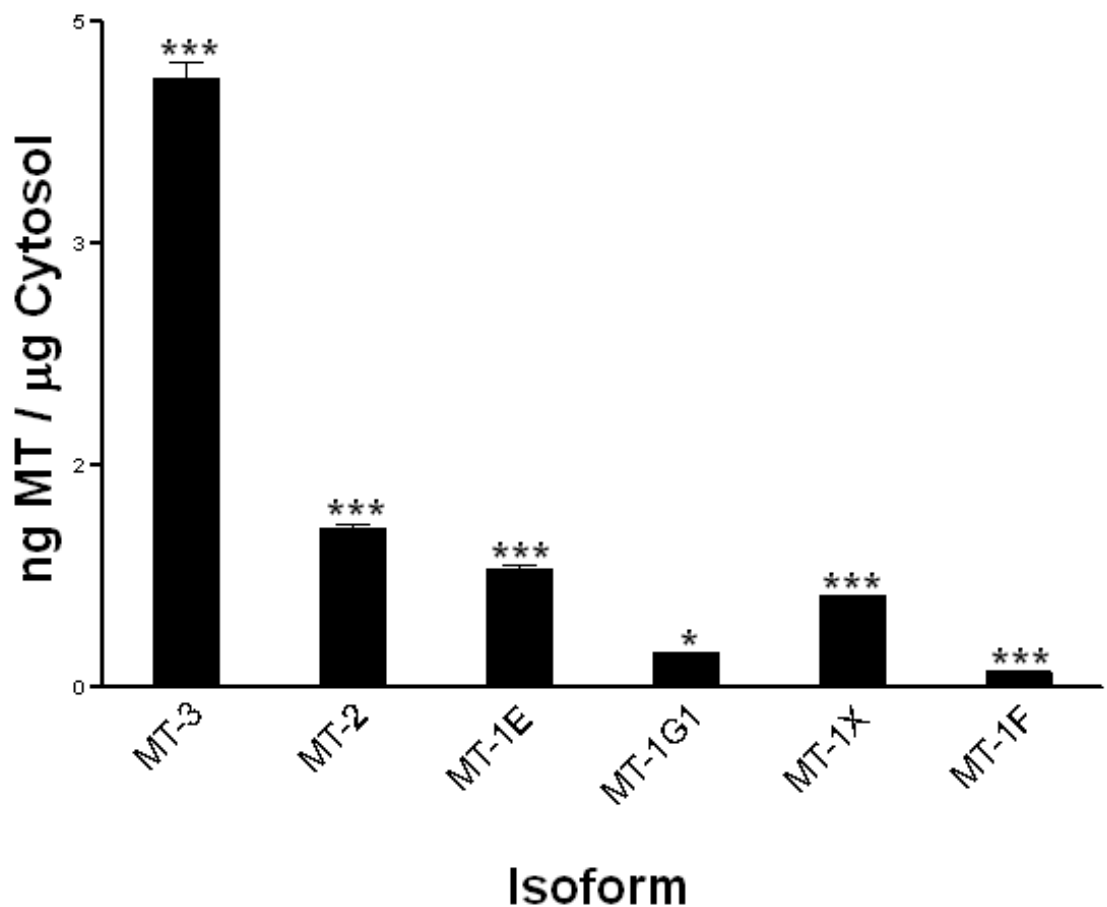


Figure 23. Absolute protein levels of the MT isoforms in human cerebrum brain tissue. Protein data represents biological replicates where n=1. Error bars indicate the standard deviation around the mean from 3 independent technical replicates of 1 biological replicate. A One-way analysis of variation was run on all data sets. * P < 0.05, ** P < 0.01, and *** P < 0.001.

confirms what others have reported of the abundance of MT-3 for this type of tissue but again this is only representative of one tissue sample and more samples need to be analyzed to adequately characterize this type of tissue.

Extraction of pure intact MT-3 from human urine for proteomic analysis

A side project of this study was to develop a method for extracting MTs out of urine for proteomic analysis, more specifically quantitation of the individual MTs in the urine for use as potential noninvasive biomarkers of renal cell carcinoma (RCC) or bladder cancer. There is evidence that MTs are over expressed in both bladder and kidney cancer and their under expression has been implicated in carcinogenesis. Additionally, certain MT isoforms may only be present in malignant tissues of the bladder or kidney. Measuring MT levels in the nearest biological fluid is an attractive means for developing a prognostic, diagnostic, and/or therapeutic decision-making biomarker of these diseases. Since a proteomic MT quantitation method was in place, the main problem that needed to be addressed with this part of the project was how to extract MTs out of the urine and also see if the protein or peptides were being modified by the urine since urine contains many salts, metabolites, vitamins, etc. There are different ways of extracting proteins out of urine but finding the most efficient way to specifically extract MTs is paramount for reproducibility and significance of findings. The need for reliable MT extraction is further amplified by the fact that urine is highly variable in protein content which is largely due to diet. There were two main protein extraction methods that were compared in this study, an organic precipitation of proteins and ultrafiltration using a size exclusion membrane (3000 Da MWCO). The details for these extractions are

listed in the Methods section. Very briefly, 5 µg of pure MT-3 protein was spiked into 1 ml of reconstituted human urine or then incubated for 5 hrs at 37 °C to mimic conditions in the human bladder. The protein was then extracted out of samples by each of these methods and was quantified through use of reversed-phase HPLC AUC analysis using 214 nm absorbance. A direct injection of 5 µg of the pure protein was run to compare extraction efficiencies of the different methods. The organic precipitation yielded the greatest recovery of the intact MT-3 protein (~72%) while the ultrafiltration method yielded a poorer recovery (~35%) which is about half the yield. After extraction and measuring recoveries, the protein was digested with trypsin. The peptides were then separated via nano-rpHPLC then MS and MSMS was performed. The only modification seen from incubating the protein in urine was oxidation of methionine which was expected. Ultrafiltration of urinary proteins is probably the most common technique for isolating proteins out of this fluid. The reason this method was poor for MTs is still unknown. Perhaps the MTs are leaking through the membrane during centrifugation or they may be interacting (sticking) to the membrane via the abundant cysteine residues. It may be worthwhile alkylating the cysteines before this step and retrying. A reversed-phase column extraction was also attempted which entails binding the urinary proteins to the column then washing and eluting the proteins off the column with acetonitrile. This method failed (no recovery of MT-3), however, 75 % acetonitrile was used to elute the intact proteins and perhaps this concentration irreversibly precipitated the proteins. This method should be revisited with a lower concentration of acetonitrile or a different

organic, perhaps methanol which has more hydroxyl groups that could potentially aid the proteins to re-solublize.

All methods are limited to the volume of urine that can be processed. The reversed-phase technique is attractive since large volumes could be passed through a column while still binding and concentrating the proteins.

Proteomic analysis of formalin-fixed paraffin-embedded uterine specimens

Another side project of this study was to try proteomic analysis of formalin-fixed paraffin-embedded (FFPE) tissue with the hopes of eventually being able to identify and quantify MT levels in these specimens. A big benefit of this type of tissue is that there is a lot of clinical data associated with these specimens that have been collected over a span of decades, such as patient treatments and outcomes. FFPE tissue represents a valuable resource for retrospective studies and biomarker discovery. Uterine FFPE specimens from hysterectomy patients were used for this work since there was more of this tissue available. The FFPE tissues underwent immunohistochemistry prior to proteomic work to verify that MTs were in fact present in the tissues used for analysis (data not shown).

There were two main methods tested for extraction of proteins out of FFPE tissue for proteomic analysis. The first tested was a commercially available kit from Qiagen. Proteins were extracted using the manufacturers standard protocol and recommendation of the amount of tissue to use for analysis (2 X 10 μ M) sections. The initial attempts failed using this technique (no MS identifications of proteins). It was believed that the extracted proteins were directly LC-MS friendly but that was not the

case. The contents of the extraction buffer were proprietary but the company confirmed that the extracted proteins could be used for MS analysis but special “clean-up” steps were required before performing LC-MS.

These initial attempts failed because there was likely detergent and a high concentration of reducing agent present in the extraction buffer. Both are conditions that inactivate trypsin used for digestion. It was necessary to add a FASP protocol (described in Methods) to remove any detergents or chemicals potentially interfering with LS-MS analysis.

After adding the additional “clean-up” protocol to the Qiagen protocol many protein identifications (>1000) were achieved using two-dimensional analysis (data not shown). Unfortunately, there were zero MT protein identifications. Additional attempts were made and even increasing the initial amount of tissue (3 X 10 μ M) yielded the same result of no MT identifications. Another FFPE tissue extraction method was attempted using a well-known proteomic-friendly detergent, RapiGest, yielded similar results to the Qiagen kit. Again, this was attempted multiple times along with different amounts of protein, up to 3 X 10 μ M tissue slices, and still zero MT identifications. There are potentially multiple reasons for these results. The MTs may not be getting extracted out of the tissue (still cross-linked), the MTs may be getting washed away in sample preparation, they may be getting extracted but modified in a way that hampers trypsin digestion or ionization of the peptide, or there may simply not be enough of extracted proteins so doubling or tripling the starting amount of tissue may result in MT identifications. In any case, more development and refinement of standard extraction

protocols is needed for MT analysis in FFPE tissue.

MT isoform expression in malignant and non-malignant human breast cells with different estrogen receptor (ER) status: Absolute protein quantitation

The last goal of this study was to apply this assay to four malignant (MCF-7, Hs578T, T-47D, and MDA-MB-231) and one non-malignant (MCF-10A) human breast cell lines. The MCF-7 and T-47D cell lines are estrogen receptor positive (ER⁺) while the Hs578T and MDA-MB-231 cell lines are estrogen receptor negative (ER⁻). The ¹⁵N-labeled synthetic MT peptides described earlier were used as internal standards to determine the absolute amount of human MT isoforms in these breast cells. A cocktail containing three N-terminal MT peptides observed in all breast cells (MT-2, MT-1E, and MT-1X) was added to cytosols that had been alkylated with ¹⁴N-iodoacetamide. The spiked cytosols were then trypsin-digested and the N-terminal MT peptides were enriched and analyzed as above. Metallothionein isoforms were quantified for control, ER⁺, and ER⁻ cells (Figure 24, Table 11). Absolute abundance was expressed as ng intact MT isoform per μg of total protein. 300 μg total cytosolic protein was used for each experiment which is equivalent to the cytosolic protein content of ~6.0 X 10⁶ breast cells. The protein expression for the three detected MT isoforms ranged from 0.05 (MT-1X in T-47D cells) to 1.94 (MT-2 in Hs578T cells) ng per μg total protein accounting for just over a 38-fold difference in MT isoform abundance between the ER⁺ and ER⁻ cell lines (Figure 24, Table 11). The three MTs detected in the ER⁻ Hs578T cells accounted for 0.25% of total cytosolic protein whereas the two MTs detected in ER⁺ T-47D cells accounted for 0.019% of the total cytosolic protein. In the control (MCF-10A) cells,

Table 11. Absolute quantitation values of MT proteins in human breast cells. Values are average ng/ μ g \pm S.D. and represent three biological replicates. Relative changes were calculated by comparing levels of each MT isoform from each malignant cell line to that of the MT levels found in the control (MCF-10A). Δ (no detection).

	MT-1X	Relative Change	MT-1E	Relative Change	MT-2A	Relative Change
MCF-7	.0754 \pm .0079	1.1	Δ	--	.1354 \pm .0520	0.3
T-47D	.0500 \pm .0020	0.8	Δ	--	.1350 \pm .0409	0.3
HS578T	.2888 \pm .0564	4.4	.2441 \pm .1003	3.5	1.9436 \pm .5578	3.9
231	.1602 \pm .0172	2.4	.3387 \pm .0956	4.8	1.4163 \pm .2516	2.8
MCF-10A	.0663 \pm .0188	1.0	.0707 \pm .0130	1.0	.5022 \pm .1556	1.0

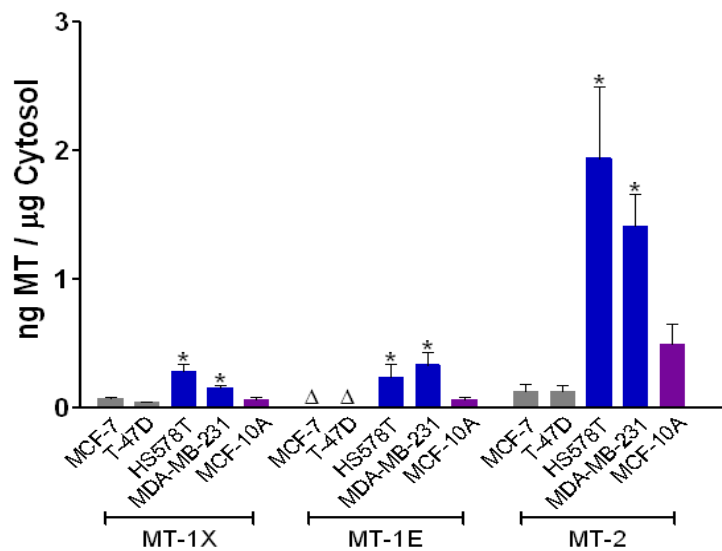


Figure 24. Absolute protein levels of the MT isoforms in human breast cells. Control (violet), ER⁺ (grey), and ER⁻ (blue) human breast cells. Protein data represents biological replicates where n=3. Error bars indicate the standard deviation around the mean. A two-way ANOVA followed with a Bonferroni posttest was run on all data sets. Significance was based on variation from control (MCF-10A). Δ (no detection). *P < .05.

0.065% of the total cytosolic proteins were MTs. This correlates to a ~13-fold higher expression of total MTs in ER⁻ compared to ER⁺ human breast cancer cell lines or a 3.9-fold increase in MT expression in ER⁻ cells compared to control or a 3.4-fold down-regulation of MTs in ER⁺ cells compared to the control. On an isoform basis, MT-2 was the dominant MT expressed throughout all the cell lines followed by MT-1E and MT-1X. There was approximately a 13-fold induction of MT-2 protein in the ER⁻ cells compared to ER⁺ cells and a 3.6-fold induction of MT-1X. MT-1E was not detected in the ER⁺ cell lines at the protein level (Figure 24, Table 11) or the transcript level (Figure 25, Table 12).

MT mRNA transcript levels in the human breast cells

The general expression pattern of the MT isoforms at the transcript level was fairly consistent with the protein levels with some exceptions (Figure 25, Table 12). The MT mRNA fold inductions were more pronounced for the MT-2 and MT-1X isoforms than was seen at the protein level. There was ~100-fold induction of MT-2 mRNA from ER⁻ cells compared to ER⁺ cells and ~44-fold induction of MT-1X. There was also a ~394-fold difference in MT mRNA isoform abundance between the MT-2 in the ER⁺ and MT-1X in the ER⁻ cell lines (Figure 25, Table 12). Noteworthy is the mRNA transcript level of MT-1E in the ER⁻ and control cells which has comparable transcript levels to MT-2 but has only 17.3% the protein compared to MT-2. The higher fold inductions seen at the mRNA compared to what was seen at the protein level could be an artifact of malignancy or another consideration may be that there is more Apo-MT in these cells which destabilizes the MTs and leaves them more susceptible to degradation.

Table 12. Absolute quantitation values of MT mRNA transcripts in human breast cells. Δ (no detection). Values are average MT transcripts/1000 18S \pm S.D. and represent three biological replicates. Fold changes were calculated by comparing levels of each MT isoform from each malignant cell line to that of the MT levels found in the control (MCF-10A).

	MT-1X	Relative Change	MT-1E	Relative Change	MT-2A	Relative Change
MCF-7	.0016 \pm .0006	0.3	Δ	--	.0058 \pm .0030	0.3
T-47D	.0003 \pm .0002	0.1	Δ	--	.0012 \pm .0009	0.1
HS578T	.0131 \pm .0040	2.0	.0535 \pm .0075	2.0	.1183 \pm .0138	5.4
231	.0044 \pm .0009	0.7	.0513 \pm .0338	1.9	.0670 \pm .0170	3.0
MCF-10A	.0065 \pm .0002	1.0	.0272 \pm .0068	1.0	.0220 \pm .0048	1.0

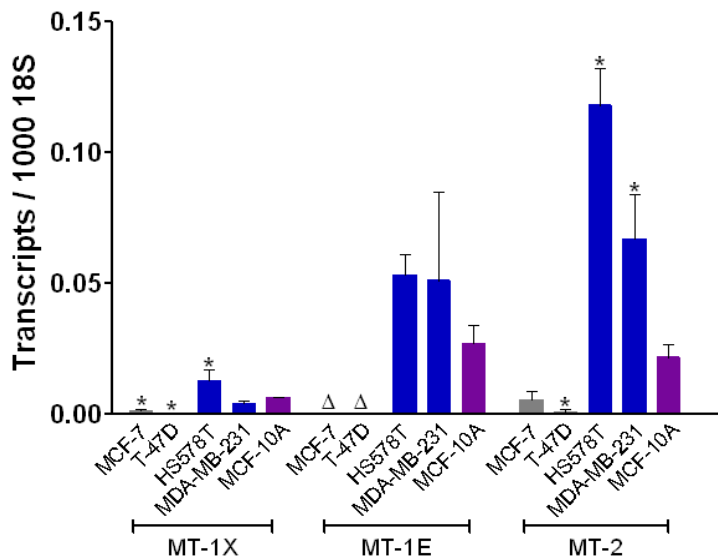


Figure 25. Absolute mRNA transcript levels of the MT isoforms in human breast cells. Control (violet), ER⁺ (grey), and ER⁻ (blue) human breast cells. Absolute mRNA transcripts were normalized to 18S. mRNA data represents biological replicates where n=3. Error bars indicate the standard deviation around the mean. A two-way ANOVA followed with a Bonferroni posttest was run on all data sets. Significance was based on variation from control (MCF-10A). Δ (no detection). *P < .05.

CHAPTER IV

DISCUSSION

In this study we describe a bottom-up proteomic-based approach leading to the development, optimization, validation, and application of an alternative means to quantify the individual MT isoforms at the protein level. While others have described top-down methods for identifying MTs using MS in induced lysates^{38,55}, to date, this is the most robust study of this type describing quantitation of the individual MT isoforms in acute metal exposure and also the application to malignant and non-malignant cells. Earlier studies describing levels of MTs in metal exposures or disease relied heavily on mRNA levels and/or the antibody-based immunohistochemistry technique using the E-9 antibody to measure total MT levels of the proteins^{4,86-90}. The result of this study provides a non-antibody-based method to quantify MT isoforms at the protein level rather than rely on traditional PCR-based methods used to quantify MTs that may or may not correlate to actual protein expression.

Since 1957 when MTs were first identified, there has been a lack in development of a robust assay to measure levels of the individual protein isoforms that have so often been implicated as diagnostic or prognostic markers of disease. The lack of development of such an assay is mostly due to the chemical (reactive) and physical (small) characteristics of the individual MTs. The high sequence homology (Table 1) is

the major reason antibody based methods used to quantify MT proteins have been hampered.

The use of mass spectrometry to characterize this family of proteins poses its own difficulties that needed to be overcome to reproducibly identify and quantitate the various MTs. These problems were addressed in this study, namely, optimizing sample preparation and LC gradients to enrich for the diagnostic acetylated N-terminal tryptic peptides. The COFRADIC approach has been used by many to gain sampling depth for proteomic studies involving complex lysates^{45,63} and optimized 2-dimensional LC-MS (methods) was employed to characterize the complex MT family in this study. Another difficulty with using MS for MTs is that the intact MT proteins are quite small and the sequence is highly conserved for all of the isoforms so when digested with trypsin many of the peptides are the same but the diagnostic N-terminal tryptic peptides have small differences in the sequence and can be identified by the mass differences. Methionine oxidation was also a very important issue that needed to be addressed in this study. It's been shown that certain peptides containing methionine demonstrate a high susceptibility to undergo methionine oxidation⁷⁹ and the diagnostic N-terminal tryptic peptides of MTs would fall in this category being prone to undergo methionine oxidation according to their results. It is likely that there is a certain level of endogenous methionine oxidation as it has been speculated that methionine oxidation is a modification that can affect the functions of the proteins⁹¹ or help protect the cell through MTs redox potential. There is also a good chance that a certain level of this modification is seen arising from a sample preparation artifact (oxygen in atmosphere

and buffers). Whether methionine oxidation results from endogenous sources, exogenous sources, or both, it was clear that this modification needed to be resolved to increase quantitation accuracy and assay sensitivity. Since a large portion of the MTs in the samples had methionine oxidation, converting the remaining reduced methionines to the oxidized forms was tested using hydrogen peroxide or sodium periodate^{92, 93}. Unfortunately, this complicated the samples more as methionine can undergo two oxidation states (mono- or di) and was not controllable. Eventually reverting the oxidized methionines back to their reduced forms with DMS^{57, 80} was tested. This successfully converted the diagnostic N-terminal peptides into one reduced form for each isoform, increasing quantitation accuracy and sensitivity. The last main challenge to overcome for characterizing the various MT isoforms using MS was to develop a reliable labeling technique for quantitation. There are various methods used for MS-based quantitation including label-free and stable Isotope labeling methods, each having their own pros and cons⁹⁴. Label-free methods of quantitation are the most inexpensive methods but are hampered by complex data analysis, normalization to achieve accurate/consistent results, and the lack at obtaining absolute protein values. Stable isotope labeling is often the most precise MS-based quantitation method used to achieve relative or absolute protein abundances but the reagents or heavy-labeled peptide standards may become costly. The use of light and heavy iodoacetamide (alkylating agent) was used in this study because the MT peptides of interest contained 5 cysteine residues which allows for adequate separation of light and heavy isotopic envelopes and the heavy iodoacetamide was not cost-prohibitive. Also, despite the 5

Da mass shift between the light and heavy peptides, they separated chromatographically identical thus allowing for precise protein quantitation.

There is an obvious need for an MS-based assay for MT proteins in the biomarker field since MTs have been studied extensively as markers of metal toxicity and disease, most notably cancers²⁴⁻³¹. MTs have a protective role against metals (mostly cadmium) in cells and tissues. It is known that cadmium accumulates in the kidney and MTs act as a sponge to bind free cadmium and protect the kidney from this carcinogenic and nephrotoxic metal⁹⁵. It has not been entirely clear yet as to which isoforms are responsible for binding metals (zinc, cadmium, copper, etc) in the cell in acute vs. chronic or low-dose vs. high-dose exposures to these heavy metals. Much of the data to date has been a reflection of the mRNA transcript levels coupled with total MT protein obtained using the E-9 antibody^{12, 29, 30, 31, 33}. The results obtained in the present study give a clearer insight as to what MTs (proteins and mRNA) are inducible or protective in acute cadmium exposure (cell culture data) and perhaps what MTs play a protective role during chronic cadmium exposure as seen from the tissue data. Although there were some similarities in expression of transcripts and proteins for the MTs, an important finding in this study was seen when these two bio-molecules were compared for the various isoforms. There were differences in the rank order and fold inductions of the MTs. This was not all that surprising since there are many variables from an mRNA transcript to a fully functional translated protein including: bio-molecule half-lives, metal stabilization of proteins, and translational efficiencies. It does, however, bring in to question the accuracy of prior MT studies that have relied heavily

on mRNA levels of the various MTs to correlate to protein levels of those isoforms. This finding further exemplifies the need for this type of assay to measure the individual proteins in metal exposures to fully understand the functional role of the isoforms.

As mentioned, MTs have been known to have altered expression in many different cancers and have been often correlated to patient prognosis. It is not entirely clear as to the functional role MTs are playing in carcinogenesis, whether they are altered due to cellular stress or if they are actually involved in the development of cancers. In certain neoplastic cells, MTs have shown to possess anti-apoptotic activity and can increase cancer cellular proliferation^{18, 96}. Either being up-regulated or down-regulated in carcinogenesis, many of the studied MT isoforms seem to increase cancer progression. MTs have also been shown to be responsible in resistance to chemotherapeutic agents by using their redox potential to inactivate free radicals that are metabolically formed due to the cancer drugs⁹⁷. Additionally, MTs have been implicated in the resistance to cisplatin by binding to the drug in cancers treated with this chemotherapeutic⁹⁸.

According to PCR-based methods of quantitation, there are studies that suggest MT-1G acts as a tumor suppressor gene in hepatocellular, breast, and thyroid cancer^{99, 100, 101}. Recently, it has been suggested that increased levels of MT-1F and MT-2A are potential biomarkers of poor outcome of non-small cell lung cancer patients¹⁰². In colorectal cancer, MT-1G, 1E, 1F, 1H, and 1M were shown to be significantly down-regulated (assumed to be epigenetically regulated by hypermethylation) and correlate with worse prognosis³⁷ and a separate study by this same group suggests that

correlating MT expression with p53 proteins enhances the prognostic power of each individual marker by predicting the progression of the disease¹⁰³. In glioma, it is postulated that MT-1E enhances the migration and invasion of glioma cells by inducing MMP-9 inactivation via upregulation of NF- κ B p50¹⁰⁴. Other studies show overexpression of MT-1F and MT-2A in breast cancer is responsible for cell proliferation and in MCF-7 cells could be responsible for chemoresistance to doxorubicin^{31, 32, 105-107}. An earlier study from our lab suggests that MT-1E may mediate cancer cell differentiation in breast cancer with relation to the estrogen receptor status of the cell²⁹.

The results from the breast cancer portion of this study demonstrated similar results in some aspects but also different from what has been proposed about the individual MT isoforms in these cancer cell lines based on PCR and antibody data. There are significant differences in expression of the MT isoforms when comparing ER⁻ to ER⁺ cell lines, not only at mRNA, but protein level as well. An interesting finding was that the transcript levels of MT-2A and MT-1E were significantly overexpressed in ER⁻ cells, but at the protein level, MT-2 was 6- to 8-fold more abundant than MT-1E. Also notable, was the complete absence of expression for MT-1E at both the protein and mRNA levels in the ER⁺ breast cancer cells.

The previous MT studies in breast cancer have relied heavily on PCR data and the transcript levels for MT-2A and MT-1E in the ER⁻ cells was comparable to what has been published, suggesting that these two isoforms are highly expressed. Some reports claim MT-1E was highly expressed at the transcript level in breast cancer cells and/or tissues³⁰

while a larger study claims that MT-2A was the most abundant isoform³¹. This current study demonstrates that MT-1E and MT-2A expressed comparable transcript levels with MT-2 displaying slightly higher (without significance) levels in this study which is in good agreement that these two isoforms are highly expressed in ER⁻ breast cancers. The most notable finding in this study, compared to what has been published in the past, is the fact that we are now able to identify which MTs at the protein level are responsible for the difference in expression previously seen with the antibody when comparing ER⁻ to ER⁺ breast cancer cells. In these cells, MT-2 is the isoform that is responsible for the major differences seen at the protein level when comparing ER⁻ to ER⁺ cells. From a biomarker standpoint, the power to detect and quantify the individual MT isoforms at the protein level increases the usefulness of this type of assay for biomarker detection and classifying tumors based on their MTs status may provide a good alternative to their traditional ER-status.

Urine remains an attractive noninvasive biological fluid to screen for biomarkers of kidney and urologic diseases with MS. Urinary protein analysis can be challenging but potentially can give helpful information regarding urinary tract diseases. The difficulty in measuring urinary proteins lies in the variation of urine composition between individuals and sampling times. Typical urine protein concentration varies considerably (1-10 mg/dl) and albumins are abundant, assuming ~50% yield for extracted protein from urine this corresponds to ~0.5-20 ml of normal urine. The high salt content of urine is an additional challenge in MS-based urinary proteomics. Once these challenges are overcome the result is a urinary protein library that may contain potential

biomarkers of disease once validated. To date, several candidate biomarkers of bladder cancer have been identified through proteomic approaches^{108, 109}. Since MT-3 and other MTs are known to show altered expression in bladder and kidney cancer, it would be plausible that cancer cells could be shed into urine and MTs could be used as markers of disease. The potential to detect MT-3 in the urine and/or to see if this protein was modified was also examined in this study. Although human urine samples from volunteers were not analyzed in this study, reconstituted (freeze-dried) human urine was obtained and spiked with purified MT-3 protein. It was found that organic precipitation of proteins in urine achieved the highest recovery of MT-3 and that there were no other modifications due to the fluid besides oxidation of methionine (which was expected). The next step would be to apply this method to a larger study of diseased (bladder/kidney cancer) and healthy volunteers to look for significant changes in abundance of the individual MTs.

Recently there have been more studies demonstrating the viability of using FFPE tissue specimens for shotgun proteomic analysis that could offer a retrospective biomarker discovery of certain diseases¹¹⁰⁻¹¹⁶. The proteins in FFPE tissues have undergone extensive modifications due to the formaldehyde reaction with the amino groups of lysines and free protein N-termini. Although these tissues have been fixed, labs have reported obtaining >90% recovery of FFPE tissue proteomes compared to those generated from frozen tissue¹¹⁷. Most studies in this type of tissue use more of a global analysis of the FFPE proteome searching potential biomarkers of disease followed with validation steps but we aim to study targeted FFPE proteomics for MTs since we

already know MTs display altered expression in certain diseases. Tissue from uterine sections was used in this study to attempt analyzing MT levels from these specimens. Using the E-9 antibody, the tissues stained positive for MTs in a single mono epithelial layer prior to MS attempts. Multiple attempts to detect MTs using published FFPE protocols for protein extractions coupled to the optimized MS MT protocols failed to identify any isoforms in this family. In retrospect, the amount of extracted protein from these samples was low which was the likely reason for no detections of MTs. Three 10 μ m uterine tissue slices was the maximum amount used for protein extractions and using 10-15 X 10 μ m would likely give a better likelihood of identifying MTs. There were many (500-1000) protein (non-MT) identifications using these different extractions in the uterine tissue despite the low amount of protein analyzed. However, recent experiments (performed by co-worker) in kidney FFPE tissue resulted in the positive identification of seven MT isoforms which were the identical seven isoforms identified and quantified in the frozen kidney tissue described in this study. In these experiments 10 X 10 μ m kidney FFPE tissue slices were used with similar protein extraction methods and the same optimized MT MS protocols described in this study that was performed on the uterine FFPE tissue. It is known from the quantitative MT analysis performed in the current study describing the frozen kidney tissue that MTs are abundant in this tissue which partly led to the successful identifications of the MTs in the kidney FFPE tissue. It is not known exactly how abundant the MTs are in the uterine FFPE tissue, the MT antibody staining appeared weak so that more than likely was also a factor for not detecting any isoforms using MS analysis for that tissue. Another important aspect that

led to the positive MT detections of the signature N-terminal peptides in kidney FFPE experiments was the increased starting tissue material (10 X 10 μ M tissue slices). These successful MT identifications in the kidney FFPE tissue leaves promise for using this type of tissue for retrospective MT studies in cancers but more work is still needed for reliable quantitative analysis.

This study describes an iodoacetamide stable isotope-labeling mass spectrometry-based method for simultaneous relative and absolute quantification of human metallothionein isoforms in complex cell or tissue lysates. Additional research on the individual MTs in cases of metal exposure and disease are needed to shed light on the functional role these isoforms in disease. This method expands the usefulness of human MT isoforms as potential biomarkers for specific diseases or environmental exposures to heavy metals.

APPENDICES

APPENDIX A

Abbreviations Used in Text

Cd ²⁺	cadmium chloride (CdCl ₂)
mRNA	messenger ribonucleic acid
RT-PCR	reverse transcription- polymerase chain reaction
NMI-BC	non-muscle invasive- bladder cancer
NaCl	sodium chloride
MeOH	methanol
EtOH	ethanol
COFRADIC	combined fractional and diagonal chromatography
BSA	bovine serum albumin
SDS	sodium dodecyl sulfate
PCR	polymerase chain reaction
HCl	hydrochloride
DTT	dithiothreitol
IgG	immunoglobulin G
BGG	bovine gamma globulin G
BCA	bicinchoninic acid assay
TBE	tris/borate/EDTA
BCP	2-Bromo-1-chloropropane

UV	ultraviolet
RNA	ribonucleic acid
DNA	deoxyribonucleic acid
DMEM	Dulbecco's modified Eagle's medium
CO ₂	carbon dioxide
EDTA	ethylenediaminetetraacetic acid
PBS	Phosphate buffered saline
NIH	National Institute of Health
AAALAC	American Association for Accreditation of Laboratory Animal Care
cDNA	complementary DNA
PAGE	polyacrylamide gel electrophoresis
TBS	tris buffered saline
DAB	diaminobenzidine
C _t	threshold cycle

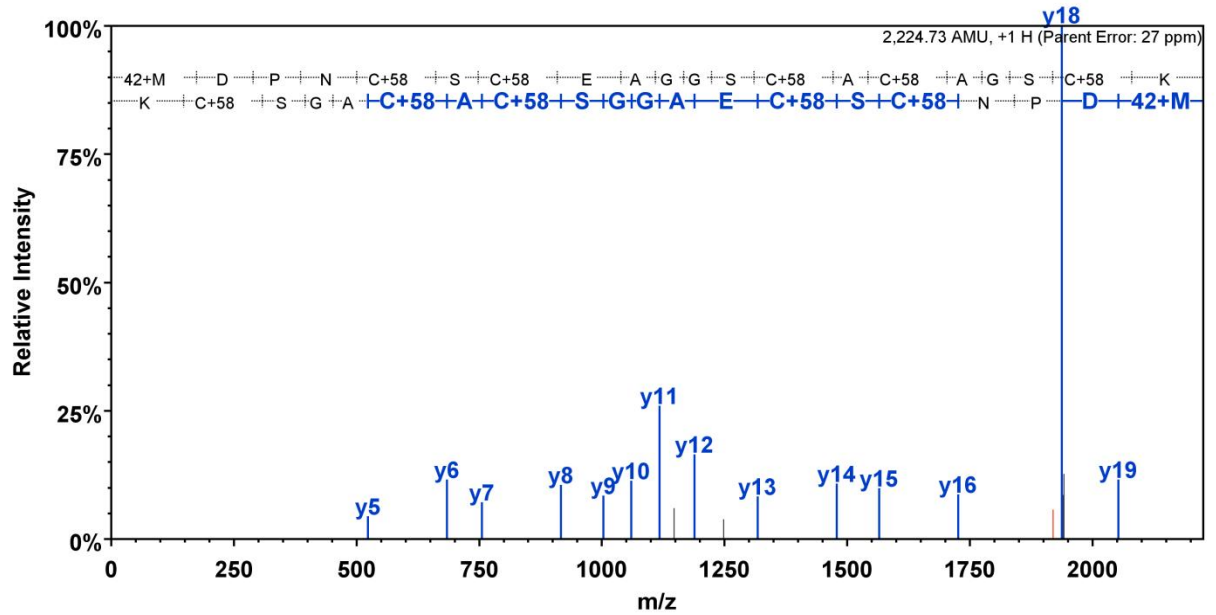
Units of Measure

cm ²	centimeters squared
°C	degrees Celsius
μM	micromolar (10 ⁻⁶ mole/liter)
mL	milliliter (10 ⁻³ liter)
μg	microgram (10 ⁻⁶ gram)
sec	second

min	minute
mM	millimolar (10^{-3} mole/liter)
ga	gauge
rpm	revolutions per minute
hr	hour
μm	micrometer (10^{-6} meter)
No.	number
mm	millimeter (10^{-3} meter)
kDa	kiloDalton

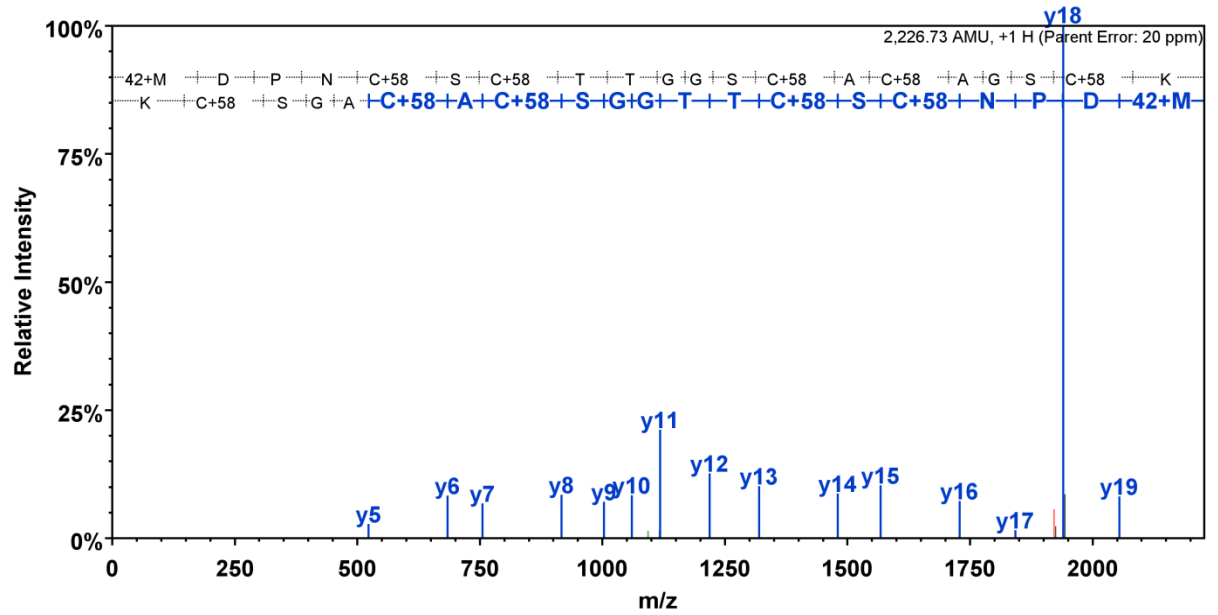
APPENDIX B

MSMS Spectra of Endogenous and Synthetic MT Peptides



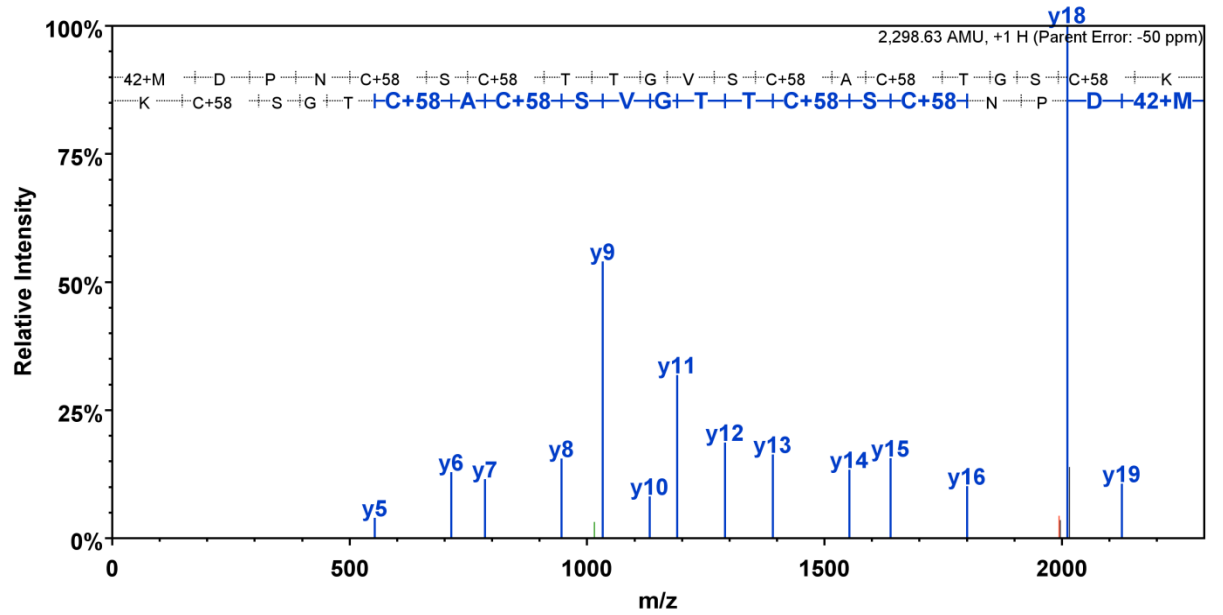
B	B Ions	B+2H	B-NH3	B-H2O	AA	Y Ions	Y+2H	Y-NH3	Y-H2O	Y
1	174.1				M+42	2,225.7		2,208.6	2,207.7	20
2	289.1			271.1	D	2,052.6		2,035.6	2,034.6	19
3	386.1			368.1	P	1,937.6		1,920.6	1,919.6	18
4	500.2		483.2	482.2	N	1,840.5		1,823.5	1,822.5	17
5	661.2		644.2	643.2	C+58	1,726.5		1,709.5	1,708.5	16
6	748.2		731.2	730.2	S	1,565.5		1,548.5	1,547.5	15
7	909.2		892.2	891.2	C+58	1,478.5		1,461.4	1,460.4	14
8	1,038.3		1,021.3	1,020.3	E	1,317.4		1,300.4	1,299.4	13
9	1,109.3		1,092.3	1,091.3	A	1,188.4		1,171.4	1,170.4	12
10	1,166.3		1,149.3	1,148.3	G	1,117.4		1,100.3	1,099.3	11
11	1,223.4		1,206.3	1,205.4	G	1,060.3		1,043.3	1,042.3	10
12	1,310.4		1,293.4	1,292.4	S	1,003.3		986.3	985.3	9
13	1,471.4		1,454.4	1,453.4	C+58	916.3		899.3	898.3	8
14	1,542.4		1,525.4	1,524.4	A	755.3		738.2	737.3	7
15	1,703.5		1,686.4	1,685.5	C+58	684.2		667.2	666.2	6
16	1,774.5		1,757.5	1,756.5	A	523.2		506.2	505.2	5
17	1,831.5		1,814.5	1,813.5	G	452.2		435.2	434.2	4
18	1,918.6		1,901.5	1,900.5	S	395.2		378.1	377.1	3
19	2,079.6		2,062.5	2,061.6	C+58	308.1		291.1		2
20	2,225.7		2,208.6	2,207.7	K	147.1		130.1		1

Supplemental Figure 1. MT-1H (¹⁵N) MSMS for synthesized human peptide.



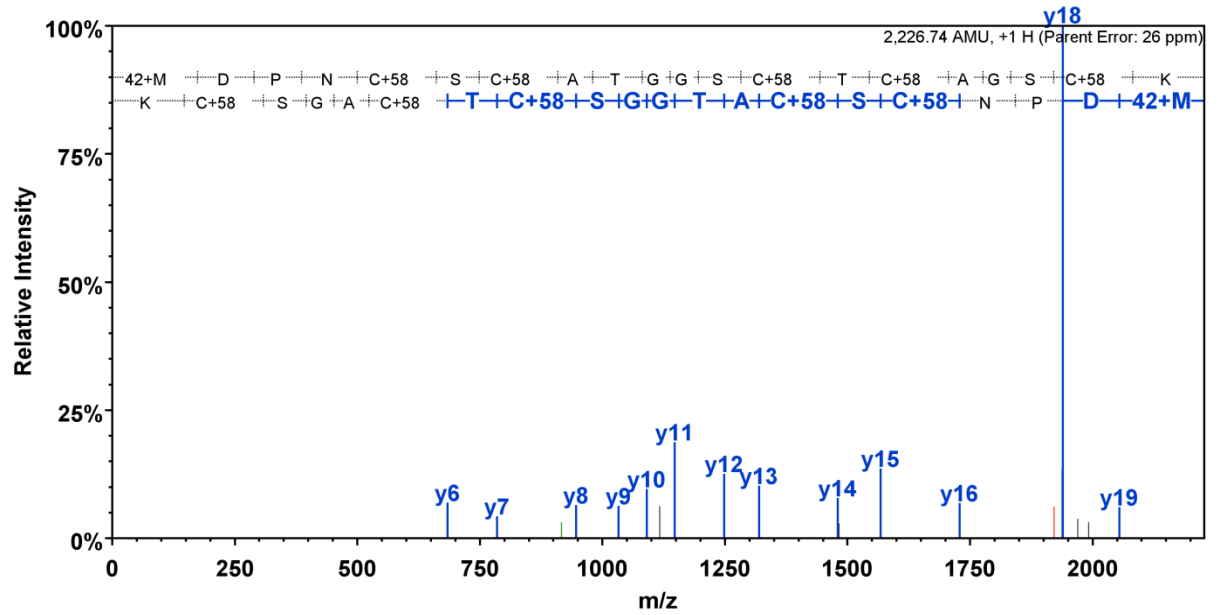
B	B Ions	B+2H	B-NH3	B-H2O	AA	Y Ions	Y+2H	Y-NH3	Y-H2O	Y
1	174.1				M+42	2,227.7		2,210.7	2,209.7	20
2	289.1			271.1	D	2,054.6		2,037.6	2,036.6	19
3	386.1			368.1	P	1,939.6		1,922.6	1,921.6	18
4	500.2		483.2	482.2	N	1,842.6		1,825.5	1,824.5	17
5	661.2		644.2	643.2	C+58	1,728.5		1,711.5	1,710.5	16
6	748.2		731.2	730.2	S	1,567.5		1,550.5	1,549.5	15
7	909.2		892.2	891.2	C+58	1,480.5		1,463.4	1,462.5	14
8	1,010.3		993.3	992.3	T	1,319.5		1,302.4	1,301.4	13
9	1,111.3		1,094.3	1,093.3	T	1,218.4		1,201.4	1,200.4	12
10	1,168.4		1,151.3	1,150.3	G	1,117.4		1,100.3	1,099.3	11
11	1,225.4		1,208.4	1,207.4	G	1,060.3		1,043.3	1,042.3	10
12	1,312.4		1,295.4	1,294.4	S	1,003.3		986.3	985.3	9
13	1,473.4		1,456.4	1,455.4	C+58	916.3		899.3	898.3	8
14	1,544.5		1,527.4	1,526.5	A	755.3		738.2	737.3	7
15	1,705.5		1,688.5	1,687.5	C+58	684.2		667.2	666.2	6
16	1,776.5		1,759.5	1,758.5	A	523.2		506.2	505.2	5
17	1,833.5		1,816.5	1,815.5	G	452.2		435.2	434.2	4
18	1,920.6		1,903.5	1,902.6	S	395.2		378.1	377.1	3
19	2,081.6		2,064.6	2,063.6	C+58	308.1		291.1		2
20	2,227.7		2,210.7	2,209.7	K	147.1		130.1		1

Supplemental Figure 2. MT-1B (¹⁵N) MSMS for synthesized human peptide.



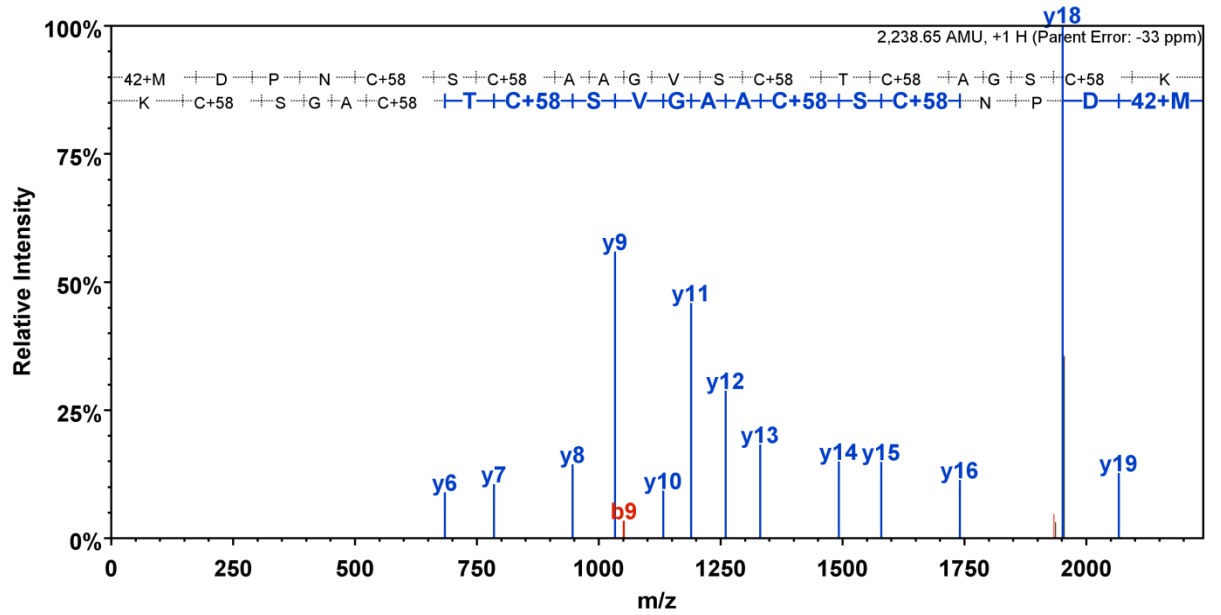
B	B Ions	B+2H	B-NH3	B-H2O	AA	Y Ions	Y+2H	Y-NH3	Y-H2O	Y
1	174.1				M+42	2,299.7		2,282.7	2,281.7	20
2	289.1			271.1	D	2,126.7		2,109.7	2,108.7	19
3	386.1			368.1	P	2,011.7		1,994.6	1,993.7	18
4	500.2		483.2	482.2	N	1,914.6		1,897.6	1,896.6	17
5	661.2		644.2	643.2	C+58	1,800.6		1,783.5	1,782.6	16
6	748.2		731.2	730.2	S	1,639.6		1,622.5	1,621.5	15
7	909.2		892.2	891.2	C+58	1,552.5		1,535.5	1,534.5	14
8	1,010.3		993.3	992.3	T	1,391.5		1,374.5	1,373.5	13
9	1,111.3		1,094.3	1,093.3	T	1,290.5		1,273.4	1,272.5	12
10	1,168.4		1,151.3	1,150.3	G	1,189.4		1,172.4	1,171.4	11
11	1,267.4		1,250.4	1,249.4	V	1,132.4		1,115.4	1,114.4	10
12	1,354.5		1,337.4	1,336.4	S	1,033.3		1,016.3	1,015.3	9
13	1,515.5		1,498.4	1,497.5	C+58	946.3		929.3	928.3	8
14	1,586.5		1,569.5	1,568.5	A	785.3		768.3	767.3	7
15	1,747.5		1,730.5	1,729.5	C+58	714.2		697.2	696.2	6
16	1,848.6		1,831.5	1,830.6	T	553.2		536.2	535.2	5
17	1,905.6		1,888.6	1,887.6	G	452.2		435.2	434.2	4
18	1,992.6		1,975.6	1,974.6	S	395.2		378.1	377.1	3
19	2,153.6		2,136.6	2,135.6	C+58	308.1		291.1		2
20	2,299.7		2,282.7	2,281.7	K	147.1		130.1		1

Supplemental Figure 3. MT-1M (¹⁵N) MSMS for synthesized human peptide.



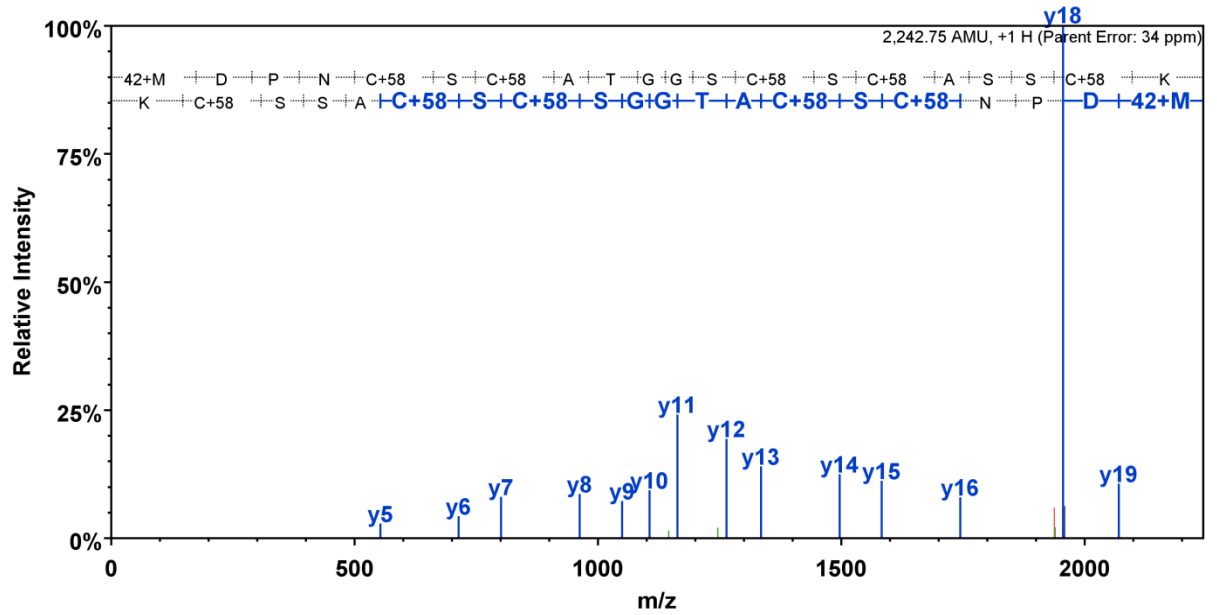
B	B Ions	B+2H	B-NH3	B-H2O	AA	Y Ions	Y+2H	Y-NH3	Y-H2O	Y
1	174.1				M+42	2,227.7		2,210.7	2,209.7	20
2	289.1			271.1	D	2,054.6		2,037.6	2,036.6	19
3	386.1			368.1	P	1,939.6		1,922.6	1,921.6	18
4	500.2		483.2	482.2	N	1,842.6		1,825.5	1,824.5	17
5	661.2		644.2	643.2	C+58	1,728.5		1,711.5	1,710.5	16
6	748.2		731.2	730.2	S	1,567.5		1,550.5	1,549.5	15
7	909.2		892.2	891.2	C+58	1,480.5		1,463.4	1,462.5	14
8	980.3		963.3	962.3	A	1,319.5		1,302.4	1,301.4	13
9	1,081.3		1,064.3	1,063.3	T	1,248.4		1,231.4	1,230.4	12
10	1,138.3		1,121.3	1,120.3	G	1,147.4		1,130.3	1,129.4	11
11	1,195.4		1,178.3	1,177.4	G	1,090.3		1,073.3	1,072.3	10
12	1,282.4		1,265.4	1,264.4	S	1,033.3		1,016.3	1,015.3	9
13	1,443.4		1,426.4	1,425.4	C+58	946.3		929.3	928.3	8
14	1,544.5		1,527.4	1,526.5	T	785.3		768.3	767.3	7
15	1,705.5		1,688.5	1,687.5	C+58	684.2		667.2	666.2	6
16	1,776.5		1,759.5	1,758.5	A	523.2		506.2	505.2	5
17	1,833.5		1,816.5	1,815.5	G	452.2		435.2	434.2	4
18	1,920.6		1,903.5	1,902.6	S	395.2		378.1	377.1	3
19	2,081.6		2,064.6	2,063.6	C+58	308.1		291.1		2
20	2,227.7		2,210.7	2,209.7	K	147.1		130.1		1

Supplemental Figure 4. MT-1E (¹⁵N) MSMS for synthesized human peptide.



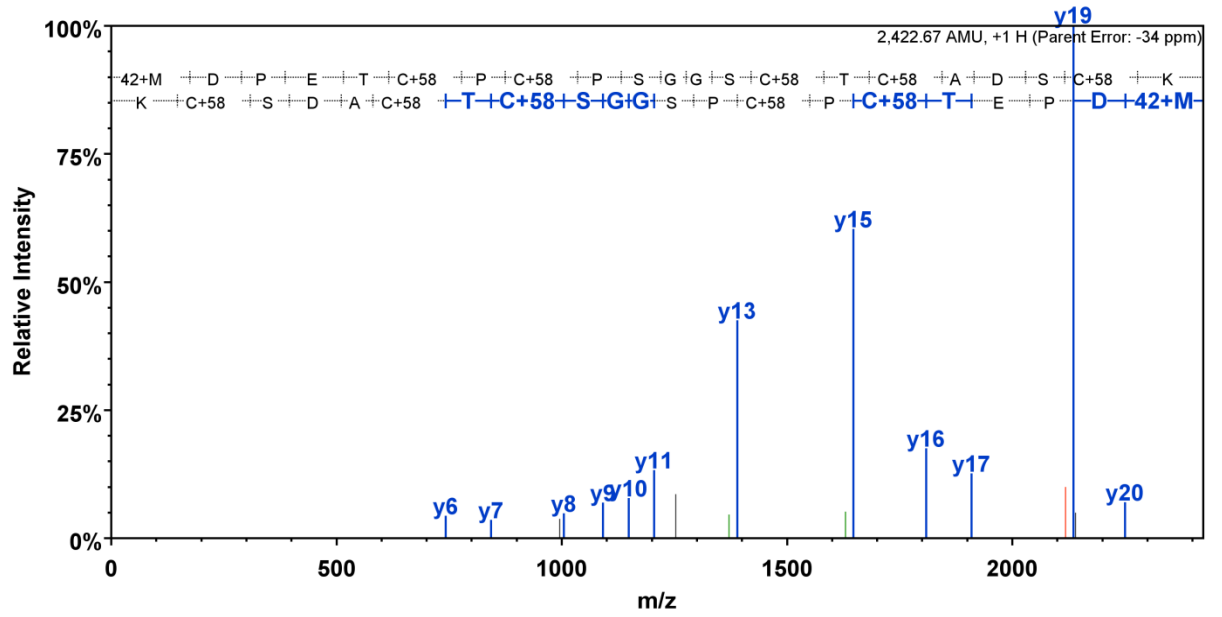
B	B Ions	B+2H	B-NH3	B-H2O	AA	Y Ions	Y+2H	Y-NH3	Y-H2O	Y
1	174.1				M+42	2,239.7		2,222.7	2,221.7	20
2	289.1			271.1	D	2,066.7		2,049.6	2,048.7	19
3	386.1			368.1	P	1,951.6		1,934.6	1,933.6	18
4	500.2		483.2	482.2	N	1,854.6		1,837.6	1,836.6	17
5	661.2		644.2	643.2	C+58	1,740.6		1,723.5	1,722.5	16
6	748.2		731.2	730.2	S	1,579.5		1,562.5	1,561.5	15
7	909.2		892.2	891.2	C+58	1,492.5		1,475.5	1,474.5	14
8	980.3		963.3	962.3	A	1,331.5		1,314.5	1,313.5	13
9	1,051.3		1,034.3	1,033.3	A	1,260.5		1,243.4	1,242.4	12
10	1,108.3		1,091.3	1,090.3	G	1,189.4		1,172.4	1,171.4	11
11	1,207.4		1,190.4	1,189.4	V	1,132.4		1,115.4	1,114.4	10
12	1,294.4		1,277.4	1,276.4	S	1,033.3		1,016.3	1,015.3	9
13	1,455.5		1,438.4	1,437.4	C+58	946.3		929.3	928.3	8
14	1,556.5		1,539.5	1,538.5	T	785.3		768.3	767.3	7
15	1,717.5		1,700.5	1,699.5	C+58	684.2		667.2	666.2	6
16	1,788.6		1,771.5	1,770.5	A	523.2		506.2	505.2	5
17	1,845.6		1,828.5	1,827.6	G	452.2		435.2	434.2	4
18	1,932.6		1,915.6	1,914.6	S	395.2		378.1	377.1	3
19	2,093.6		2,076.6	2,075.6	C+58	308.1		291.1		2
20	2,239.7		2,222.7	2,221.7	K	147.1		130.1		1

Supplemental Figure 5. MT-1F (¹⁵N) MSMS for synthesized human peptide.



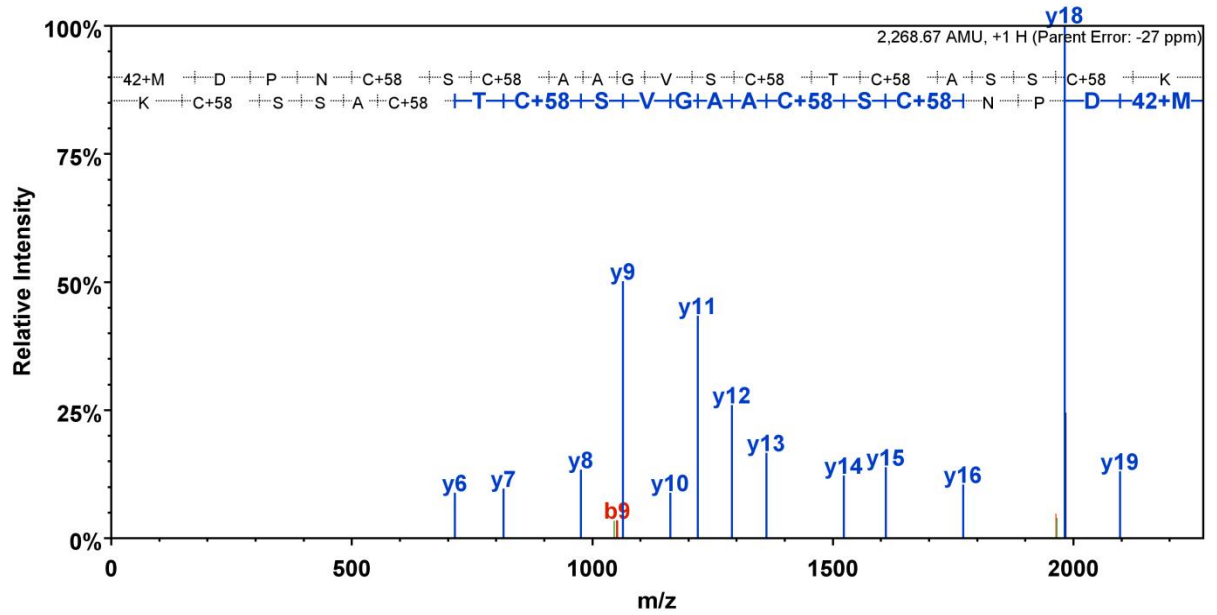
B	B Ions	B+2H	B-NH3	B-H2O	AA	Y Ions	Y+2H	Y-NH3	Y-H2O	Y
1	174.1				M+42	2,243.7		2,226.7	2,225.7	20
2	289.1			271.1	D	2,070.6		2,053.6	2,052.6	19
3	386.1			368.1	P	1,955.6		1,938.6	1,937.6	18
4	500.2		483.2	482.2	N	1,858.6		1,841.5	1,840.5	17
5	661.2		644.2	643.2	C+58	1,744.5		1,727.5	1,726.5	16
6	748.2		731.2	730.2	S	1,583.5		1,566.5	1,565.5	15
7	909.2		892.2	891.2	C+58	1,496.5		1,479.4	1,478.5	14
8	980.3		963.3	962.3	A	1,335.4		1,318.4	1,317.4	13
9	1,081.3		1,064.3	1,063.3	T	1,264.4		1,247.4	1,246.4	12
10	1,138.3		1,121.3	1,120.3	G	1,163.4		1,146.3	1,145.4	11
11	1,195.4		1,178.3	1,177.4	G	1,106.3		1,089.3	1,088.3	10
12	1,282.4		1,265.4	1,264.4	S	1,049.3		1,032.3	1,031.3	9
13	1,443.4		1,426.4	1,425.4	C+58	962.3		945.3	944.3	8
14	1,530.4		1,513.4	1,512.4	S	801.3		784.2	783.3	7
15	1,691.5		1,674.4	1,673.5	C+58	714.2		697.2	696.2	6
16	1,762.5		1,745.5	1,744.5	A	553.2		536.2	535.2	5
17	1,849.5		1,832.5	1,831.5	S	482.2		465.2	464.2	4
18	1,936.6		1,919.5	1,918.6	S	395.2		378.1	377.1	3
19	2,097.6		2,080.6	2,079.6	C+58	308.1		291.1		2
20	2,243.7		2,226.7	2,225.7	K	147.1		130.1		1

Supplemental Figure 6. MT-1L (¹⁵N) MSMS for synthesized human peptide.



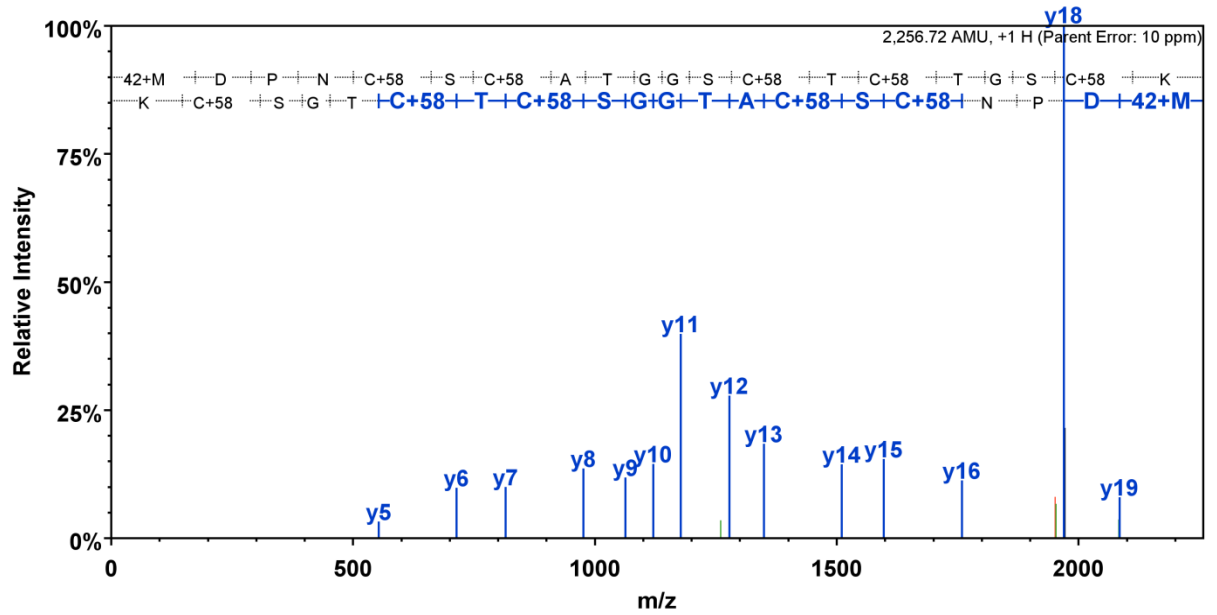
B	B Ions	B+2H	B-NH3	B-H2O	AA	Y Ions	Y+2H	Y-NH3	Y-H2O	Y
1	174.1				M+42	2,423.8		2,406.7	2,405.8	21
2	289.1			271.1	D	2,250.7		2,233.7	2,232.7	20
3	386.1			368.1	P	2,135.7		2,118.7	2,117.7	19
4	515.2			497.2	E	2,038.6		2,021.6	2,020.6	18
5	616.2			598.2	T	1,909.6		1,892.6	1,891.6	17
6	777.2			759.2	C+58	1,808.5		1,791.5	1,790.5	16
7	874.3			856.3	P	1,647.5		1,630.5	1,629.5	15
8	1,035.3			1,017.3	C+58	1,550.5		1,533.4	1,532.5	14
9	1,132.4			1,114.4	P	1,389.5		1,372.4	1,371.4	13
10	1,219.4			1,201.4	S	1,292.4		1,275.4	1,274.4	12
11	1,276.4			1,258.4	G	1,205.4		1,188.3	1,187.4	11
12	1,333.4			1,315.4	G	1,148.4		1,131.3	1,130.3	10
13	1,420.5			1,402.5	S	1,091.3		1,074.3	1,073.3	9
14	1,581.5			1,563.5	C+58	1,004.3		987.3	986.3	8
15	1,682.5			1,664.5	T	843.3		826.3	825.3	7
16	1,843.5			1,825.5	C+58	742.2		725.2	724.2	6
17	1,914.6			1,896.6	A	581.2		564.2	563.2	5
18	2,029.6			2,011.6	D	510.2		493.2	492.2	4
19	2,116.6			2,098.6	S	395.2		378.1	377.1	3
20	2,277.7			2,259.6	C+58	308.1		291.1		2
21	2,423.8		2,406.7	2,405.8	K	147.1		130.1		1

Supplemental Figure 7. MT-3 (^{15}N) MSMS for synthesized human peptide.



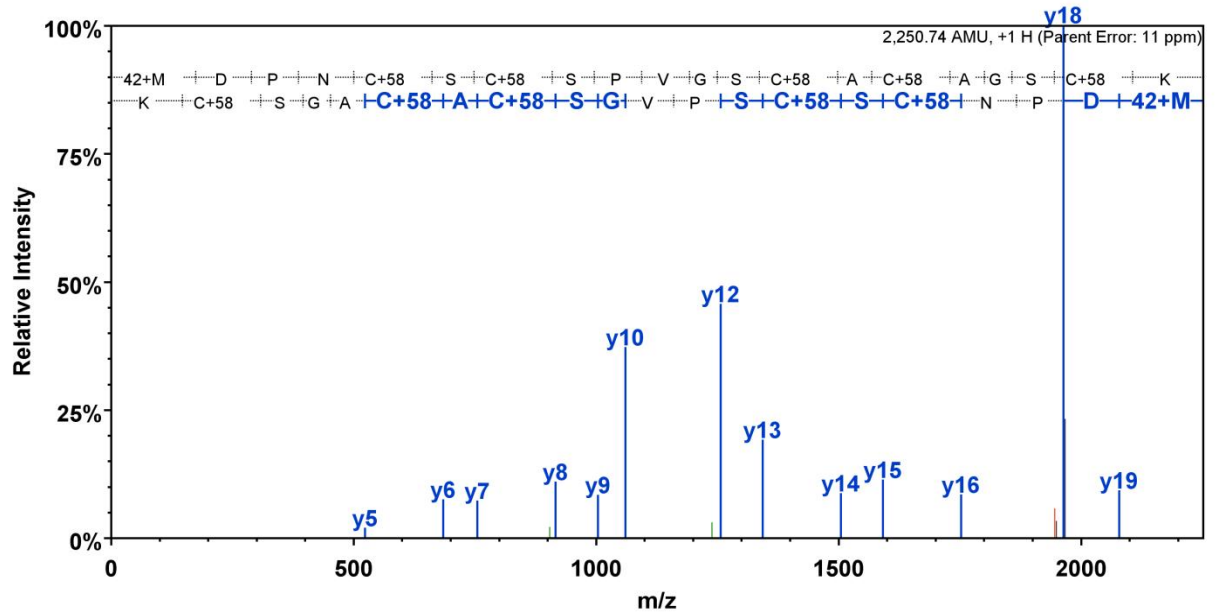
B	B Ions	B+2H	B-NH3	B-H2O	AA	Y Ions	Y+2H	Y-NH3	Y-H2O	Y
1	174.1				M+42	2,269.7		2,252.7	2,251.7	20
2	289.1			271.1	D	2,096.7		2,079.7	2,078.7	19
3	386.1			368.1	P	1,981.7		1,964.6	1,963.6	18
4	500.2		483.2	482.2	N	1,884.6		1,867.6	1,866.6	17
5	661.2		644.2	643.2	C+58	1,770.6		1,753.5	1,752.6	16
6	748.2		731.2	730.2	S	1,609.5		1,592.5	1,591.5	15
7	909.2		892.2	891.2	C+58	1,522.5		1,505.5	1,504.5	14
8	980.3		963.3	962.3	A	1,361.5		1,344.5	1,343.5	13
9	1,051.3		1,034.3	1,033.3	A	1,290.5		1,273.4	1,272.5	12
10	1,108.3		1,091.3	1,090.3	G	1,219.4		1,202.4	1,201.4	11
11	1,207.4		1,190.4	1,189.4	V	1,162.4		1,145.4	1,144.4	10
12	1,294.4		1,277.4	1,276.4	S	1,063.3		1,046.3	1,045.3	9
13	1,455.5		1,438.4	1,437.4	C+58	976.3		959.3	958.3	8
14	1,556.5		1,539.5	1,538.5	T	815.3		798.3	797.3	7
15	1,717.5		1,700.5	1,699.5	C+58	714.2		697.2	696.2	6
16	1,788.6		1,771.5	1,770.5	A	553.2		536.2	535.2	5
17	1,875.6		1,858.6	1,857.6	S	482.2		465.2	464.2	4
18	1,962.6		1,945.6	1,944.6	S	395.2		378.1	377.1	3
19	2,123.6		2,106.6	2,105.6	C+58	308.1		291.1		2
20	2,269.7		2,252.7	2,251.7	K	147.1		130.1		1

Supplemental Figure 8. MT-1G2 (¹⁵N) MSMS for synthesized human peptide.



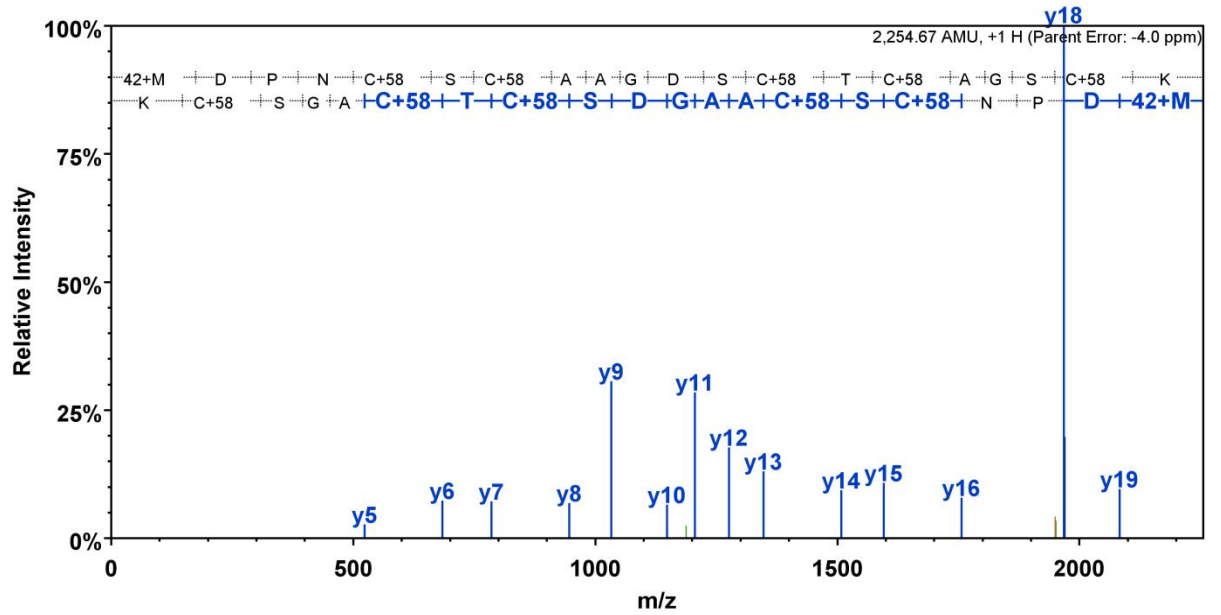
B	B Ions	B+2H	B-NH3	B-H2O	AA	Y Ions	Y+2H	Y-NH3	Y-H2O	Y
1	174.1				M+42	2,257.7		2,240.7	2,239.7	20
2	289.1			271.1	D	2,084.6		2,067.6	2,066.6	19
3	386.1			368.1	P	1,969.6		1,952.6	1,951.6	18
4	500.2		483.2	482.2	N	1,872.6		1,855.5	1,854.6	17
5	661.2		644.2	643.2	C+58	1,758.5		1,741.5	1,740.5	16
6	748.2		731.2	730.2	S	1,597.5		1,580.5	1,579.5	15
7	909.2		892.2	891.2	C+58	1,510.5		1,493.5	1,492.5	14
8	980.3		963.3	962.3	A	1,349.5		1,332.4	1,331.5	13
9	1,081.3		1,064.3	1,063.3	T	1,278.4		1,261.4	1,260.4	12
10	1,138.3		1,121.3	1,120.3	G	1,177.4		1,160.4	1,159.4	11
11	1,195.4		1,178.3	1,177.4	G	1,120.4		1,103.3	1,102.3	10
12	1,282.4		1,265.4	1,264.4	S	1,063.3		1,046.3	1,045.3	9
13	1,443.4		1,426.4	1,425.4	C+58	976.3		959.3	958.3	8
14	1,544.5		1,527.4	1,526.5	T	815.3		798.3	797.3	7
15	1,705.5		1,688.5	1,687.5	C+58	714.2		697.2	696.2	6
16	1,806.5		1,789.5	1,788.5	T	553.2		536.2	535.2	5
17	1,863.5		1,846.5	1,845.5	G	452.2		435.2	434.2	4
18	1,950.6		1,933.6	1,932.6	S	395.2		378.1	377.1	3
19	2,111.6		2,094.6	2,093.6	C+58	308.1		291.1		2
20	2,257.7		2,240.7	2,239.7	K	147.1		130.1		1

Supplemental Figure 9. MT-1A (¹⁵N) MSMS for synthesized human peptide.



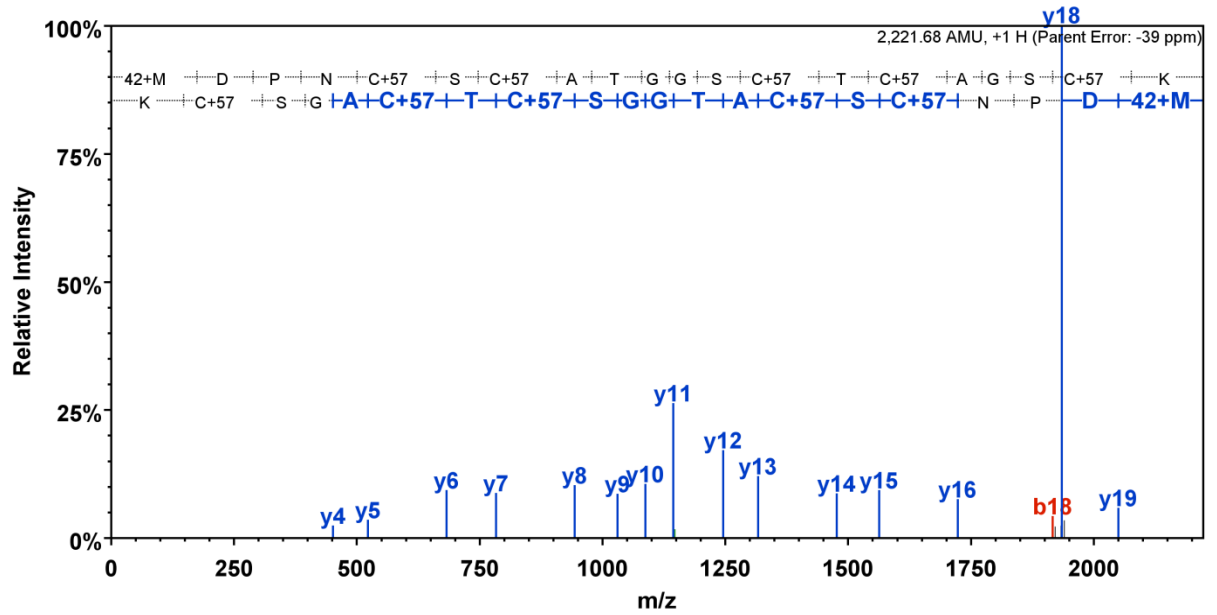
B	B Ions	B+2H	B-NH3	B-H2O	AA	Y Ions	Y+2H	Y-NH3	Y-H2O	Y
1	174.1				M+42	2,251.7		2,234.7	2,233.7	20
2	289.1			271.1	D	2,078.7		2,061.6	2,060.7	19
3	386.1			368.1	P	1,963.6		1,946.6	1,945.6	18
4	500.2		483.2	482.2	N	1,866.6		1,849.6	1,848.6	17
5	661.2		644.2	643.2	C+58	1,752.6		1,735.5	1,734.5	16
6	748.2		731.2	730.2	S	1,591.5		1,574.5	1,573.5	15
7	909.2		892.2	891.2	C+58	1,504.5		1,487.5	1,486.5	14
8	996.3		979.2	978.3	S	1,343.5		1,326.5	1,325.5	13
9	1,093.3		1,076.3	1,075.3	P	1,256.5		1,239.4	1,238.4	12
10	1,192.4		1,175.4	1,174.4	V	1,159.4		1,142.4	1,141.4	11
11	1,249.4		1,232.4	1,231.4	G	1,060.3		1,043.3	1,042.3	10
12	1,336.4		1,319.4	1,318.4	S	1,003.3		986.3	985.3	9
13	1,497.5		1,480.4	1,479.5	C+58	916.3		899.3	898.3	8
14	1,568.5		1,551.5	1,550.5	A	755.3		738.2	737.3	7
15	1,729.5		1,712.5	1,711.5	C+58	684.2		667.2	666.2	6
16	1,800.6		1,783.5	1,782.5	A	523.2		506.2	505.2	5
17	1,857.6		1,840.5	1,839.6	G	452.2		435.2	434.2	4
18	1,944.6		1,927.6	1,926.6	S	395.2		378.1	377.1	3
19	2,105.6		2,088.6	2,087.6	C+58	308.1		291.1		2
20	2,251.7		2,234.7	2,233.7	K	147.1		130.1		1

Supplemental Figure 10. MT-1X (¹⁵N) MSMS for synthesized human peptide.



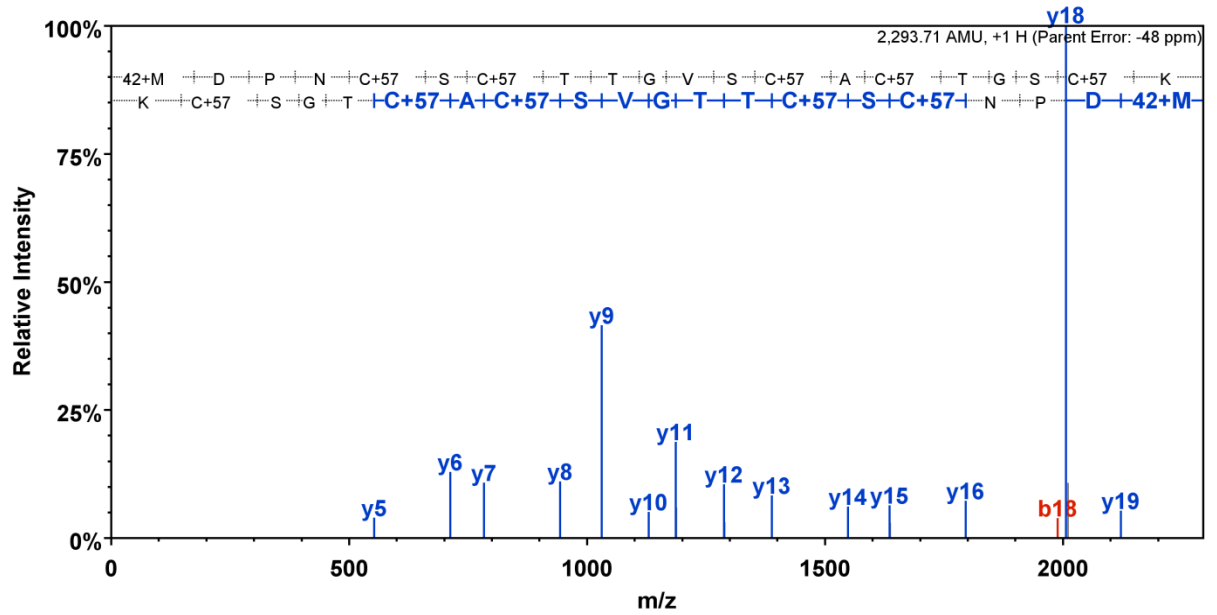
B	B Ions	B+2H	B-NH3	B-H2O	AA	Y Ions	Y+2H	Y-NH3	Y-H2O	Y
1	174.1				M+42	2,255.7		2,238.7	2,237.7	20
2	289.1			271.1	D	2,082.6		2,065.6	2,064.6	19
3	386.1			368.1	P	1,967.6		1,950.6	1,949.6	18
4	500.2		483.2	482.2	N	1,870.6		1,853.5	1,852.5	17
5	661.2		644.2	643.2	C+58	1,756.5		1,739.5	1,738.5	16
6	748.2		731.2	730.2	S	1,595.5		1,578.5	1,577.5	15
7	909.2		892.2	891.2	C+58	1,508.5		1,491.4	1,490.5	14
8	980.3		963.3	962.3	A	1,347.4		1,330.4	1,329.4	13
9	1,051.3		1,034.3	1,033.3	A	1,276.4		1,259.4	1,258.4	12
10	1,108.3		1,091.3	1,090.3	G	1,205.4		1,188.3	1,187.4	11
11	1,223.4		1,206.3	1,205.4	D	1,148.4		1,131.3	1,130.3	10
12	1,310.4		1,293.4	1,292.4	S	1,033.3		1,016.3	1,015.3	9
13	1,471.4		1,454.4	1,453.4	C+58	946.3		929.3	928.3	8
14	1,572.5		1,555.4	1,554.4	T	785.3		768.3	767.3	7
15	1,733.5		1,716.4	1,715.5	C+58	684.2		667.2	666.2	6
16	1,804.5		1,787.5	1,786.5	A	523.2		506.2	505.2	5
17	1,861.5		1,844.5	1,843.5	G	452.2		435.2	434.2	4
18	1,948.6		1,931.5	1,930.6	S	395.2		378.1	377.1	3
19	2,109.6		2,092.6	2,091.6	C+58	308.1		291.1		2
20	2,255.7		2,238.7	2,237.7	K	147.1		130.1		1

Supplemental Figure 11. MT-2 (¹⁵N) MSMS for synthesized human peptide.



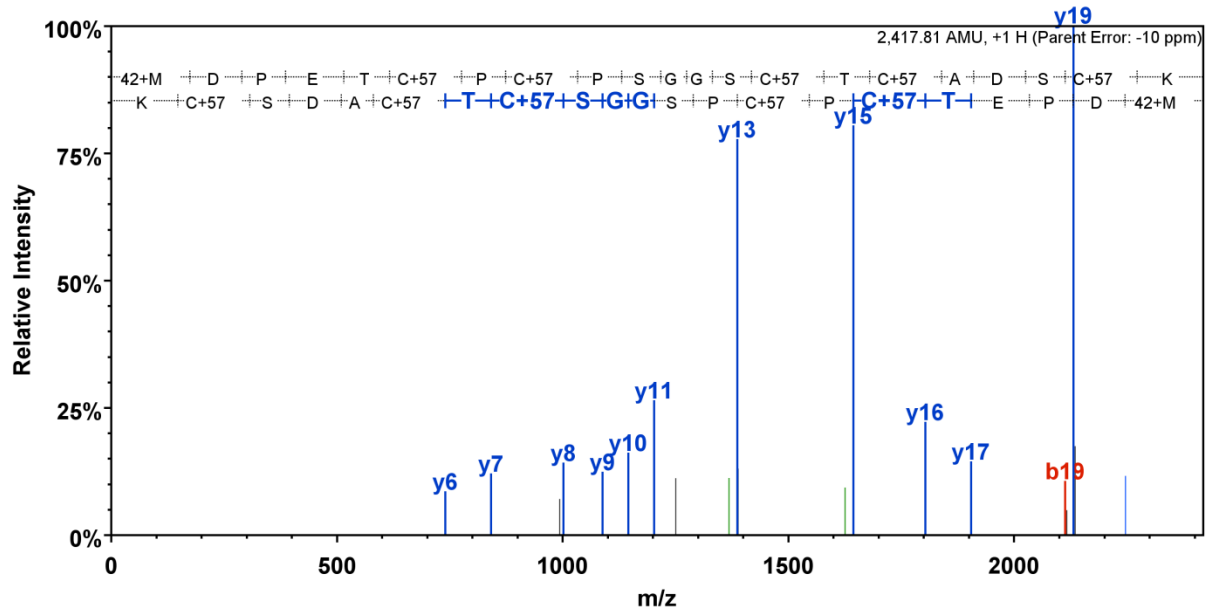
B	B Ions	B+2H	B-NH3	B-H2O	AA	Y Ions	Y+2H	Y-NH3	Y-H2O	Y
1	174.1				M+42	2,222.8		2,205.7	2,204.8	20
2	289.1			271.1	D	2,049.7		2,032.7	2,031.7	19
3	386.1			368.1	P	1,934.7		1,917.7	1,916.7	18
4	500.2		483.2	482.2	N	1,837.6		1,820.6	1,819.6	17
5	660.2		643.2	642.2	C+57	1,723.6		1,706.6	1,705.6	16
6	747.2		730.2	729.2	S	1,563.6		1,546.5	1,545.6	15
7	907.3		890.2	889.3	C+57	1,476.5		1,459.5	1,458.5	14
8	978.3		961.3	960.3	A	1,316.5		1,299.5	1,298.5	13
9	1,079.4		1,062.3	1,061.3	T	1,245.5		1,228.4	1,227.5	12
10	1,136.4		1,119.4	1,118.4	G	1,144.4		1,127.4	1,126.4	11
11	1,193.4		1,176.4	1,175.4	G	1,087.4		1,070.4	1,069.4	10
12	1,280.4		1,263.4	1,262.4	S	1,030.4		1,013.3	1,012.4	9
13	1,440.5		1,423.4	1,422.5	C+57	943.3		926.3	925.3	8
14	1,541.5		1,524.5	1,523.5	T	783.3		766.3	765.3	7
15	1,701.5		1,684.5	1,683.5	C+57	682.3		665.2	664.3	6
16	1,772.6		1,755.6	1,754.6	A	522.2		505.2	504.2	5
17	1,829.6		1,812.6	1,811.6	G	451.2		434.2	433.2	4
18	1,916.6		1,899.6	1,898.6	S	394.2		377.1	376.2	3
19	2,076.7		2,059.6	2,058.7	C+57	307.1		290.1		2
20	2,222.8		2,205.7	2,204.8	K	147.1		130.1		1

Supplemental Figure 13. Endogenous MT-1E (¹⁴N) MSMS.



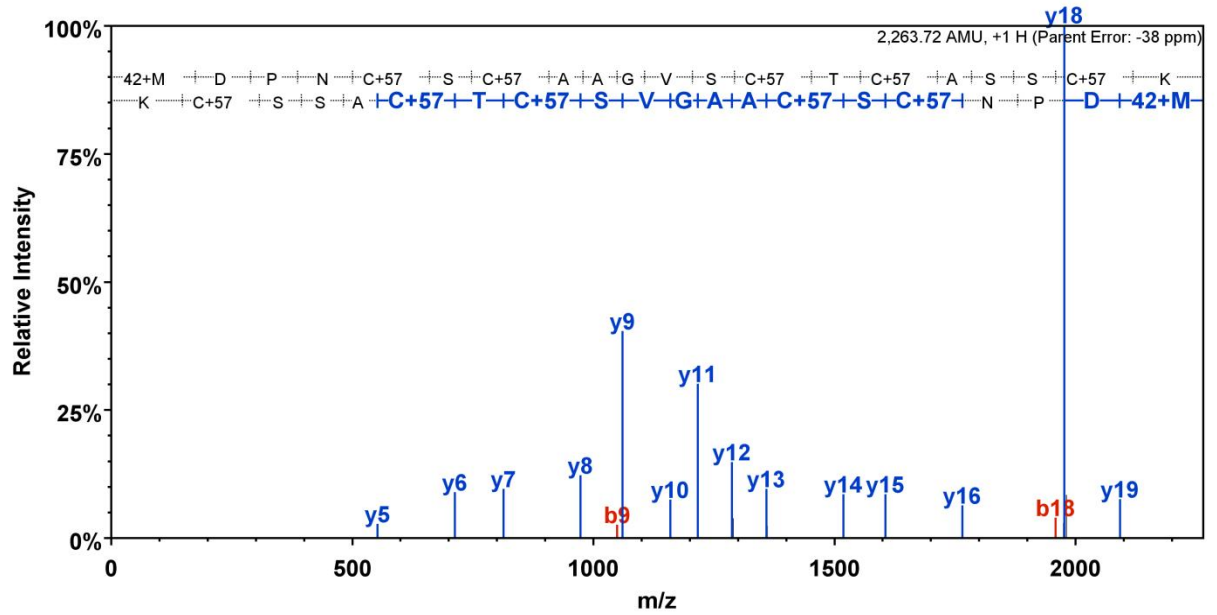
B	B Ions	B+2H	B-NH3	B-H2O	AA	Y Ions	Y+2H	Y-NH3	Y-H2O	Y
1	174.1				M+42	2,294.8		2,277.8	2,276.8	20
2	289.1			271.1	D	2,121.8		2,104.7	2,103.8	19
3	386.1			368.1	P	2,006.7		1,989.7	1,988.7	18
4	500.2		483.2	482.2	N	1,909.7		1,892.7	1,891.7	17
5	660.2		643.2	642.2	C+57	1,795.7		1,778.6	1,777.6	16
6	747.2		730.2	729.2	S	1,635.6		1,618.6	1,617.6	15
7	907.3		890.2	889.3	C+57	1,548.6		1,531.6	1,530.6	14
8	1,008.3		991.3	990.3	T	1,388.6		1,371.5	1,370.5	13
9	1,109.4		1,092.3	1,091.4	T	1,287.5		1,270.5	1,269.5	12
10	1,166.4		1,149.4	1,148.4	G	1,186.5		1,169.4	1,168.5	11
11	1,265.5		1,248.4	1,247.4	V	1,129.4		1,112.4	1,111.4	10
12	1,352.5		1,335.5	1,334.5	S	1,030.4		1,013.3	1,012.4	9
13	1,512.5		1,495.5	1,494.5	C+57	943.3		926.3	925.3	8
14	1,583.6		1,566.5	1,565.5	A	783.3		766.3	765.3	7
15	1,743.6		1,726.6	1,725.6	C+57	712.3		695.2	694.3	6
16	1,844.6		1,827.6	1,826.6	T	552.2		535.2	534.2	5
17	1,901.7		1,884.6	1,883.6	G	451.2		434.2	433.2	4
18	1,988.7		1,971.7	1,970.7	S	394.2		377.1	376.2	3
19	2,148.7		2,131.7	2,130.7	C+57	307.1		290.1		2
20	2,294.8		2,277.8	2,276.8	K	147.1		130.1		1

Supplemental Figure 14. Endogenous MT-1M (¹⁴N) MSMS.



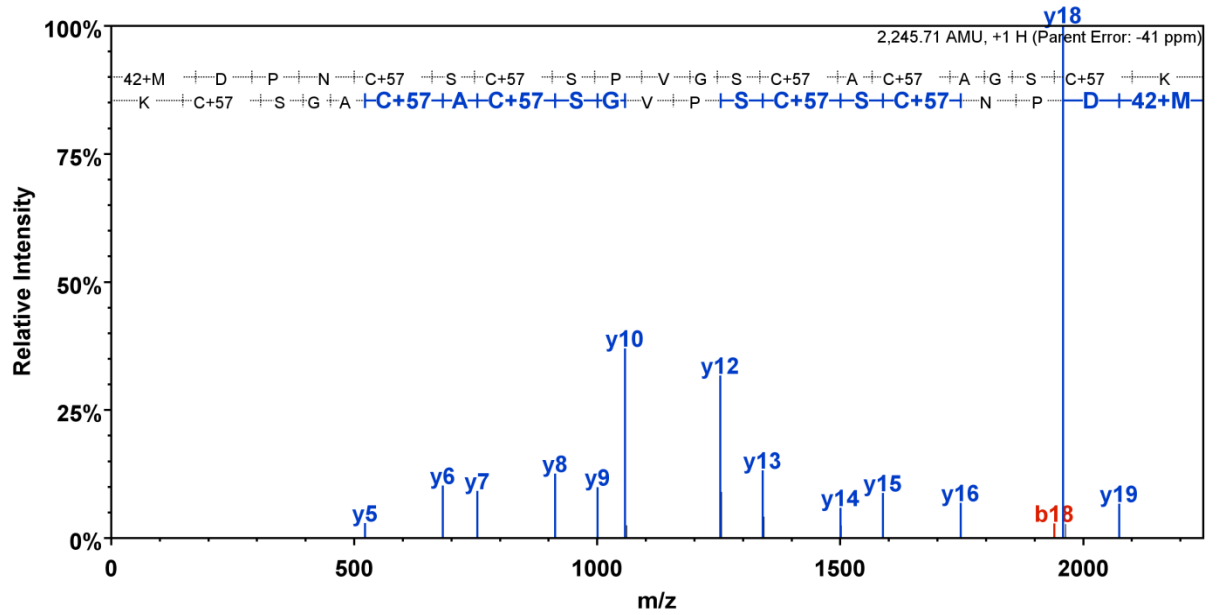
B	B Ions	B+2H	B-NH3	B-H2O	AA	Y Ions	Y+2H	Y-NH3	Y-H2O	Y
1	174.1				M+42	2,418.8		2,401.8	2,400.8	21
2	289.1			271.1	D	2,245.8		2,228.8	2,227.8	20
3	386.1			368.1	P	2,130.8		2,113.7	2,112.8	19
4	515.2			497.2	E	2,033.7		2,016.7	2,015.7	18
5	616.2			598.2	T	1,904.7		1,887.6	1,886.7	17
6	776.3			758.2	C+57	1,803.6		1,786.6	1,785.6	16
7	873.3			855.3	P	1,643.6		1,626.6	1,625.6	15
8	1,033.3			1,015.3	C+57	1,546.5		1,529.5	1,528.5	14
9	1,130.4			1,112.4	P	1,386.5		1,369.5	1,368.5	13
10	1,217.4			1,199.4	S	1,289.5		1,272.4	1,271.4	12
11	1,274.4			1,256.4	G	1,202.4		1,185.4	1,184.4	11
12	1,331.5			1,313.5	G	1,145.4		1,128.4	1,127.4	10
13	1,418.5			1,400.5	S	1,088.4		1,071.4	1,070.4	9
14	1,578.5			1,560.5	C+57	1,001.3		984.3	983.3	8
15	1,679.6			1,661.6	T	841.3		824.3	823.3	7
16	1,839.6			1,821.6	C+57	740.3		723.2	722.3	6
17	1,910.6			1,892.6	A	580.2		563.2	562.2	5
18	2,025.7			2,007.7	D	509.2		492.2	491.2	4
19	2,112.7			2,094.7	S	394.2		377.1	376.2	3
20	2,272.7			2,254.7	C+57	307.1		290.1		2
21	2,418.8		2,401.8	2,400.8	K	147.1		130.1		1

Supplemental Figure 15. Endogenous MT-3 (¹⁴N) MSMS.



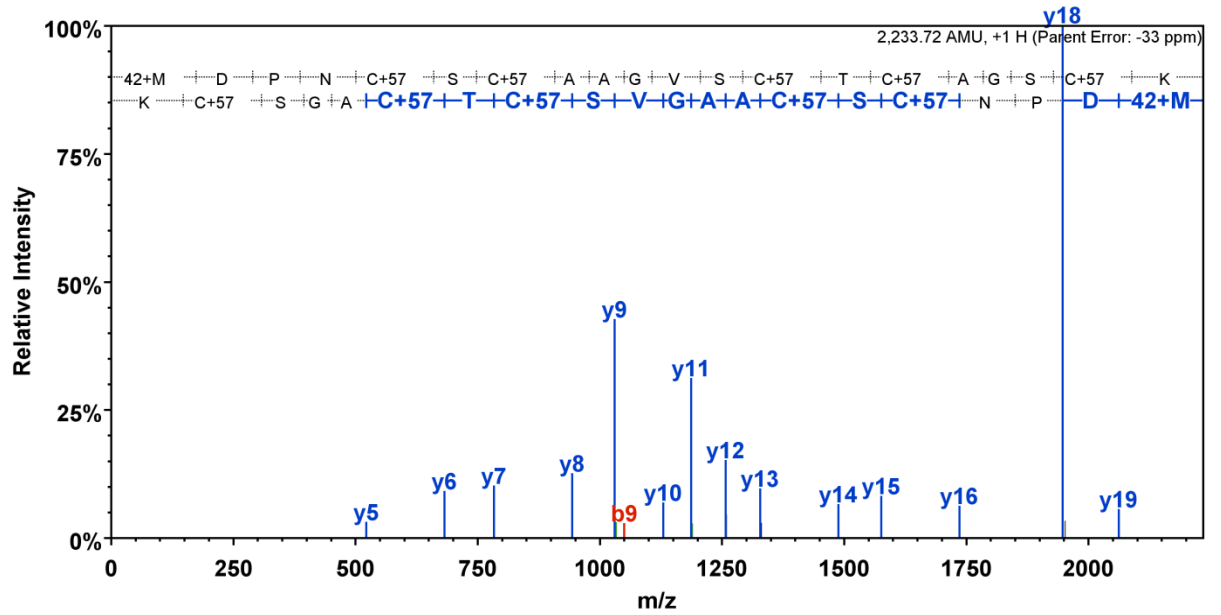
B	B Ions	B+2H	B-NH3	B-H2O	AA	Y Ions	Y+2H	Y-NH3	Y-H2O	Y
1	174.1				M+42	2,264.8		2,247.8	2,246.8	20
2	289.1			271.1	D	2,091.8		2,074.7	2,073.8	19
3	386.1			368.1	P	1,976.7		1,959.7	1,958.7	18
4	500.2		483.2	482.2	N	1,879.7		1,862.7	1,861.7	17
5	660.2		643.2	642.2	C+57	1,765.6		1,748.6	1,747.6	16
6	747.2		730.2	729.2	S	1,605.6		1,588.6	1,587.6	15
7	907.3		890.2	889.3	C+57	1,518.6		1,501.6	1,500.6	14
8	978.3		961.3	960.3	A	1,358.5		1,341.5	1,340.5	13
9	1,049.3		1,032.3	1,031.3	A	1,287.5		1,270.5	1,269.5	12
10	1,106.4		1,089.3	1,088.4	G	1,216.5		1,199.4	1,198.5	11
11	1,205.4		1,188.4	1,187.4	V	1,159.5		1,142.4	1,141.4	10
12	1,292.5		1,275.4	1,274.5	S	1,060.4		1,043.4	1,042.4	9
13	1,452.5		1,435.5	1,434.5	C+57	973.4		956.3	955.3	8
14	1,553.5		1,536.5	1,535.5	T	813.3		796.3	795.3	7
15	1,713.6		1,696.6	1,695.6	C+57	712.3		695.2	694.3	6
16	1,784.6		1,767.6	1,766.6	A	552.2		535.2	534.2	5
17	1,871.6		1,854.6	1,853.6	S	481.2		464.2	463.2	4
18	1,958.7		1,941.7	1,940.7	S	394.2		377.1	376.2	3
19	2,118.7		2,101.7	2,100.7	C+57	307.1		290.1		2
20	2,264.8		2,247.8	2,246.8	K	147.1		130.1		1

Supplemental Figure 16. Endogenous MT-1G2 (¹⁴N) MSMS.



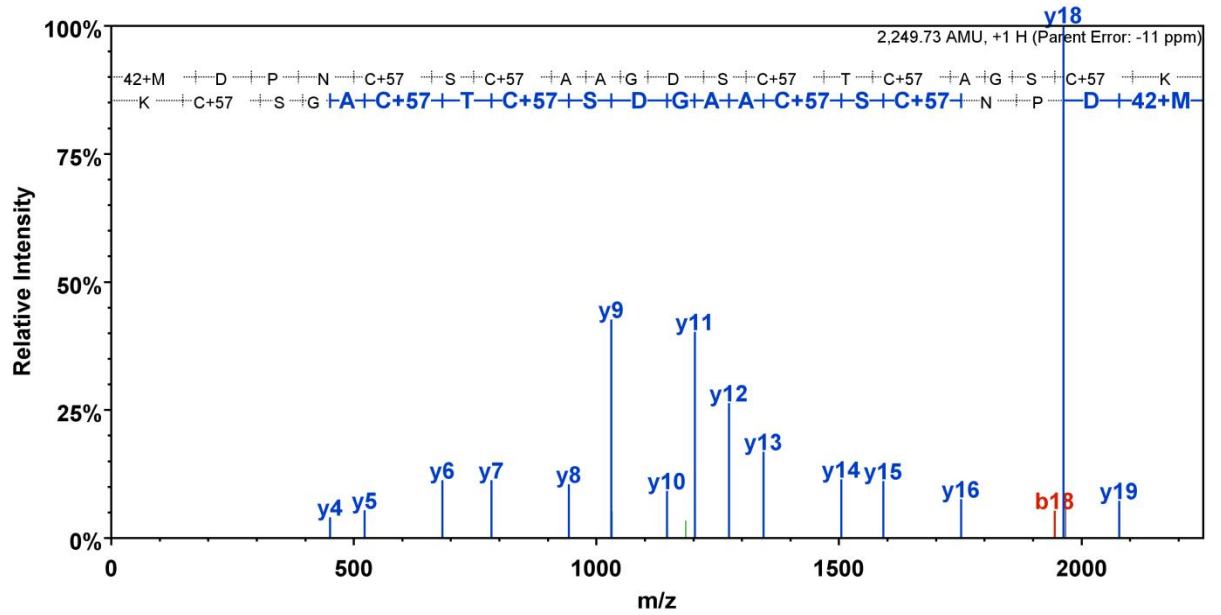
B	B Ions	B+2H	B-NH3	B-H2O	AA	Y Ions	Y+2H	Y-NH3	Y-H2O	Y
1	174.1				M+42	2,246.8		2,229.8	2,228.8	20
2	289.1			271.1	D	2,073.8		2,056.7	2,055.7	19
3	386.1			368.1	P	1,958.7		1,941.7	1,940.7	18
4	500.2		483.2	482.2	N	1,861.7		1,844.6	1,843.7	17
5	660.2		643.2	642.2	C+57	1,747.6		1,730.6	1,729.6	16
6	747.2		730.2	729.2	S	1,587.6		1,570.6	1,569.6	15
7	907.3		890.2	889.3	C+57	1,500.6		1,483.5	1,482.6	14
8	994.3		977.3	976.3	S	1,340.5		1,323.5	1,322.5	13
9	1,091.4		1,074.3	1,073.3	P	1,253.5		1,236.5	1,235.5	12
10	1,190.4		1,173.4	1,172.4	V	1,156.5		1,139.4	1,138.4	11
11	1,247.4		1,230.4	1,229.4	G	1,057.4		1,040.4	1,039.4	10
12	1,334.5		1,317.5	1,316.5	S	1,000.4		983.3	982.4	9
13	1,494.5		1,477.5	1,476.5	C+57	913.3		896.3	895.3	8
14	1,565.5		1,548.5	1,547.5	A	753.3		736.3	735.3	7
15	1,725.6		1,708.6	1,707.6	C+57	682.3		665.2	664.3	6
16	1,796.6		1,779.6	1,778.6	A	522.2		505.2	504.2	5
17	1,853.6		1,836.6	1,835.6	G	451.2		434.2	433.2	4
18	1,940.7		1,923.6	1,922.7	S	394.2		377.1	376.2	3
19	2,100.7		2,083.7	2,082.7	C+57	307.1		290.1		2
20	2,246.8		2,229.8	2,228.8	K	147.1		130.1		1

Supplemental Figure 17. Endogenous MT-1X (¹⁴N) MSMS.



B	B Ions	B+2H	B-NH3	B-H2O	AA	Y Ions	Y+2H	Y-NH3	Y-H2O	Y
1	174.1				M+42	2,234.8		2,217.8	2,216.8	20
2	289.1			271.1	D	2,061.8		2,044.7	2,043.7	19
3	386.1			368.1	P	1,946.7		1,929.7	1,928.7	18
4	500.2		483.2	482.2	N	1,849.7		1,832.6	1,831.7	17
5	660.2		643.2	642.2	C+57	1,735.6		1,718.6	1,717.6	16
6	747.2		730.2	729.2	S	1,575.6		1,558.6	1,557.6	15
7	907.3		890.2	889.3	C+57	1,488.6		1,471.5	1,470.6	14
8	978.3		961.3	960.3	A	1,328.5		1,311.5	1,310.5	13
9	1,049.3		1,032.3	1,031.3	A	1,257.5		1,240.5	1,239.5	12
10	1,106.4		1,089.3	1,088.4	G	1,186.5		1,169.4	1,168.5	11
11	1,205.4		1,188.4	1,187.4	V	1,129.4		1,112.4	1,111.4	10
12	1,292.5		1,275.4	1,274.5	S	1,030.4		1,013.3	1,012.4	9
13	1,452.5		1,435.5	1,434.5	C+57	943.3		926.3	925.3	8
14	1,553.5		1,536.5	1,535.5	T	783.3		766.3	765.3	7
15	1,713.6		1,696.6	1,695.6	C+57	682.3		665.2	664.3	6
16	1,784.6		1,767.6	1,766.6	A	522.2		505.2	504.2	5
17	1,841.6		1,824.6	1,823.6	G	451.2		434.2	433.2	4
18	1,928.7		1,911.6	1,910.7	S	394.2		377.1	376.2	3
19	2,088.7		2,071.7	2,070.7	C+57	307.1		290.1		2
20	2,234.8		2,217.8	2,216.8	K	147.1		130.1		1

Supplemental Figure 18. Endogenous MT-1F (¹⁴N) MSMS.



B	B Ions	B+2H	B-NH3	B-H2O	AA	Y Ions	Y+2H	Y-NH3	Y-H2O	Y
1	174.1				M+42	2,250.8		2,233.7	2,232.8	20
2	289.1			271.1	D	2,077.7		2,060.7	2,059.7	19
3	386.1			368.1	P	1,962.7		1,945.7	1,944.7	18
4	500.2		483.2	482.2	N	1,865.6		1,848.6	1,847.6	17
5	660.2		643.2	642.2	C+57	1,751.6		1,734.6	1,733.6	16
6	747.2		730.2	729.2	S	1,591.6		1,574.5	1,573.5	15
7	907.3		890.2	889.3	C+57	1,504.5		1,487.5	1,486.5	14
8	978.3		961.3	960.3	A	1,344.5		1,327.5	1,326.5	13
9	1,049.3		1,032.3	1,031.3	A	1,273.5		1,256.4	1,255.5	12
10	1,106.4		1,089.3	1,088.4	G	1,202.4		1,185.4	1,184.4	11
11	1,221.4		1,204.4	1,203.4	D	1,145.4		1,128.4	1,127.4	10
12	1,308.4		1,291.4	1,290.4	S	1,030.4		1,013.3	1,012.4	9
13	1,468.5		1,451.4	1,450.4	C+57	943.3		926.3	925.3	8
14	1,569.5		1,552.5	1,551.5	T	783.3		766.3	765.3	7
15	1,729.5		1,712.5	1,711.5	C+57	682.3		665.2	664.3	6
16	1,800.6		1,783.5	1,782.6	A	522.2		505.2	504.2	5
17	1,857.6		1,840.6	1,839.6	G	451.2		434.2	433.2	4
18	1,944.6		1,927.6	1,926.6	S	394.2		377.1	376.2	3
19	2,104.7		2,087.6	2,086.6	C+57	307.1		290.1		2
20	2,250.8		2,233.7	2,232.8	K	147.1		130.1		1

Supplemental Figure 19. Endogenous MT-2 (¹⁴N) MSMS.

BIBLIOGRAPHY

1. M. Margoshes, B.L. Vallee A cadmium protein from equine kidney cortex *J Am Chem Soc*, 79 (1957), pp. 4813–4814
2. Laukens D, Waeytens A, De Bleser, P, Cuvelier C, De Vos, Martin. (2009) Human metallothionein expression under normal and pathological conditions: mechanisms of gene regulation based on in silico promoter analysis. *Crit Rev Eukary Gene Express* 19:301-317.
3. Andrews GK. (2000) Regulation of metallothionein gene expression by oxidative stress and metal ions. *Biochem Pharmacol* 59:95-104.
4. Hamer DH. (1986) Metallothionein. *Ann Rev Biochem* 55:913-951.
5. Sakurai A, Hara S, Okano N, Kondo Y, Inoue J, Imura N. (1999) Regulatory role of metallothionein in NF-kappaB activation. *FEBS Lett* 455:55-58.
6. Kim CH, Kim JH, Lee J, Ahn YS. (2003) Zinc-induced NF-kappaB inhibition can be modulated by changes in the intracellular metallothionein level. *Toxicol Appl Pharmacol* 190:189-196.
7. Ostrakhovitch EA, Olsson PE, Jiang S, Cherian MG. (2006) Interaction of metallothionein with tumor suppressor p53 protein. *FEBS Lett* 580:1235-1238.
8. Zeng J, Heuchel R, Schaffner W, Kagi JH. (1991) Thionein (apometallothionein) can modulate DNA binding and transcriptional activation by zinc finger containing factor Sp1. *FEBS Lett* 279:310-312.
9. Schmidt CJ, Jubier MF, Hamer DH. (1985) Structure and expression of two human metallothionein-I isoform genes and a related pseudogene. *J Biol Chem* 260:7731-7737.
10. Andrews, G.K., (2000) Regulation of metallothionein gene expression by oxidative stress and metal ions. *Biochem Pharmacol*. 59, 95-104.
11. P.J. Thornalley, M. Vašák. (1985) Possible role for metallothionein in protection against radiation induced oxidative stress. Kinetics and mechanism of its reaction with superoxide and hydroxyl radicals *Biochim Biophys Acta*, 827 pp. 36–44.
12. Albrecht A.L., Singh R.K., Somji S., Sens M.A., Sens D.A., Garrett S.H. (2008) Basal and metal-induced expression of metallothionein isoform 1 and 2 genes in the RWPE-1 human prostate epithelial cell line. *J. Appl. Toxicol.* 28:283–293.
13. Penkowa M., Giralt M., Thomsen P. S., Carrasco J., Hidalgo J. (2001) Zinc or copper deficiency-induced impaired inflammatory response to brain trauma may be caused by the concomitant metallothionein changes. *J. Neurotrauma* 18, 447–463
14. Hamer, D.H., (1986), Metallothionein1,2. *Annual Review of Biochemistry*. 55, 913-951.

15. Gasull T., Giralt M., Hernandez J., Martinez P., Bremner I., Hidalgo J. (1994) Regulation of metallothionein concentrations in rat brain. Effect of glucocorticoids, zinc, copper, and endotoxin. *Am. J. Physiol.* 266, E760–E767
16. Penkowa M., Moos T., Carrasco J., Hadberg H., Molinero A., Bluethmann H., Hidalgo J. (1999) Strongly compromised inflammatory response to brain injury in interleukin-6-deficient mice. *Glia* 25, 343–357
17. Carrasco J., Hernandez J., Gonzalez B., Campbell I. L., Hidalgo J. (1998) Localization of metallothionein-I and -III expression in the CNS of transgenic mice with astrocyte-targeted expression of interleukin 6. *Exp. Neurol.* 153, 184–194
18. Cherian MG, Jayasurya A, Bay B-H: Metallothioneins in human tumors and potential roles in carcinogenesis. *Mut Res* 2003, 533:201-209.
19. Kim JH, Nam YP, Jeon SM, Han HS, Suk K. (2012) Amyloid neurotoxicity is attenuated by metallothionein: dual mechanisms at work. *J Neurochem.* 121(5):751-62
20. Ghanizadeh A: Gold implants and increased expression of metallothionein-I/II as a novel hypothesized therapeutic approach for autism. *Toxicology* 2011, 283(1):63-64.
21. Hashimoto K, Hayashi Y, Watabe K, Inuzuka T, Hozumi I. (2011) Metallothionein-III prevents neuronal death and prolongs life span in amyotrophic lateral sclerosis model mice. *Neuroscience.* 189:293-8.
22. Michael GJ, Esmailzadeh S, Moran LB, Christian L, Pearce RK, Graeber MB. Up-regulation of metallothionein gene expression in parkinsonian astrocytes. *Neurogenetics.* 2011;12(4):295–305.
23. Vidal E, Acin C, Foradada L, Monzon M, Marquez M, Monleon E, Pumarola M, Badiola JJ, Bolea R: Immunohistochemical characterisation of classical scrapie neuropathology in sheep. *J Comp Pathol* 2009, 141:135-146
24. Pedersen MO, Larsen A, Stoltenberg M, Penkowa M: The role of metallothionein in oncogenesis and cancer prognosis. *Prog Histochem Cytochem* 2009, 44(1):29-64.
25. Hoey JG, Garrett SH, Sens MA, Todd JH, Sens DA: Expression of MT-3 mRNA in human kidney, proximal tubule cell cultures, and renal cell carcinoma. *Toxicol Lett* 1997, 92:149-160.
26. Garrett SH, Sens MA, Todd JH, Somji S, Sens DA: Expression of MT-3 protein in the human kidney. *Toxicol Lett* 1999, 105:207-214.
27. Somji S, Garret SH, Toni C, Zhou XD, Zheng Y, Ajjimaporn, A, Sens MS, Sens DA: Differences in the epigenetic regulation of MT-3 gene expression between parental and Cd⁺² or As⁺³ transformed human urothelial cells. *Cancer Cell Int* 2011; 11:2.
28. Sens MA, Somji S, Lamm DL, Garrett SH, Slovinsky F, et al. (2000) Metallothionein isoform 3 as a potential biomarker for human bladder cancer. *Environ Health Perspect* 108: 413–418.
29. Friedline, J. A., S. H. Garrett, S. Somji, J. H. Todd, and D. A. Sens. 1998. Differential expression of the MT-1E gene in estrogen-receptor-positive and -negative human breast cancer cell lines. *Am. J. Pathol.* 152:23-27.
30. Jin R, Bay BH, Chow VTK, et al. Metallothionein 1E mRNA is highly expressed in oestrogen receptor-negative human invasive ductal breast cancer. *Br J Cancer* 2000;83:319–23.

31. Jin R, Chow VT, Tan PH, Dheen ST, Duan W, Bay BH. Metallothionein 2A expression is associated with cell proliferation in breast cancer. *Carcinogenesis* 2002; 23:81-6.
32. Garrett SH, Sens MA, Todd JH, Somji S, Sens DA. (1999). Expression of MT-3 protein in the human kidney. *Toxicol Lett* 105:207-214.
33. Jasani B, Schmid KW. (1997). Significance of metallothionein overexpression in human tumours. *Histopathology* 31:211-214.
34. Theocharis SE, Margeli, AP, Klijanienko JT, Kouraklis GP. (2004). Metallothionein expression in human neoplasia. *Histopathology* 45:103-118.
35. Namdarghanbari M, Wobig W, Krezoski S, Tabatabai NM, Petering DH. (2011). Mammalian metallothionein in toxicology, cancer, and cancer chemotherapy. *J Biol Inorgan Chem* 16:1087-1101.
36. Mididoddi S, McGuirt JP, Sens MA, Todd JH, Sens DA (1996). Isoform-specific expression of metallothionein mRNA in the developing and adult human kidney. *Toxicol Lett* 85:17-27.
37. Arriaga JM, Levy ES, Bravo AI, Bayo SM, Amat M, Aris M, Hannois A, Bruno L, Roberti MP, Loria FS, Pairola A, Huertas E, Mordon J, Bianchini M. (2011). Metallothionein expression in colorectal cancer: relevance for different isoforms for tumor progression and patient survival. *Human Pathol* 43:197-208.
38. Wang R, Sens DA, Albrecht A, Garrett S, Somji S, Sens MA, and Lu X (2007) Simple method for identification for metallothionein isoforms in cultured human prostate cells by MALDI-TOF/TOF mass spectrometry. *Anal Chem* 79:4433-4441.
39. Huang I-Y, Kimura M, Hata A, Tsunoo H and Yoshida A (1981) Complete amino acid sequence of mouse liver metallothionein-II. *J Biochem* 89:1839-1845
40. Huang I-Y, Yoshida A, Tsunoo H, and Nakajima H (1977) Mouse liver metallothioneins: complete amino acid sequence of Metallothionein-I. *J Biol Chem* 252:8217-8221
41. Kissling MM and Kägi JHR (1977) Primary structure of human hepatic metallothionein. *FEBS Lett* 82:274-250
42. Kojima Y, Berger C, Vallee BL and Kägi JHR (1976) Amino acid sequence of equine renal metallothionein-1B. *Proc Natl Acad Sci USA* 73:3413-3417
43. Winge DR, Nielson KB, Zeikus RD, and Gray WR (1984) Structural characterization of the isoforms of neonatal and adult rat liver metallothionein. *J Biol Chem* 259:11419-11425
44. Boissel J-P, Kasper T, and Bunn HF (1988) Cotranslational amino-terminal processing of cytosolic proteins: cell-free expression of site-directed mutants of human hemoglobin. *J Biol Chem* 263:8443-8449
45. Arnesen T, Van Damme P, Polevoda B, Helsens K, Evjenth R, Colaert N, Varhaug JE, Vandekerckhove J, Lillehaug JR, Sherman F, and Gevaert K (2009) Proteomics analyses reveal the evolutionary conservation and divergence of N-terminal acetyltransferases from yeast and humans. *Proc Natl Acad Sci USA* 106:8157-8162
46. Helbig AO, Gauci S, Raijmakers R, van Breukelen B, Slijper M, Mohammed S, and Heck AJR (2010) *Mol Cell Proteomics* 9:928-939

47. Knudsen CB, Bjornsdottir I, Jons O, and Hansen SH (1998) Detection of metallothionein isoforms from three different species using on-line capillary electrophoresis-mass spectrometry. *Anal Biochem* 265:167-175
48. Beattie JH, Wood AM, and Duncan GJ (1999) Rat metallothionein-2 contains N-acetylated and unacetylated forms. *Electrophoresis* 20:1613-1618.
49. Van Vyncht G, Bordin A and Rodriguez AR (2000) Rabbit liver metallothionein subisoform characterization using liquid chromatography hyphenated to diode array detection and electrospray ionization mass spectrometry. *Chromatographia* 52:745-752
50. Andón B, Barbosa J, Sanz-Nebot V (2006) Separation and characterization of rabbit liver apothioneins by capillary electrophoresis coupled to electrospray ionization time-of-flight mass spectrometry. *Electrophoresis* 27:3661-3670
51. Ray WJ and Koshland DE (1962) Identification of amino acids involved in phosphoglucomutase action. *J Biol Chem* 237:2493-2505
52. Savige WE and Fontana A (1977) Interconversion of methionine and methionine sulfoxide. *Meth Enzymol* 47:453-459
53. Gross E (1967) The cyanogen bromide reaction. *Meth Enzymol* 11:238-255
54. Alvarez L, Gonzalez-Iglesias H, Garcia M, Ghosh S, Sanz-Medel A, and Coca-Prados M (2012) The stoichiometric transition from Zn₆Cu₁-metallothionein to Zn₇-metallothionein underlies the up-regulation of metallothionein (MT) expression: quantitative analysis of MT-metal load in eye cells. *J Biol Chem* 287:28456-28469
55. Mounicou S, Ouerdane L, L'Azou B, Passagne I, Ohayon-Courtès C, Szpunar J, and Lobinski R (2010) Identification of metallothionein subisoforms in HPLC using accurate mass and online sequencing by electrospray hybrid linear ion trap-orbital ion trap mass spectrometry. *Anal Chem* 82:6947-6957
56. Desiere F, Deutsch EW, Nesvizhskii AI, Mallick P, King NL, Eng JK, Adereem A, Boyle R, Brunner E, Donohoe S, Fausto N, Hafen E, Hood L, Katze MG, Kennedy KA, Kregenow F, Lee, H, Lin B, Martin D, Ranish JA, Rawlings DJ, Samelson LE, Shii Y, Watts JD, Wollscheid B, Wright ME, Yan W, Yang L, Yi EC, Zhang H, and Aebersold R (2004) Integration with the human genome of peptide sequences obtained by high-throughput mass spectrometry. *Genome Biol* 6:R9
57. Desiere F, Deutsch EW, King NL, Nesvizhskii AI, Mallick P, Eng J, Chen S, Edes J, Loevenich SN and Aebersold R (2006) The PeptideAtlas project. *Nucl Acids Res* 34:D655-D658
58. Beck M, Schmidt A, Malmstroem J, Claasen M, Ori A, Szymborska A, Herzog F, Rinner O, Ellengerg J, and Aebersold R (2011) The quantitative proteome of a human cell line. *Mol Syst Biol* 7:549
59. Geiger T, Wehner A, Schaab C, Cox J, and Mann M (2012) Comparative proteomic analysis of eleven common cell lines reveals ubiquitous but varying expression of most proteins. *Mol Cell Proteomics* 11:1-11
60. Munoz J, Low TY, Kok YJ, Chin A, Frese CK, Ding V, Choo A, and Heck AJR (2011) The quantitative proteomes of human induced pluripotent stem cells and embryonic stem cells. *Mol Syst Biol* 7:550

61. Nagaraj N, Wisniewski JR, Geiger T, Cox J, Kircher M, Kelso J, Pääbo S, and Mann M (2011) Deep proteome and transcriptome mapping of a human cancer cell line. *Mol Syst Biol* 7:548
62. Phanstiel DH, Brumbaugh J, Wenger CD, Tian S, Probasco MD, Bailey DJ, Swaney DL, Tervo MA, Bolin JM, Ruotti V, Stewart R, Thomson JA, and Coon JJ (2011) Phosphoproteomic comparison of human ES and iPS cells. *Nat Meth* 8:821-827
63. Gevaert, K., Goethals, M., Martens, L., Van Damme, J., Staes, A., Thomas, G.R. and Vandekerckhove, J. (2003) Exploring proteomes and analyzing protein processing by mass spectrometric identification of sorted N-terminal peptides. *Nat. Biotechnol* 21, 566–569.
64. Sechi, S., Chait, B. T. (1998) Modification of cysteine residues by alkylation. A tool in peptide mapping and protein identification. *Anal. Chem* 70, 5150–5158.
65. Gygi SP, Rist B, Gerber SA, Turecek F, Gelb MH, Aebersold R. (1999) Quantitative analysis of complex protein mixtures using isotope-coded affinity tags. *Nat. Biotechnol* 17:994–999.
66. Niwayama S, Kurono S, and Matsumoto H (2001) Synthesis of d-labeled N-alkylmaleimides and application to quantitative peptide analysis by isotope differential mass spectrometry. *Bioorg Med Chem Lett* 13:2913-2916
67. Niwayama S, Kurono S, and Matsumoto H (2003) Synthesis of ¹³C-labeled iodoacetanilide and application to quantitative peptide analysis by isotope differential mass spectrometry. *Bioorg Med Chem Lett* 11:2257-2261
68. Sebastiano R, Citterio A, Lapadula M, and Righetti PG (2003) A new deuterated alkylating agent for quantitative proteomics. *Rapid Commun Mass Spec* 17:2380-2386
69. Shen M, Guo L, Wallace A, Fitzner J, Eisenman J, Jacobson E, and Johnson RS (2003) Isolation and isotope labeling of cysteine- and methionine-containing tryptic peptides. *Mol Cell Proteomics* 2:315-324
70. Pasquarello C, Sanchez J-C, Hochstrasser DF, and Corthals GL (2004) N-t-butyl-iodoacetamide and iodoacetanilide: two new cysteine alkylating reagents for relative quantitation of proteins. *Rapid Commun Mass Spec* 18:117-127
71. Niwayama S, Kurono S, Cho H, and Matsumoto H (2006) Synthesis of D-labeled naphthyl-iodoacetamide and application to quantitative peptide analysis by isotope differential mass spectrometry. *Bioorg Med Chem Lett* 16:6054-6057
72. Zhang R and Regnier FE (2002) Minimizing resolution of isotopically coded peptides in comparative proteomics. *J Proteome Res* 1:139-147
73. Conrads TP, Alving K, Weenstra TD, Belov ME, Anderson GA, Anderson DJ, Lipton MS, Paša-Tolić L, Udseth HR, Chrisler WB, Thrall BD, and Smith RD (2001) Quantitative analysis of bacterial and mammalian proteomes using a combination of cysteine affinity tags and ¹⁵N-metabolic labeling. *Anal Chem* 73:2132-2139
74. Kim, D., Garrett, S. H., Sens, M. A., Somji, S., and Sens, D. A. (2002). Metallothionein isoform 3 and proximal tubule vectorial active transport. *Kidney Int.* 61, 464–472.

75. Somji, S., Garrett, S. H., Sens, M. A., Gurel, V., and Sens, D. A. (2004). Expression of metallothionein isoform 3 (MT-3) determines the choice between apoptotic or necrotic cell death in Cd⁺²-exposed human proximal tubule cells. *Toxicol. Sci.* 80, 358–366.
76. Shechter Y (1986) Selective oxidation and reduction of methionine residues in peptides and proteins by oxygen exchange between sulfoxide and sulfide. *J Biol Chem* 261:66-70
77. Dormeyer W, Mohammed S, van Breukelen B, Krijgsveld J, and Heck AJR (2007) Targeted analysis of protein termini. *J Proteome Res* 6:4634-4645.
78. Landon M (1977) Cleavage at aspartyl-prolyl bonds. *Meth Enzymol* 47:145-149
79. Ghesqui re B, Jonkheere V, Colaert N, Van Durme J, Timmerman E, Goethals M, Schymkowitz J, Rousseau F, Vandekerckhove J, and Gevaert K (2011) Redox proteomics of protein-bound methionine oxidation. *Molec Cell Proteomics* 10:1-12
80. Lipton SH and Bodwell CE (1976) Specific oxidation of methionine to methionine sulfoxide. *J Agric Food Chem* 24:26-31
81. Cousins RJ (1979) Metallothionein synthesis and degradation: relationship to cadmium metabolism. *Environ Health Persp* 28: 131-136
82. Monia, B.P., Butt, T.R., Ecker, D.J., Mirabelli, C.K., Crooke, S.T. (1986) Metallothionein turnover in mammalian cells. *J Biol Chem* 24:10957-10959
83. Winge, D. R., Miklossy, K. A. (1982) Domain nature of metallothionein. *J. Biol. Chem.* 257, 3471–3476.
84. Nielson, K. B., Winge, D. R. (1983) Order of metal binding in metallothionein. *J. Biol. Chem.* 258, 13063–13069.
85. Nielson, K. B., Atkin, C. L., Winge, D. R. (1985) Distinct metal-binding configurations in metallothionein. *J. Biol. Chem.* 260, 5342–5350.
86. Werynska B, Pula B, Muszczyńska-Bernhard B, Gomulkiewicz A, Piotrowska A, Prus R, Podhorska-Okolow M, Jankowska R, Dziegiel P. (2013) Metallothionein IF and 2A overexpression predicts poor outcome of non-small cell lung cancer patients. *Exp Mol Path*: 94(1):301-8.
87. Zhang R, Zhang H, Wei H, et al. (2000) Expression of metallothionein in invasive ductal breast cancer in relation to prognosis. *J Environ Pathol Toxicol Oncol* 19: 95-97.
88. Vazquez-Ramirez FJ, Gonzalez-Campora JJ, Hevia-Alvarez E, et al. (2000) P-glycoprotein, metallothionein and NM23 protein expressions in breast carcinoma. *Pathol Res Pract* 196: 553-559.
89. Jin R, Chow VT, Tan PH, et al. (2002) Metallothionein 2A expression is associated with cell proliferation in breast cancer. *Carcinogenesis* 23: 81-86.
90. Ioachim E, Tsanou E, Briasoulis E, et al. (2003) Clinicopathological study of the expression of hsp27, pS2, cathepsin D and metallothionein in primary invasive breast cancer. *Breast* 12: 111-119.
91. Levine, R.L., Moskovitz, J., Stadtman, E.R. (2000) Oxidation of Methionine in Proteins: Roles in Antioxidant Defense and Cellular Regulation. *Life*. 50: 301-307.

92. Drozdź R, Naskalski JW, Sznajd J, (1988) Oxidation of amino acids and peptides in reaction with myeloperoxidase, chloride, and hydrogen peroxide. *Biochim Biophys Acta.* 2; 957 (1) 47-52.
93. Yamasaki RB, Osuga DT, Feeney RE. (1982) Periodate oxidation of methionine in proteins. *Anal Biochem.* 126(1): 183-9.
94. Arsova B, Zauber H, Schulze WX. (2012) Precision, Proteome Coverage, and Dynamic Range of Arabidopsis Proteome Profiling Using ¹⁵N Metabolic Labeling and Label-free Approaches. *Mol Cell Proteomics.* 11(9): 619-28.
95. Klaasen, CD, Liu, J, Diwan, BA. (2009) Metallothionein protection of cadmium toxicity. *Toxicol Appl Pharm.* 238:215-220.
96. Santon, A., et al., (2004) Evaluation of MT Expression and detection of apoptotic cells in LEC rat kidney. *Biochimica et Biophysica Acta.* 1668, 223-231.
97. Koropatnick, J., et al., (1995) Metallothionein expression and resistance to cisplatin in human germ cell tumor cell line. *Jour of Pharm Exp. Ther.* 275, 1681-1687.
98. Surowiak, P., et al., (2007) Nuclear metallothionein expression correlates with cisplatin resistance of ovarian cancer cells and poor clinical outcome. *Virchows Archiv.* 450, 279-285.
99. Ferrario, C., et al., (2008) Metallothionein 1G acts as an oncosuppressor in papillary thyroid carcinoma. *Laboratory investigation.* 88, 474-481.
100. Kanda, M., et al., (1991) Detection of Metallothionein 1G as a methylated tumor suppressor gene in human hepatocellular carcinoma using a novel method of double combination array analysis. *Int Jour Oncology.* 35, 477-483.
101. Tai, S.K., et al., (2003) Differential expression of metallothionein 1 and 2 isoform in breast cancer lines with different invasive potential identification of a novel nonsilent metallothionein- 1H mutant variant. *Amer Jour Pathology.* 163, 2009-2019.
102. Werynska, B., et al., (2013) Metallothionein 1F and 2A overexpression predicts poor outcome of non-small cell lung cancer patients. *Exp and Mol Pathology.* 94, 301-308.
103. Arriaga JM, Bravo IA, Bruno L, Morales Bayo S, Hannois A, Sanchez Loria F, Pairola F, Huertas E, Roberti MP, Rocca YS, Aris M, Barrio MM, Baffa Trasci S, Levy EM, Mordoh J, Bianchini M. (2012) Combined metallothioneins and p53 proteins expression as a prognostic marker in patients with Dukes stage B and C colorectal cancer. *Hum Pathol.* 2012 Oct; 43(10):1695-703.
104. Ryu HH, Jung S, Jung TY, Moon KS, Kim IY, Jeong YI, Jin SG, Pei J, Wen M, Jang WY. Role of metallothionein 1E in the migration and invasion of human glioma cell lines. *Int J Oncol:* 41: 1305-1313, 2012.
105. Jin, R., et al., (2001) Metallothionein 1F mRNA expression correlates with histological grade in breast carcinoma. *Breast Canc Res and Treatment.* 66, 265-272.
106. Yap, X., et al., (2009) Over-expression of metallothionein predicts chemoresistance in breast cancer. *Jour of Path.* 217, 563-570.
107. Lim, D., et al., (2009) Silencing the Metallothionein-2A gene inhibits cell cycle progression from G1-to-S-phase involving ATM and cdc25A signaling in breast cancer cells. *Cancer Letters.* 276, 109-117.

108. Theodorescu, D., et al., (2006) Discovery and validation of new protein biomarkers for urothelial cancer: a prospective analysis. *Lancet Oncol.* 7, 230-240.
109. Linden, M., et al., (2012) Proteomic analysis of urinary biomarker candidates for nonmuscle invasive bladder cancer. *Proteomics.* 12, 135-144.
110. Hood, B.L., et al., (2005) Proteomic analysis of formalin-fixed prostate cancer tissue. *Mol. Cell. Proteomics.* 4, 1741-1753.
111. Xu, H., et al., (2008) Antigen retrieval for proteomic characterization of formalin-fixed and paraffin-embedded tissues. *J. Proteome Res.* 7, 1098-1108.
112. Crockett, D.K., et al., (2005) Identification of proteins from formalin-fixed paraffin-embedded cells by LC-MS/MS. *Lab. Invest.* 85, 1405-1415.
113. Hwang, S.I., et al., (2007) Direct cancer tissue proteomics: a method to identify candidate cancer biomarkers from formalin-fixed paraffin-embedded archival tissues. *Oncogene.* 26, 65-76.
114. Jiang, X., et al., (2007) Development of efficient protein extraction methods for shotgun proteome analysis of formalin-fixed tissues. *J. Proteome Res.* 6, 1038-1047.
115. Palmer-Toy, D.E., et al., (2005) Efficient method for the proteomic analysis of fixed and embedded tissues. *J. Proteome Res.* 4, 2404-2411.
116. Shi, S.R., et al., (2006) Protein extraction from formalin-fixed, paraffin-embedded tissue sections: quality evaluation by mass spectrometry. *J. Histochem. Cytochem.* 54, 739-743.
117. Sprung, Jr., R.W. et al., (2009) Equivalence of protein inventories obtained from formalin-fixed paraffin-embedded and frozen tissue in multidimensional liquid chromatography-tandem mass spectrometry shotgun proteomic analysis. *Mol Cell Prot.* 8, 1988-1998.